

UNIVERSITY OF OKLAHOMA

GRADUATE COLLEGE

HEME AND HEMOGLOBIN TRANSPORT
SYSTEMS OF LISTERIA MONOCYTOGENES

A DISSERTATION

SUBMITTED TO THE GRADUATE FACULTY

in partial fulfillment of the requirements for the

Degree of

DOCTOR OF PHILOSOPHY

By

QIAOBIN XIAO
Norman, Oklahoma
2010

HEME AND HEMOGLOBIN TRANSPORT
SYSTEMS OF LISTERIA MONOCYTOGENES

A DISSERTATION APPROVED FOR THE
DEPARTMENT OF CHEMISTRY AND BIOCHEMISTRY

BY

Dr. Phillip E. Klebba, Chair

Dr. Randall S. Hewes

Dr. Helen I. Zgurskaya

Dr. Michael T. Ashby

Dr. Jun Li

© Copyright by QIAOBIN XIAO 2010
All Rights Reserved.

Acknowledgements

Five years ago, when I started my study at OU, I basically knew nothing about bacterial genetics and membrane transport. It is from this lab that I began to have this knowledge. So I would like to thank my major professor, Dr. Phillip E. Klebba, who gave me the chance to work in his lab and had always been offering great advice for my Ph.D study. His patience and financial support helped me to finish this work. I would also like to thank Dr. Salet M. Newton, who trained me a lot and was always ready to offer me suggestions whenever I had problems with my experiments.

My sincere gratitude also goes to all my committee members, Dr. Helen I. Zgurskaya, Dr. Randall S. Hewes, Dr. Valentin V. Rybenkov, Dr. Michael T. Ashby and Dr. Jun Li, for their guidance and helps throughout my Ph.D study.

I would also like to take the chance to say thanks to all the previous and current members in Dr. Klebba's lab: Hualiang Pi, Yi Shao, Xiaoxu Jiang, Li Ma, Wallace Kaserer, Daniel Schuerch, Kyle Moore, Chuck Smallwood, Vy Trinh, Zhiguo Wang, Lorne Jordan, Muthuvelan Soundarajan, John Best, Amparo Gala Marco, Lynn Mercer, Justin Rosinski, Dilip Mahale. Thanks for their helps in my experiments and the helpful discussions.

My special thanks go to my dearest wife, Hualiang Pi. It is her constant love, understanding and support that has supported and is supporting me to go through all the hard times, not to mention the help she gave to me in those time-consuming and labor-consuming binding and transport experiments.

I also want to thank my parents, my brothers and my sister. They always love me and are always proud of me.

Last, but not least, I want to thank my daughter and my son, Ruby and Fred. It is their laugh that makes me feel happy and makes my life a little bit easier.

Table of contents

Chapter 1 Introduction	1
1.1 Cell envelope of bacteria and bacterial iron transport systems.....	1
1.2 Heme uptake in bacteria.....	6
1.2.1 Heme uptake in Gram-negative bacteria.....	6
1.2.1.1 Hemophore-independent heme uptake	6
1.2.1.2 Hemophore-mediated heme uptake	8
1.2.2 Heme uptake in Gram-positive bacteria	12
1.2.2.1 Protein sorting to the cell wall in Gram-positive bacteria	12
1.2.2.2 Heme uptake by <i>S. aureus</i> through Isd system	14
1.2.2.3 Crystal structures of Isd proteins	18
1.2.2.4 The Hts system is the primary membrane heme uptake system in <i>S.aureus</i>	20
1.3 Heme toxicity and its detoxification	20
1.4 Iron and Heme uptake regulation in bacteria	23
1.5 <i>Listeria monocytogenes</i>	25
1.6 Iron transport systems in <i>Listeria monocytogenes</i> and their relevance to virulence..	27
1.7 Significance of this research	29
1.8 TonB in <i>E.coli</i>	30
Chapter 2 Materials and Methods	33
2.1 Bacteria strains and plasmids	33
2.2 Growth media	35
2.3 Oligonucleotides	36
2.4 Preparation of chromosomal DNA from <i>Listeria monocytogenes</i> strain EGD-e....	39

2.5 Preparation of <i>E. coli</i> competent cells for electroporation	40
2.6 Preparation of competent cells of <i>Listeria monocytogenes</i> for electroporation	40
2.7 Site-directed chromosomal deletions in <i>Listeria monocytogenes</i>	41
2.8 Complementation of $\Delta hupD$	42
2.9 Expression and purification of His-tagged HupD	45
2.10 Nutrition test with <i>Listeria monocytogenes</i>	48
2.11 Synthesis of [⁵⁹ Fe]-hemin	48
2.12 [⁵⁹ Fe]-hemin uptake in <i>L.monocytogenes</i>	49
2.13 Generation of polyclonal mouse anti-HupD antibody	50
2.14 Immunoblots with cell fractions of <i>Listeria monocytogenes</i>	51
2.15 Growth of <i>Listeria monocytogenes</i> in MOPS-L media	52
2.16 Intrinsic tryptophan fluorescence quenching	53
2.17 Synthesis of [⁵⁹ Fe]-Ferric Citrate	53
2.18 [⁵⁹ Fe]-Ferric Citrate uptake in <i>Listeria monocytogenes</i>	53
2.19 Binding of peptidoglycan to TonB C-terminus	54
Chapter 3 Site-directed Chromosomal Deletions in <i>Listeria</i>	55
3.1 Target genes for deletion.....	55
3.2 Chromosomal deletions.....	57
3.2.1 Deletion of <i>hupD</i>	57
3.2.2 Deletion of <i>hupCDG</i>	60
3.2.3 Construction of <i>lmo</i> Δ 2183/ Δ <i>hupCDG</i>	63
3.2.4 Construction of <i>lmo</i> Δ 2185/ Δ <i>hupCDG</i>	66
3.2.5 Construction of <i>lmo</i> Δ 0641/ Δ <i>hupCDG</i>	66

3.2.6 Construction of <i>lmo</i> Δ 1960/ Δ <i>hup</i> CDG.....	71
3.2.7 Construction of <i>lmo</i> Δ 2183/ Δ <i>hup</i> CDG/ Δ 1960.....	71
3.2.8 Construction of <i>lmo</i> Δ 2183/ Δ 1960.....	71
3.3 Complementation of Δ <i>hupD</i>	78
Chapter 4 Characterization of Binding Specificity of HupD.....	85
4.1 Expression and purification of HupD.....	85
4.2 Binding specificity of HupD.....	91
Chapter 5 Hemin Binding and Uptake by <i>Listeria monocytogenes</i>	96
5.1 Putative or demonstrated Hemin uptake systems in <i>Listeria monocytogenes</i>	96
5.2 Nutrition tests.....	97
5.2.1 Nutrition tests with Δ <i>hupD</i> and Δ <i>hup</i>	98
5.2.2 Nutrition tests with deletion mutants in <i>srtB</i> locus and <i>fhu</i> locus.....	100
5.3 [⁵⁹ Fe]-Hn binding and uptake.....	102
5.3.1 Development of the [⁵⁹ Fe]-Hn uptake protocol.....	102
5.3.2 The <i>hup</i> operon in Hn binding and uptake.....	103
5.3.3 Sortase B and Lmo2185 in Hn binding and uptake.....	106
5.4 Expression and localization of HupD in <i>Listeria monocytogenes</i>	107
Chapter 6 Heme export by <i>Listeria monocytogenes</i>	110
6.1 Potential function of <i>lmo0641</i>	110
6.2 Nutrition tests.....	110
6.3 Growth assays.....	112
6.4 Hn uptake.....	114
Chapter 7 Discussion.....	117

Chapter 8 Binding of peptidoglycan to TonB.....	123
8.1 Sequence relationship between TonB and YcsF.....	123
8.2 Peptidoglycan precipitated MalE-TonB69C.....	124
References	128

List of Tables

Table 2.1 Bacterial strains and plasmids used in this study.....	34
Table 2.2 Media used in this study.....	35
Table 2.3 Primers used in this study.....	36
Table 3.1 Chromosomal deletion mutants made for this study.....	56
Table 5.1 Binding and transport properties of EGD-e and its mutant derivatives.....	105

List of Figures

Figure 1.1 Structures of ferrichrome and ferric-enterobactin.....	5
Figure 1.2 Structure of PhuT compared with BtuF and FhuD.....	12
Figure 1.3 Isd-mediated heme uptake in <i>S. aureus</i>	17
Figure 1.4 Schematic representation of Isd surface proteins.....	18
Figure 1.5 Putative and demonstrated iron transport loci in the genome of <i>L. monocytogene</i>	28
Figure 3.1 Schematic representation of the construction of $\Delta hupD$	58
Figure 3.2 Construction of $\Delta hupCDG$	61
Figure 3.3 Construction of $lmo\Delta 2183/\Delta hupCDG$	64
Figure 3.4 Construction of $lmo\Delta 2185/\Delta hupCDG$	67
Figure 3.5 Construction of $lmo\Delta 0641/\Delta hupCDG$	69
Figure 3.6 Construction of $lmo\Delta 1960/\Delta hupCDG$	72
Figure 3.7 Construction of $lmo\Delta 2183/\Delta hupCDG/\Delta 1960$	74
Figure 3.8 Construction of $lmo\Delta 2183/\Delta 1960$	76
Figure 3.9 Complementation clone of <i>hupD</i> with pKSV7.....	80
Figure 3.10 Plasmid map of pPL2.....	81
Figure 3.11 Complementation clone with pPL2.....	82
Figure 3.12 Cloning of <i>hupD</i> into pPro and replacement of the native promoter.....	83
Figure 3.13 Cloning <i>hupD</i> and its native promoter into pMAD.....	84
Figure 4.1 Signal peptidase II recognition sequence of HupD in EGD-e.....	86
Figure 4.2 Schematic depiction of insertion of the <i>hupD</i> fragment into pET28a.....	87

Figure 4.3 Cloning of hupD into pET28a and transformation of BL21 with pETHupDΔ18.....	88
Figure 4.4 HupD expression check by Western Immunoblot with anti-Histag antibody..	89
Figure 4.5 Cloning of hupD into pET28a and transformation of BL21 with pETHupDΔ20.....	89
Figure 4.6 Expression and purification of HupD.....	90
Figure 4.7 Separation of Hn from HupD by SDS-denaturation.....	93
Figure 4.8 Binding specificity of HupD.....	94
Figure 4.9 UV-visible wavelength scan of purified HupD.....	95
Figure 5.1 Nutrition tests of EGD-e, Δ <i>hupD</i> and Δ <i>hup</i>	99
Figure 5.2 Nutrition tests with mutants in <i>srtB</i> and <i>fhu</i> loci.....	101
Figure 5.3 [⁵⁹ Fe]-Hn binding and uptake by EGD-e and its derivatives.....	104
Figure 5.4 Expression and localization of HupD in <i>L. monocytogenes</i>	108
Figure 6.1 Nutrition tests with EGD-e, Δ <i>0641</i> and Δ <i>0641/comp</i>	111
Figure 6.2 Growth of EGD-e and its derivatives in BHI broth and MOPS-L.....	113
Figure 6.3 [⁵⁹ Fe]-Hn uptake by EGD-e and Δ <i>lmo0641</i>	115
Figure 6.4 [⁵⁹ Fe]-citrate uptake by EGD-e and Δ <i>lmo0641</i>	116
Figure 8.1 CLUSTALW analysis of YcfS homologs.....	125
Figure 8.2 Affinity of the TonB C terminus for PG.....	126

Abstract

Heme (Hn) is an important iron source for *Listeria monocytogenes*, an intracellular pathogen that causes listeriosis. I characterized listerial Hn acquisition by two Fur-regulated genetic systems: the *hup* region that produces an ABC transporter for Hn and hemoglobin (Hb) and the *srtB* region that produces an ABC transporter and other proteins with currently unknown functions. Intrinsic fluorescence titration assay showed HupD binds Hn with high affinity ($K_d=40$ nM). Western immunoblot analysis with listerial fractions identified its localization in the envelope of *L. monocytogenes*. Nutrition tests showed that the deletions in either *hup* region or the *srtB* region reduced the uptake of Hn and Hb. To quantitatively characterize Hn acquisition by *L. monocytogenes*, I synthesized [^{59}Fe]-Hn and for the first time measured thermodynamic and kinetic parameters of its binding and transport. The [^{59}Fe]-Hn binding and uptake assay showed that *L. monocytogenes* binds Hn with high affinity ($K_d\approx 2$ nM) and imports it with a V_{\max} (23 pMol/ 10^9 cells/min) comparable to those of ferric siderophore import systems. The Hup system was responsible for the majority of Hn uptake ($V_{\max}=16$ pMol/ 10^9 cells/min). The residual uptake system (in Δhup) also had high affinity ($K_d\approx 2$ nM) but lower rate ($V_{\max}=7$ pMol/ 10^9 cells/min). This quantitative assay also showed that the sortase B-anchored protein Lmo2185 binds Hn and deletions of *lmo2185* or *srtB* severely impaired the uptake of [^{59}Fe]-Hn by *L. monocytogenes* at low concentrations (≤ 20 nM). However, at higher concentrations (≥ 50 nM), Hn directly adsorbs to its high affinity binding protein of cytoplasmic membrane transporter. Deletion of sortase A, on the other hand, had no effect on Hn/Hb acquisition, in nutrition tests or [^{59}Fe]-Hn binding and uptake assay.

These data showed the participation of at least two cytoplasmic membrane permeases in Hn/Hb acquisition and the involvement of the SrtB-anchored cell envelope protein Lmo2185 in binding and uptake of Hn at low external concentrations. SrtA-anchored proteins, on the other hand, apparently do not function in Hn transport by *L. monocytogenes*.

Intracellular Hn concentration is tightly regulated. To prevent Hn toxicity, bacteria export excess Hn. Deletion of *lmo0641* rendered the mutant intolerant to a moderate concentration of Hn/Hb (2 μ M), implying its defect in Hn detoxification. [59 Fe]-Hn uptake assay supported the hypothesis that Lmo0641 functions as a heme exporter: Δ *lmo0641* accumulated intracellularly 1.6 fold higher amount of Hn than the wild type EGD-e did. [59 Fe]-citrate uptake assay, on the other hand, displayed no difference in the ability of the two strains to uptake ferric citrate: the V_{max} of [59 Fe]-citrate uptake for EGD-e was 51.4 pMol/ 10^9 cells/min and 55 pMol/ 10^9 cells/min for Δ 0641; the K_M was 44.2 nM for EGD-e and 48.4 nM for Δ 0641.

TonB has been proposed to be an energy transducer for the active transport of metal complexes across the OM of Gram-negative bacteria. Sequence analysis revealed homology in the TonB C terminus to *E. coli* YcfS, a proline-rich protein that contains the lysin (LysM) peptidoglycan-binding motif. My experiments confirmed that TonB physically binds to the peptidoglycan: the purified peptidoglycan precipitated MalE-TonB69C from solution, but not MalE nor FepB.

Chapter 1 Introduction

1.1 Cell envelopes of bacteria and bacterial iron transport systems

Bacteria are classified into two categories based on whether or not they retain the crystal-violet dye (Gram stain): Gram-negative bacteria and Gram-positive bacteria. Gram-negative bacteria envelopes contain an outer membrane (OM), a periplasmic space (PP), and an inner membrane (IM, or cytoplasmic membrane). In the periplasmic space, a cell wall composed of 7 to 8 nm thick peptidoglycan layer is closely attached to the outer membrane (Vollmer and Holtje, 2004). Gram-positive bacteria, on the other hand, have no outer membrane, and the cytoplasmic membrane (CM) is surrounded by a much thicker cell wall (20 to 80 nanometers) (Navarre et al, 1999; Dmireiev et al, 1999) that makes Gram-positive bacteria susceptible to Gram stain.

Besides its structural function, the cell envelope is an extremely important interface between the cell and its external surroundings. A cell relies on its envelope to sense and respond to the environmental changes, to acquire nutrients from and exclude toxic molecules or metabolic wastes to its surrounding environments. With few exceptions, iron is an essential nutrient to all organisms. Many important biological processes, such as energy generation, oxygen transport, DNA synthesis, photosynthesis and detoxification of oxygen radicals (Neilands, 1976; Neilands, 1995; Weinberg, 1990; Wrigglesworth and Baum, 1980), require iron or are regulated by iron. The iron requirement for maximal cell growth is 0.4 - 4.0 μM (Weinberg, 1978) and the minimal iron requirement is 10^{-8} M (Neilands, 1995; Braun and Killmann, 1999; Wandersman and

Delepelaire, 2004) in order to maintain the required 10^{-6} M internal concentration (Braun and Killmann, 1999). However, iron is not readily available despite being the second most abundant metal in the earth's crust. Under aerobic conditions, Fe^{2+} is readily oxidized to Fe^{3+} and then precipitates as hydroxide polymers, reducing the free iron concentration to 10^{-18} M (Schneider and Schwyn, 1987). In animal body fluids, iron is also sequestered by some eukaryotic iron-binding proteins, such as transferrin (Tfn), lactoferrin (Lfn), hemoglobin (Hb) and ferritin (Fn). This further reduces free iron concentration to about 10^{-24} M (Raymond et al, 2003). To overcome this iron acquisition barrier, efficient pathogens develop three ways. One way is to produce siderophores (Neilands, 1976; Neilands, 1995). Siderophores are low molecular weight organic compounds that have sufficient higher affinities to either scavenge free iron at very low concentrations or directly capture iron from iron-containing proteins. There are two major types of siderophores: catecholate and hydroxamate, based on the functional groups that chelate iron. Both types are given one example in Figure 1.1. A second way is to directly utilize eukaryotic iron-binding proteins like Hb, Tfn and Lfn as iron sources. The third way is to utilize insoluble ferric iron (Fe^{3+}) by reducing it to ferrous iron (Fe^{2+}). Among the three ways, the second one is a more common attribute among pathogenic bacteria (Cornelissen and Sparling, 1994). A brief description of the 3 iron acquisition ways is given below.

For many bacteria, siderophore-mediated iron uptake is the main way to acquire iron and is well-studied in Gram-negative bacteria. One example is ferric enterobactin (FeEnt) uptake in *Escherichia coli*. Enterobactin is a catecholate type siderophore. The FeEnt uptake system of *E. coli* constitutes an outer membrane receptor FepA, a periplasmic

binding protein FepB, and an ABC transporter FepCDG. Under low iron conditions, enterobactin is synthesized and excreted to the extracellular environment, where it chelates ferric iron with extremely high affinity ($K_d=10^{-52}\text{M}$) (Carl and Raymond, 1979). FepA recognizes FeEnt and binds it with high affinity ($K_d=10^{-10}\text{M}$) (Newton et al, 1999). The translocation of FeEnt across the OM through FepA is believed to be energized by TonB, a potential energy transducer. However, the exact mechanism about how FeEnt is transported across the OM and how it is released from the periplasmic side still remains unclear. Comparison of the available structural data of FepA (Buchanan et al, 1999), ligand free and ferrichrome-bound FhuA (the OM receptor for ferrichrome) (Locher et al, 1998) suggests that binding of FeEnt to FepA induces conformational change on the periplasmic side of FepA, promoting the interactions between the N-terminal “TonB box” of FepA and TonB. FeEnt is then transported across the OM through FepA. Once inside the periplasmic space, it is bound by FepB and delivered to the inner membrane ABC transporter FepCDG. It is still not sure whether there is an interaction between FepA and FepB which helps delivery of FeEnt to FepB (Newton et al, 2010). FeEnt is then transported into the cytoplasm, degraded and iron is released.

In addition to the secretion of siderophores, many bacteria also have the ability to directly utilize eukaryotic iron-containing proteins. In terms of iron availability for bacteria, animal body fluid is an extremely harsh environment. Virtually no free iron is available because most of the iron is sequestered by eukaryotic iron-binding proteins and 99% of total body iron is localized intracellularly (Stojiljkovic and Perkins-Balding, 2002). Usually these iron-binding proteins are only 30% to 40% saturated (Perkins-Balding et al, 2004). To survive under this tough condition, bacteria have developed efficient ways to

directly utilize host iron-containing proteins as important iron sources. For example, *Neisseria meningitidis*, a Gram-negative bacterium, can strip iron from transferrin and lactoferrin. Extensive studies about iron uptake from Tf and Lfn in *Neisseria meningitides* have been conducted. It was reported that the OM receptors for Tf and Lfn consist of two protein components, with TbpA/TbpB for Tf and LbpA/LbpB for Lfn, respectively (Perkins-Balding et al, 2004). TbpA and LbpA are believed to be membrane proteins inserted into the OM while TbpB and LbpB are lipoproteins anchored to outer leaflet of the OM. Mutants deficient in TbpB (LbpB) are still able to utilize iron from Tf (Lfn) with a level significantly less than the wild type. However, mutants deficient in TbpA (LbpA) can no longer utilize Tf (Lfn) as an iron source (Perkins-Balding et al, 2004). This indicates that TbpB (LbpB) play a facilitatory role in the usage of Tf (Lfn) as an iron source. Such kind of OM receptors with two protein components is not common in TonB-dependent iron transport systems. As iron sources, neither the whole Tf nor the whole Lfn is internalized across the OM. It was reported that binding of Tf (Lfn) to its receptor may cause conformational changes both in the ligand and the receptor, resulting in removal of iron from the ligand and binding of iron to the receptor (Perkins-Balding et al, 2004). Specific interactions between TbpB and Tf have been reported (Retzer et al, 1999). The iron is then delivered to FbpA, a periplasmic iron-binding protein. A recent study using the closely related *N. gonorrhoeae* demonstrated that this iron transfer involves interaction between TbpA and FbpA (Siburt et al, 2009). It was also showed that TbpA interacts with apo-FbpA with higher affinity than holo-FbpA which could facilitate the dissociation of holo-FbpA from the TbpA/B receptor. The iron-FbpA complex is then bound by FbpB/FbpC complex, a putative inner membrane ABC transporter, and the

ferric iron is internalized across the IM through FbpB/FbpC (Perkins-Balding et al, 2004).

Besides the synthesis of siderophore and direct utilization of eukaryotic iron-containing proteins, some bacteria can reduce extracellular ferric iron to ferrous iron on the surface of cell envelope (Cartron et al, 2006; Deneer et al, 1995). However, little is known about the mechanism or components of extracellular-ferric iron reduction in bacteria. Unlike the ferric form, ferrous iron is relatively soluble (0.1 M at pH 7) (Cartron et al, 2006). The feo system of *E. coli* K-12 was the first bacterial ferrous iron transport system reported (Hantke 1987).

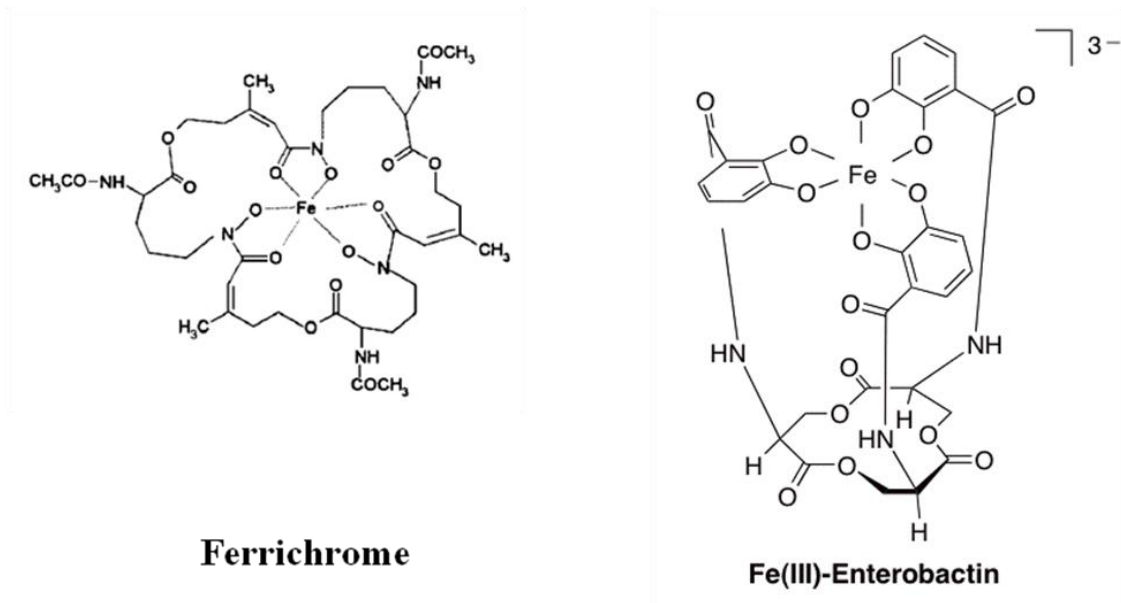


Figure 1.1 Structures of ferrichrome and ferric-enterobactin

Left panel: apoferrichrome complexed with iron, apoferrichrome is a prototypical hydroxamate type siderophore; Right panel: enterobactin complexed with iron, enterobactin is a prototypical catecholate type siderophore (Neilands, 1995).

1.2 Heme uptake in bacteria

A 70-kg adult human has an iron pool around 5g (Braun and Killmann, 1999) and heme iron source constitutes two thirds of it (Wandersman and Delepelaire, 2004). Most of heme is bound to either hemoglobin or myoglobin. Free heme or hemoglobin is scarce in animal body fluids. Spontaneous hemolysis or local hemolysis release heme or hemoglobin, but they are complexed immediately by hemopexin or haptoglobin with high affinity. Haptoglobin and hemopexin are glycoproteins found in serum or plasma, respectively. Heme is a hydrophobic molecule that can easily intercalate into membranes (Wandersman and Delepelaire, 2004). It also promotes redox reactions. Thus makes heme highly toxic. While micromolar iron is required for bacterial growth, nanomolar heme is sufficient (Wandersman and Delepelaire, 2004).

1.2.1 Heme uptake in Gram-negative bacteria

Heme-uptake systems in Gram-negative bacteria can be classified into two groups depending on whether hemophore, a protein secreted by bacteria to the extracellular environment to scavenge heme sources, is involved to mediate the uptake of heme. One group involves direct binding of heme or heme-containing host proteins to specific OM receptors while the other group relies on hemophores to present heme to the specific OM receptors. And then heme is transported across the cell envelope in a defined way.

1.2.1.1 Hemophore-independent heme uptake

This type of heme uptake systems in Gram-negative bacteria relies on their OM receptors to directly bind heme or heme-containing proteins. Basically all OM receptors for varying iron sources share some common characteristics. Although their primary

sequence homology is low with the amino terminus being the most conserved part, they all show a quite similar overall structure: a 22-stranded β -barrel with a N-terminal plug folded inside the barrel. For heme source OM receptors, there are 2 groups: one group recognizes diverse heme sources and the other only recognize and utilize one or two specific heme source (Wandersmann and Stojiljkovic, 2000). All known heme receptors share the conserved FRAP/NPL domain (Wandersmann and Stojiljkovic, 2000) and are all TonB-ExbB-ExbD dependent.

An example of the first group is HemR, the OM receptor of *Y. enterocolitica*. HemR can recognize many different heme-containing compounds, including heme, hemoglobin, myoglobin, hemoglobin-haptoglobin complex, heme-hemopexin complex, heme-albumin complex (Bracken et al, 1999). Site-directed mutagenesis have identified two conserved histidine residues, one located in the plug , most likely on one apex, and the other in the β -barrel on an extracellular loop, essential for heme acquisition by HemR (Bracken et al, 1999). Examples of the second group include HutA and HmbR. HutA is the OM receptor for heme and hemoglobin in *Vibrio cholera* (Henderson and Payne, 1994). HmbR is the OM receptor for hemoglobin and heme in *Neisseria meningitides* (Stojiljkovic et al, 1995; Stojiljkovic et al, 1996). In general, heme uptake in Gram-negative bacteria is similar with other OM receptor-mediated iron uptake process. Both of them are TonB-ExbB-ExbD dependent.

Two heme uptake systems have been identified in *N. meningitides*. One system involves HmbR which recognizes and binds hemoglobin with a high affinity, with a K_d around 13 nM (Stojiljkovic et al, 1995). HmbR strips heme from Hb and transports it across the OM (Stojiljkovic et al, 1995). The other system involves HpuAB, the bipartite OM receptor

which recognizes and binds a broader spectrum of heme sources, including hemoglobin, haptoglobin and hemoglobin-haptoglobin complexes. Similar to other bipartite receptors TbpAB/LbpAB in *Neisseria*, HpuAB consists of a lipoprotein HpuA and a transmembrane protein HpuB (Perkins-Balding et al, 2004). While TbpB/LbpB is not essential for utilization of Tf/Lfn as an iron source, both HpuA and HpuB are required for Hb utilization (Stojiljkovic and Schryvers, 1999). During HmbR or HpuAB-mediated heme uptake process, only heme, but not heme-containing proteins, is internalized (Stojiljkovic et al, 1995). Both HmbR and HpuAB are TonB-ExbB-ExbD dependent. A specific interaction between HmbR and TonB has been reported (Perkins-Balding et al, 2004). Little is known about the mechanism of heme transport from periplasm to cytoplasm. But the Fbp system is not involved (Khun et al, 1998).

1.2.1.2 Hemophore-mediated heme uptake

Hemophore is a small protein secreted by some Gram-negative bacteria through an ABC transporter under iron-deficient conditions (Letoffe et al, 1994). The secretion signal is located in the C-terminus (Letoffe et al, 1994). The first identified hemophore is HasA from *S.marcescens* (Letoffe et al, 1994; Arnoux et al, 1999; Arnoux et al, 2000). It consists of a β -sheet layer and a layer of 4 α -helices (Krieg et al, PNAS 2009). HasA binds b-type heme with high affinity ($K_d \sim 10^{-11}$ M) (Deniau et al, 2003). Its homologues have been found in *P. aeruginosa* (Letoffe et al, 1998; Letoffe et al, 2000), *Pseudomonas fluorescens* (Idei et al, 1999), *Y. pestis* (Rossi et al, 2001) and *Y. enterocolitica* (Stojiljkovic and Hantke, 1994). The OM receptor for HasA is HasR and the binding interaction between them was proposed to be HasB-dependent (HasB is a TonB-like protein) (Lefevre et al, 2008). The crystal structure of HasR-HasA complex has recently

been solved (Krieg et al, PNAS 2009). Like other TonB-dependent receptors, HasR consists of a C-terminal 22-stranded β -barrel and an N-terminal plug localized inside the β -barrel. HasR superimposes well with the known structures of other TonB-dependent receptors except for the extracellular loops. It binds heme with a significant lower affinity ($K_d=10^{-6}$ M) (Letoffe et al, 2004) than HasA. The lower affinity of HasR raises a question about how HasR gets heme from HasA. The formation of HasR-HasA complex and interactions between HasR and holo-HasA have been reported (Izadi et al,1997; Letoffe et al,1999; Caillet-Saguy et al, 2006; Caillet-Saguy et al, 2009). HasR binds HasA with a $K_d=7$ nM. It was proposed that once HasR binds holo-HasA, the equilibrium between high-spin species and low-spin species of heme shifts toward the high-spin species, inverting the affinity order of HasA and HasR for heme (Caillet-Saguy et al, 2006). As a result, heme transfers from HasA to HasR. It has been observed that holo-HasA docking to HasR breaks 1 of the 2 axial heme coordinations of HasA. The other axial coordination is then ruptured by subsequent displacement of heme by a HasR residue, leading to heme transfer into HasR. While heme transfer from HasA to HasR is energy-independent, heme transfer from HasR into the periplasm requires energy provided by HasB-ExbB-ExbD complex, just like other OM receptor-mediated iron uptake processes. Besides serving as hemophore receptors, HasR in *S. marcescens* also function as heme receptors by directly binding free heme and hemoglobin (Ghigo et al, 1997). There is also another uncommon type of hemophore: HxuA. HxuA was first identified in *H. influenza* (Hanson et al, 1992). The main difference between HxuA and HasA is that HxuA only strips heme from heme-loaded hemopexin while HasA strips heme from a broad spectrum of heme sources (Wandersman and Delepelaire, 2004; Tong and Guo, 2009). HxuA binds heme-

hemopexin suggesting heme transfer through protein-protein interactions (Hanson et al, 1992). On the other hand, both coimmunoprecipitation and analytical ultracentrifugation methods failed to detect stable complexes between HasA and myoglobin or hemoglobin, suggesting a mechanism of heme transfer from these proteins to HasA by passive heme transfer because of the higher affinity of HasA (Wandersman and Delepelaire, 2004). While HxuA is absolutely required for heme uptake from hemopexin, HasA is not essential in the *has* system of *S. marcescens* (Stojiljkovic and Perkins-Balding, 2002). Under some conditions, HxuA itself also functions as a heme receptor (Cope et al, 1998; Wong et al, 1994; Cope et al, 1995). The molecular weight of HxuA is about 100 KDa, 5 times larger than HasA (19 KDa) (Tong and Guo, 2009).

Once heme inside the periplasm, it is believed that it uses a common heme transport system to deliver heme from periplasm into the cytoplasm. However, little is known about how heme is transported from periplasm into the cytoplasm.

One well-studied periplasmic heme binding protein is PhuT from *P. aeruginosa* (Ho et al, 2007). The *phu* locus in *P.aeruginosa* is involved in heme uptake (Ochsner et al, 2000; Tong and Guo, 2007). It contains an OM heme receptor PhuR, a periplasmic heme binding protein PhuT, a putative IM ABC transporter PhuUVW and a putative cytoplasmic heme storage/chaperone protein PhuS (Tong and Guo, 2009). PhuR recognizes a broad spectrum of heme iron sources, including heme, hemoglobin, myoglobin, haptoglobin-hemoglobin, hemopexin (Tong and Guo, 2009). Heme is internalized into the periplasm through PhuR. PhuT is then proposed to bind and deliver heme to the IM permease PhuUVW through which heme is transported into the cytoplasm where it is bound by PhuS (Tong and Guo, 2009). Recently, the crystal

structures of apo-PhuT and holo-PhuT have been solved (Ho et al, 2007). PhuT belongs to Class III periplasmic binding proteins (PBPs) which are featured by a long, rigid α -helix joining two topologically similar globular domains (Borths et al, 2002; Karpowich et al, 2003; Quioco and Ledvina et al, 1996). Members of this group with available crystal structures include BtuF (Borths et al, 2002; Karpowich et al, 2003) and FhuD (Clarke et al, 2000; Clarke et al, 2002), two *E. coli* periplasmic binding proteins that binds vitamin B12 and hydroxamate-type siderophores, respectively. Proteins of this group only show minor conformational changes upon ligand binding. For example, BtuF shows only 1Å shrinking of the B12 binding pocket upon B12 binding (Borths et al, 2002; Karpowich et al, 2003). Another periplasmic heme binding protein, ShuT from *Shigella dysenteriae*, also has its crystal structure available at the same time as PhuT (Ho et al, 2007). The overall structures of PhuT and ShuT are quite similar, although the detailed architectures of the heme binding pockets in PhuT and ShuT are quite different (Ho et al, 2007). For both proteins, heme binds in a narrow cleft between the N- and C-terminal binding domains (Ho et al, 2007). It has been proposed that heme binding to PhuT/ShuT may only induce a minor conformational change in the heme binding pocket (Ho et al, 2007). The crystal structures of PhuT, BtuF and FhuD are shown in Figure 1.2. Once in the periplasm, the periplasmic heme binding protein shuttles heme between inner and outer membranes. Heme transport across the inner membrane involves an inner membrane permease and an ATPase on the cytoplasmic side. It is proposed that heme binding to its PBPs induces conformational changes in the PBPs, allowing interaction between PBPs and the IM permease. Heme is then delivered to the IM permease and transported across the IM at the expenditure of ATP (Tong and Guo, 2009).

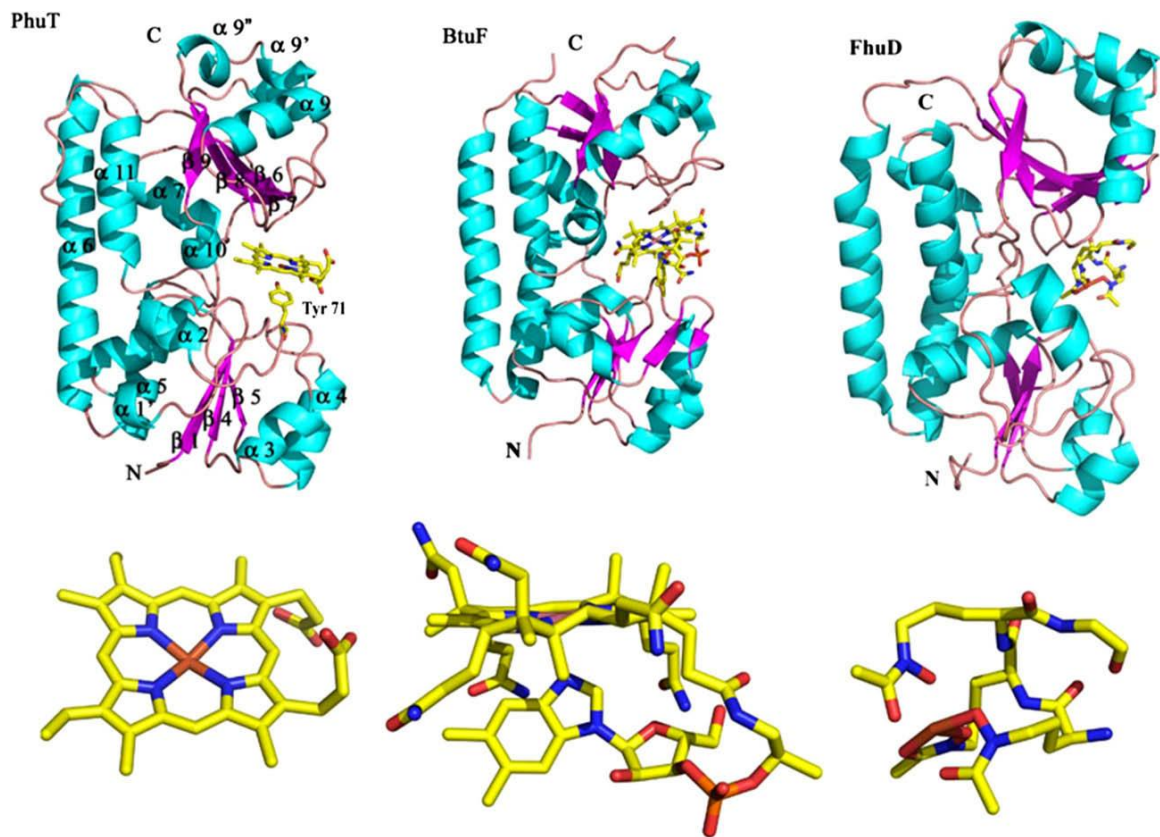


Figure 1.2 Structure of PhuT compared with BtuF and FhuD (adapted from: Tong and Guo, 2009)

The major elements of the secondary structure according to the BtuF structure are shown on the PhuT structure. The ligands for each protein are also shown right below.

1.2.2 Heme uptake in Gram-positive bacteria

1.2.2.1 Protein sorting to the cell wall in Gram-positive bacteria

Gram-positive bacteria have no OM. Instead, they have a quite thick cell wall composed of the murein sacculus and the attached polysaccharides, teichoic acids, and cell wall

proteins (Navarre and Schneewind, 1999). The cell wall of Gram-positive bacteria lies at the interface of the interaction between the bacterial cell and its external environment. It is thus of unique importance for Gram-positive bacteria. Through the cell wall, Gram-positive bacterial cells sense and respond to changes of their environment, and also exchange substances with their environment. All these must rely on cell wall proteins. This raised a series of interesting questions related to these cell wall proteins: How are they anchored? Where are they localized--exposed on the surface or buried inside the cell wall? What are the factors that determine their final destinations? Over the past decades, significant progress has been made to answer these questions. Several different mechanisms have been identified, including sortase-mediated covalent linking, binding to choline containing teichoic acids and binding to lipoteichoic acids (Ton-That et al, 2004). A brief review about sortase-mediated anchoring mechanism is provided as following. Sortase is a membrane-anchored transpeptidase (Marraffini et al, 2006). Many surface proteins, including some virulence factors, proteins involved in iron uptake, and the protein components of pilus, are anchored to the cell wall by sortases (Marraffini et al, 2006). Sortase-anchored surface proteins typically contain an N-terminal signal peptide and a C-terminal sorting signal. The C-terminal sorting signal consists of a short pentapeptide motif, typically LPXTG, followed by a hydrophobic domain and a positively charged tail (Schneewind et al, 1992). Two sortases, SrtA and SrtB have been reported to be involved in iron uptake in *Staphylococcus aureus* (Mazmanian et al, 2003). Three residues in SrtA, His (120), Cys (184), and Arg (197), are absolutely conserved in sortase enzymes from Gram-positive bacteria (Zong et al, 2004). The anchoring reaction with SrtA starts with a nucleophilic attack of Cys (184) on the peptide bond between T

and G of the pentapeptide motif, LPXTG, giving rise to a thioester-linked acyl intermediate. This was followed by a second nucleophilic attack on the thioester bond performed by the amino group of the pentaglycine cross bridge of the cell wall. The enzyme is then regenerated and the surface protein is attached to the cell wall (Huang et al, 2003; Ton-That et al, 2000). On the other hand, SrtB, the other sortase involved in iron uptake in *S. aureus*, recognizes the sequence motif NPQTN and anchors IsdC, a heme-binding protein, to the cell wall (Mazmanian et al, 2001, 2002). The catalytic mechanisms of SrtA and SrtB are quite similar (Marraffini 2006). Both the two sortases have also been identified in *Listeria monocytogenes* (Bierne et al, 2002a, 2002b, 2004; Newton et al, 2005), a Gram-positive bacterium that is the subject of this study. *L. monocytogenes* internalin A (InIA), a known surface virulence factor, carries a LPXTG motif and is the substrate of SrtA (Bierne et al, 2002a). Two proteins encoded by the *srtB* genetic locus of *L. monocytogenes*, Lmo2185 and Lmo2186, contain an NKVTN and an NAKTN motif, respectively (Newton et al, 2005). Both of them have been reported to be anchored to the cell wall by SrtB (Bierne et al, 2004; Pucciarelli et al, 2005).

1.2.2.2 Heme uptake by *S. aureus* through Isd system

While extensive studies have been carried out about heme transport in Gram-negative bacteria, only until recent ten years this research has been emerging in Gram-positive bacteria. Heme uptake systems have been reported in Gram-positive bacteria *Corynebacterium diphtheriae* (Burkhard and Wilks, 2008), *Streptococcus pyogenes*, group A streptococcus (GAS) (Bates et al, 2003; Lei et al, 2002; Lei et al, 2003) and *S. aureus* (Mazmanian et al, 2003; Skaar et al, 2004a). Relatively extensive studies have been conducted in *S. aureus*. The *isd* (iron-regulated surface determinant) locus in *S.*

aureus was identified to be involved in heme uptake (Mazmanian et al, 2003). This locus contains 8 genes (Figure 1.3) and all of them have been reported to be involved in heme iron source acquisition (Mazmanian et al, 2003; Marraffini et al, 2006). Except SrtB, all of them bound heme. Three proteins (IsdA, IsdB and IsdC) were tested to see if they bind human Hb, only IsdB bound. While IsdA, IsdB and IsdH contain LPXTG sorting signals and are anchored to the cell wall by sortase A, IsdC contain NPQTN sorting signal and is anchored to the cell wall by sortase B. Proteinase K susceptibility assay suggested that IsdB and IsdH were completely surface-exposed, IsdA partially exposed and IsdC completely buried in the cell wall. IsdEF is a CM ABC transporter consisting of a putative lipoprotein IsdE and a permease IsdF. IsdD is thought to be inserted into the CM. Once inside cytoplasm, heme may be degraded by IsdG or IsdI, the heme oxygenases (Figure 1.3; Skaar et al, 2004b). Alternatively, heme may be directly incorporated into the respiratory proteins of the bacterial membrane as an enzyme cofactor (Skaar et al, 2004a) or may be pumped out of the cell if the heme concentration is too high (Friedman et al, 2006). Two genes located outside *isd* locus, *isdH* and *isdI*, encode two other proteins of the Isd system. IsdH was reported to bind haptoglobin and haptoglobin-hemoglobin (Dryla et al, 2003). A group led by Dr. Skaar at Vanderbilt University also reported that IsdB, but not IsdA or IsdH, binds hemoglobin on the bacterial surface and removes heme from hemoglobin (Torres et al, 2006). Recently they also reported that IsdA and IsdB were localized to discrete regions within the cell wall and the distribution of both IsdA and IsdB are iron-regulated (Pishchany et al, 2009). They also observed that IsdA and IsdB physically interact with each other as evidenced by the colocalization of IsdA and IsdB on the cell surface. Using electrospray ionization

mass spectrometry (ESI-MS) and magnetic circular dichroism (MCD), a recent report demonstrated that heme transfer occurred in a unidirectional pathway: either from IsdB to IsdA to IsdC then to IsdE or from IsdH to IsdA to IsdC then to IsdE (Muryoi et al, 2008). Specific protein-protein interactions were proposed for the transfer to occur. They also found that Heme can transfer bidirectionally between IsdH and IsdB. Another group led by Dr Lei at Montana State University also showed direct heme transfer from IsdA to IsdC through the formation of holo-IsdA-apo-IsdC complex, using stopped-flow spectrophotometer. This transfer is driven by the higher affinity of IsdC for heme (Liu et al, 2008). In another report, they further showed that IsdB directly capture hemin from metHb, suggesting formation of the complex metHb-apo-IsdB (Zhu et al, 2008). Hemin is then transferred either directly or through IsdA to IsdC, then to IsdE. These findings support a hypothesis that the locations of the Isd proteins in the cell envelope define the pathway of heme uptake (Figure 1.3; Grigg et al, 2010). The passage of heme across the cytoplasm membrane has been proposed to be mediated by IsdF, a putative CM permease (Figure 1.3; Mazmanian et al, 2003). The role of IsdD is still not clear.

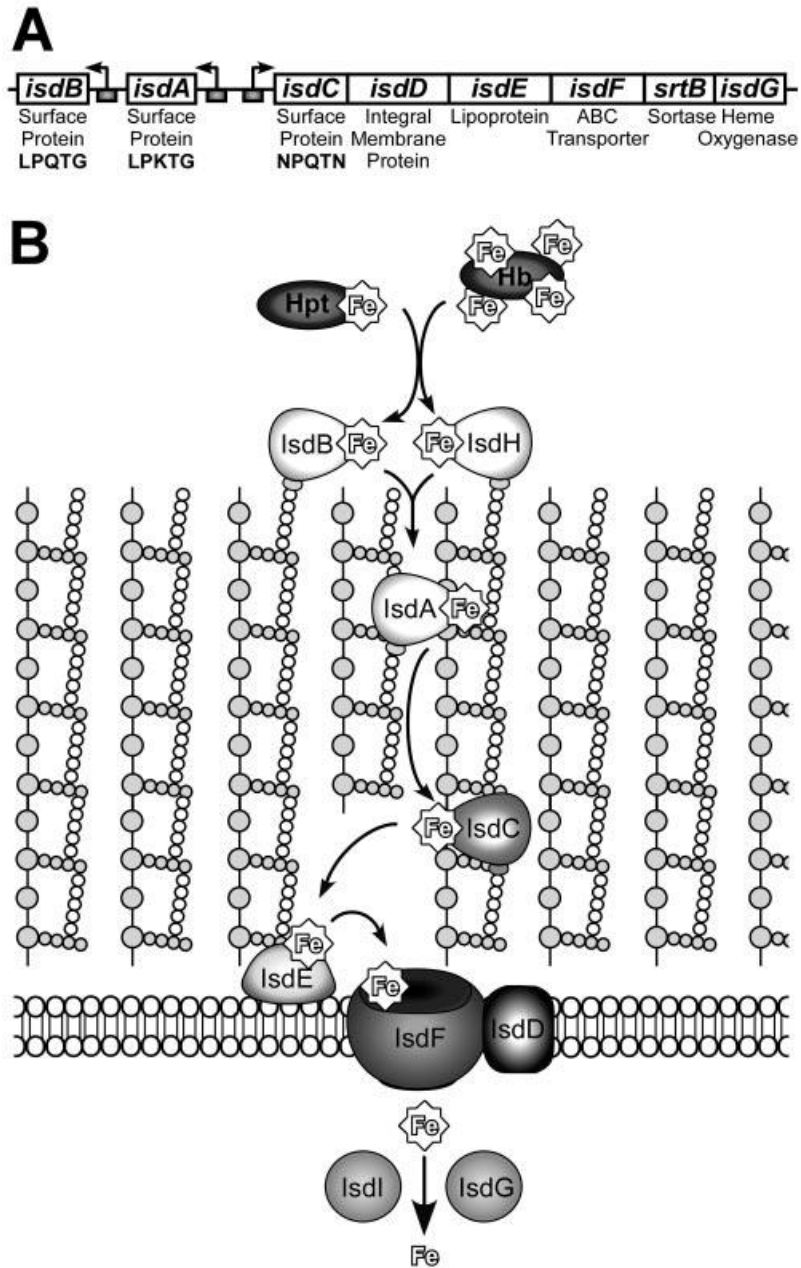


Figure 1.3 Isd-mediated heme uptake in *S. aureus* (adapted from: Marraffini et al, 2006)

A. The *isd* locus. B. A model for Isd-mediated heme uptake across the cell wall of *S. aureus*. IsdA, IsdB, and IsdH function as receptors for hemoprotein ligands, including haptoglobin (Hpt), hemoglobin (Hb), or heme. Upon binding to Isd receptors, heme is released from the hemoproteins by an unknown mechanism and passed through the cell

wall in an IsdC-dependent manner. The heme molecule is then transported through the membrane transport system composed of IsdDEF into the cytoplasm. Upon entry into the cytoplasm, heme is degraded by IsdG and IsdI heme monooxygenases. This leads to the release of free iron for use by the bacterium as a nutrient source (Marraffini et al, 2006).

1.2.2.3 Crystal structures of Isd proteins

4 proteins of the Isd system, IsdA, IsdB, IsdC and IsdH, are anchored to the cell wall. Each of them contains one to three copies of a conserved domain: NEAT (near iron transport) domain (Figure 1.4; Grigg et al, 2010). The domain acquired its name because the proteins featured by this domain are normally near putative ABC transporters of iron in Gram-positive bacteria, including *Staphylococcus*, *Listeria*, *Streptococcus*, *Bacillus*, and *Clostridium* species (Andrade et al, 2002).

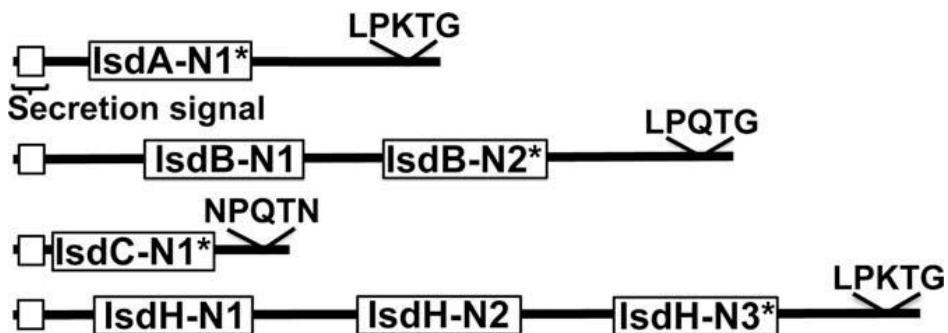


Figure 1.4 Schematic representation of Isd surface proteins (adapted from: Grigg et al, 2010)

NEAT domains are indicated as IsdX-Ny, where “X” indicates the unique protein designation, N indicates the NEAT domain and “y” indicates the order of the NEAT domain numbered from the N-terminus of the protein (Andrade et al, 2002).

Structures of several NEAT domains in the Isd system have been reported, including apo (1.6 Å) and heme-bound IsdA-N1(1.9Å) (Grigg et al, 2007a), the heme-bound IsdC-N1(1.5Å) (Sharp et al, 2007), apo and Zn²⁺-protoporphyrin IX IsdC-N1(Villareal et al, 2008) , apo IsdH-N1, apo and heme-bound IsdH-N3 (Pilpa et al, 2006; Watanabe et al, 2008). All of these NEAT domains have a similar eight-stranded immunoglobulin-like β -sandwich fold and are well superimposed. Heme is bound in the hydrophobic pockets of the NEAT domains through conserved contacts.

The crystal structure of the soluble portion of the lipoprotein IsdE in complex with heme has been reported (Grigg et al, 2007b). This structure reveals a bi-lobed topology formed by an N- and C-terminal domain bridged by a single α -helix, typical of Class III periplasmic binding protein family. Heme is bound to IsdE in a large groove of the domain interface. It has been demonstrated that there was minor conformational change between the heme-bound and heme-free IsdE (Pluym et al, 2007).

The crystal structures of IsdG and IsdI are also available (Wu et al, 2005). Both IsdG and IsdI exist as homodimers. Their structures exhibit a ferredoxin-like $\alpha+\beta$ sandwich fold and a β -barrel is formed at the dimer interface, representing the emerging of a new family of heme oxygenase different from HmuO, the first identified bacterial heme-degrading enzyme from *C. diphtheria* (Schmitt, 1997). In contrast to IsdG/IsdI, HmuO exists as a monomer and adopts a predominantly α -helical fold (Unno et al, 2004). This structure is similar to vertebrate heme oxygenase (HO) (Schuller et al, 1999). While HO-like enzymes have been identified in both Gram-positive and Gram-negative bacteria, IsdG-like enzymes have been exclusively identified in Gram-positive bacteria. Besides the structural difference between IsdG/IsdI and HO-like enzymes, their catalytic mechanisms

and degradation products are also different. For more information about heme oxygenase, please refer to (Grigg et al, 2010; Reniere et al, 2007; Wu et al, 2005; Lee et al, 2008; Unno et al, 2007).

1.2.2.4 The Hts system is the primary membrane heme uptake system in *S.aureus*

Although the Isd system is the first system identified in *S.aureus* to be involved in Hn/Hb uptake, it has been reported not to be the primary system. Using the technique of Inductively Coupled Plasma Mass Spectrometry (ICP-MS), Skaar et al reported that *S.aureus* exhibited iron source preference for heme iron and identified a new heme uptake system, Hts (heme transport system) system, responsible for this heme iron preference and as the primary membrane heme uptake system (Skaar et al, 2004b). However, the Hts system has been less well studied. It consists of a putative lipoprotein (HtsA) and two putative membrane permeases (HtsB and HtsC). Sequence analysis revealed that HtsB and HtsC closely resemble HemU and HmuU, the permease components of the heme transport systems in *Yersinia enterocolitica* (Stojiljkovic and Hantke, 1994) and *Corynebacterium diphtheriae* (Drazek et al, 2000), respectively. A canonical Fur box is immediately preceding HtsA.

1.3 Heme toxicity and its detoxification

Although heme is an essential element to almost all organisms and serves as a valuable iron source for microorganisms, heme is also highly toxic. Heme is a hydrophobic molecule with a molecular weight around 620 Da, rendering it capable of intercalating into membranes. This finally leads to damage of lipid bilayers and organelles (Ryter and

Tyrrell, 2000). Heme also catalyzes the Fenton reaction, generating highly reactive oxygen species which cause damage to proteins, lipids, nucleic acids (Everse and Hsia, 1997). As a way of protection against heme toxicity, in vertebrates, most of the free heme or hemoglobin released into the plasma upon hemolysis are immediately complexed either by hemopexin, a 60-kDa plasma glycoprotein which binds heme with a high affinity ($K_d \sim 10^{-12} \text{M}$) (Zunszain et al, 2003), or by serum albumin, the most abundant plasma protein with a lower affinity ($K_d \sim 10^{-8} \text{M}$) for heme compared to hemopexin (Zunszain et al, 2003), or by haptoglobin, a serum glycoprotein which binds hemoglobin with high affinity ($K_d \sim 10^{-12} \text{M}$) (Wejman et al, 1984). Then they are transported to the liver, decomposed and removed. In bacteria, several ways to fight against heme toxicity at high concentration have been reported. Generally, there are three possible ways to deal with heme toxicity intracellularly: store it, degrade it, or export it. Degradation of heme with heme oxygenase has been described previously in this chapter. Storage of heme with heme storage proteins has not been unambiguously identified. It was reported that HmuS in *Y. pestis* (Thompson et al, 1999; Wyckoff et al, 1998) or HutZ in *Vibrio cholerae* (Wyckoff et al, 2004) may function as heme storage proteins. However, further survey is needed to support that speculation. Recently a heme-regulated transport (Hrt) system has been identified in *S. aureus* (Friedman et al, 2006). Current data strongly suggest that this system functions as a heme exporter (Friedman et al, 2006; Torres et al, 2007; Stauff et al, 2007; Stauff et al, 2008).

The Hrt system consists of a putative ATPase HrtA and a putative membrane permease HrtB. Exposure of *S. aureus* to 10 μM hemin increased the expression of HrtA 45-fold. Moreover, growth of either $\Delta hrtA$ or $\Delta hrtB$ with 10 μM hemin as the sole iron source was

severely inhibited. Interestingly, the Hrt system is neither iron- nor Fur-regulated. Instead, its expression is controlled by the heme sensor system (Hss) which responds to heme exposure (Torres et al, 2007). Hss is a two component system composed of HssR (Hss regulator) and HssS (Hss sensor, a histidine kinase). Inactivation of either HssR or HssS also severely impaired the growth of *S.aureus* with 10 uM hemin as the sole iron source. Furthermore, transcription of *hrtA* in the mutant strain $\Delta hssR$ upon hemin exposure was not detectable while providing a wild-type copy of *hssR* in *trans* restored *hrtA* transcription. Genomic analyses revealed that Hrt and Hss systems are highly conserved across Gram-positive bacteria, including *Staphylococcus epidermidis*, *Bacillus anthracis*, *Listeria monocytogenes*, and *Enterococcus faecalis*. A direct repeat DNA sequence within the *hrtAB* promoter essential for heme-induced, HssRS-dependent transcription of *hrtAB* has been identified (Stauff et al, 2007). Signaling between HssS and HssR is necessary for the regulated expression of *hrtAB*. Upon exposure of exogenous heme, HssS undergoes autophosphorylation and then phosphorylates HssR. Phosphorylated HssR binds the direct repeat DNA sequence, resulting in the activation of expression of *hrtAB*. This direct DNA repeat sequence is also conserved across Gram-positive bacteria, including *Staphylococcus epidermidis*, *Bacillus anthracis*, *Bacillus cereus*, *L.monocytogenes*. Studies about the Hss and Hrt systems have been further extended by a recent report which demonstrated the ATPase activity of HrtA (Stauff et al, 2008).

1.4 Iron and Heme uptake regulation in bacteria

As discussed previously, heme is a valuable nutrient with high toxicity for bacteria. Regulation of heme uptake by bacteria is thus necessary for bacterial cell metabolism. In bacteria, a common way to regulate iron/heme uptake is to modulate the function of the protein Fur (ferric iron uptake regulator), a global iron uptake regulator. The Fur protein was identified 30 years ago as a repressor of iron-regulated genes in *Salmonella typhi* and *E.coli* (Ernst et al, 1978; Hantke, 1981). It is a homodimer consisting of a N-terminal DNA binding domain and a C-terminal dimerization domain (Pohl et al, 2003). The function of Fur as the repressor of the expression of iron-regulated genes needs ferrous iron as a corepressor (Lavrrar et al, 2002). Under iron rich conditions, Fur is iron-loaded and capable of binding the Fur box, a well-conserved 19-bp DNA sequence (GATAATGATAATCATTATC) characteristic of iron-regulated genes (Stojiljkovic et al, 1994). The transcription of these genes is then inhibited by the binding of Fur to the Fur box. It was proposed that two Fur dimers bind at each Fur box on opposite faces of the DNA helix (Lavrrar et al, 2002). Under iron-starved conditions, Fur is free of iron and incapable of binding Fur box. RNA polymerase then gains access to the promoter region and transcription happens.

Another repressor of iron/heme uptake genes, DtxR (diphtheria toxin repressor), was first identified in a Gram-positive bacterium *Corynebacterium diphtheria* (Schmitt et al, 1991) and later was found in both Gram-positive and Gram-negative bacteria (Hill et al, 1998; Brett et al, 2008). Despite little sequence homology, DtxR and Fur proteins show substantial structural similarities (Schiering et al, 1995;Pohl et al, 2003). Like Fur, DtxR

is also a homodimer and behaves similarly to Fur: it binds or dissociates from the DtxR box (also an AT-rich 19 bp sequence), depending on the availability of ferrous iron in the cytoplasm (Wandersman and Delepelaire, 2004).

As a global iron uptake regulator, Fur is capable of controlling the transcription of those genes involved in iron uptake not only directly (as described above) but also indirectly, through extra cytoplasmic function (ECF) sigma factors or through other factors.

Because iron is an essential nutrient for most bacteria, they have different iron uptake systems corresponding to different iron sources. Certainly, it is a huge waste of material and energy to turn on all those systems in response to iron limitation irrespective of the nature of the iron source available. Indeed, many systems are positively regulated by their cognate iron source via a variety of regulatory mechanisms.

A well studied way is to employ ECF sigma factors. Iron-responsive ECF sigma factors are highly conserved and form a distinct branch in the ECF sigma factor subfamily (Braun et al, 2003). Most ECF sigma factors are found associated with membrane-bound antisigma factors.

A classical example of ECF sigma regulation of iron uptake is the *E.coli* ferric citrate uptake system (Braun et al, 2003). Transcription of the *fecABCDE* genes, which encode the ferric citrate transport system in *E.coli*, is positively regulated by FecIR whose encoding genes are located upstream of *fecABCDE*. A well conserved Fur box is present in the promoters of both the *fecIR* transcriptional unit and the *fecABCDE* transcriptional unit, enabling iron-loaded Fur to turn off their transcription when intracellular iron is abundant. Under iron strict conditions, however, transcription of *fecABCDE* doesn't necessarily happen, unless ferric citrate is present extracellularly. Iron starvation

derepresses the expression of FecIR, the iron-starvation ECF sigma factor (FecI) and anti-sigma factor (FecR). The binding of extracellular ferric citrate to its OM receptor, FecA, induces conformational changes in FecA. This leads to interaction between the N-terminal extension of FecA and C-terminal extension of FecR, the IM-localized anti-sigma factor. As a result, FecI dissociates from FecR and binds to the core RNA polymerase. Transcription of the *fecABCDE* then occurs.

Similar regulation systems exist for heme uptake. In *Bordetella pertussis* and *Bordetella bronchiseptica*, the heme acquisition system and their corresponding regulation systems are encoded by the *bhuRSTUV* and *hurIR* loci, respectively (Brickman et al, 2007). Similar to the *fec* system described above, the transcription of the *bhu locus* is regulated by Fur, the ECF sigma factor (HurI), anti-sigma factor (HurR), the OM receptor (BhuR) of the Bhu system and heme. While transcription of *hurIR* is iron-regulated and heme-independent, expression of *bhuRSTUV* requires both iron shortage and the presence of heme.

1.5 *Listeria monocytogenes*

Listeria monocytogenes is a rod-shaped Gram-positive bacterium. It was first described by Murray et al in 1926 based on six cases of sudden death in young rabbits (Murray et al, 1926). *L. monocytogenes* has a very broad host range and is widely distributed in nature (Gray and Killinger, 1966). It has been found in at least 37 mammals, 17 fowls, ticks, fish, fly, crustaceans. It inhabits stream water, mud, sewage, raw milk, cheeses, raw vegetables. It is able to grow at 4°C. The best pH for its growth is neutral to slightly

alkaline but it still grows at pH as high as 9.6. At pH lower than 5.6, it dies (Gray and Killinger, 1966). All these together make *L. monocytogenes* one of the leading causes of many foodborne diseases. When grown at or below 30°C, *L. monocytogenes* synthesizes flagella responsible for its motility (Gray and Killinger, 1966). At 37°C, basically no flagellum is produced. However, *L. monocytogenes* moves within eukaryotic cells by polymerization of host cell's actin filaments (Lambrechts et al, 2008).

L. monocytogenes causes many serious diseases. Listeriosis, a serious infection caused by eating food contaminated with the bacteria, has recently been recognized as an important public health problem in the United States. Up to 30 percent of the patients diagnosed with listeriosis finally die (Ramaswamy et al, 2007). The occurrence of listeriosis is especially high with newborns, pregnant women, immunocompromised people or elders (McLauchlin, 1990). Every year, in USA there are approximately 2500 illnesses and 500 deaths caused by *L. monocytogenes* (Dharmarha, 2008). This high mortality rate of listeriosis is largely because the infection often leads to neurological damage. The two main clinical manifestations of listeriosis are sepsis and meningitis.

L. monocytogenes is an intracellular pathogen. It proliferates in many types of mammalian cells, including macrophages and epithelial cells. The ability of *Listria* to evade attacks by its host immune system is a determinant of its pathogenicity. The life cycle of *L. monocytogenes* consists of three stages: adherence and entrance into the cell, escape from a vacuole, and cell to cell spread (Cossart, 2002; Kreft et al, 2002). The bacterium can invade a cell either by phagocytosis or by active invasion. It then escapes from a host vacuole, enters the cytoplasm and begins to grow rapidly. During the third stage, it utilizes host actin to move to the surface of the host cell, where a bacteria

containing protrusion forms and is engulfed by adjacent cells, including non-professional phagocytes (Mounier et al, 1990; Tilney et al, 1989). Then the bacterium escapes from the double membrane vacuole of the secondary cell and enters the cytoplasm again. By such a mechanism, direct cell-to-cell spread of *Listeria* in an infected tissue may occur without an extracellular stage.

The entry of *L. monocytogenes* into nonphagocytic cells requires two major virulence factors, internalin A (InlA) and internalin B (InlB) (Vazquez-Boland et al, 2001). InlA and InlB recognize their host cell receptors to promote the entry of *L. monocytogenes* into cells (Bergmann et al, 2002; Dramsi et al, 1995; Bierne and Cossart, 2002). Once inside the cells, *L. monocytogenes* becomes trapped in phagosomes which are acidified by proton pumps. At acidic pH listeriolysin O (LLO) (Portnoy et al, 2002), a hemolytic exotoxin and a phosphatidyl-inositol phospholipase C (PI-PLC) (Marques et al, 1989) together disrupt the phagosomal membrane and release the bacteria. A membrane-anchored protein, ActA, promotes the polymerization of host actin on the bacterial surface (Mounier et al, 1990; Tilney et al, 1989; Lambrechts et al, 2008). The bacteria then multiply and the growing actin sheet drives the bacteria across the cytoplasm until they finally reach the surface of the host cell.

1.6 Iron transport systems in *Listeria monocytogenes* and their relevance to virulence

Iron is an essential nutrient for the growth of pathogenic bacteria. Over past decades, the correlation between bacterial iron uptake and bacterial virulence has been well

established (Cornelissen and Sparling, 1994; Furman et al, 1994; Bearden et al, 1998; Pradel et al, 2000; Mazmanian et al, 2003; Stork et al, 2004; Skaar et al, 2004b; Braun, 2005). The complete genome of *L. monocytogenes* has been available since 2001 (Glaser et al, 2001). Four loci in the genome, the *fur-fhu* region at 2.031 Mb, the *feo* region at 2.184 Mb, the *srtB* region at 2.27 Mb and the *hup* region at 2.499 Mb, contain well-conserved Fur boxes (Figure 1.5; Jin et al, 2006). The *srtB* locus was reported to be iron-regulated and is similar to the *isd* locus in *S. aureus* (Newton et al, 2005). The *hup* locus and *fur-fhu* locus have been reported to be involved in iron uptake from Hn/Hb and ferric hydroxamates, respectively (Jin et al, 2006). The *feo* locus is potentially involved in ferrous iron uptake. Deletion of a gene in *hup* locus, *lmo2429*, decreased the virulence of *L. monocytogenes* 50-fold in mice. On the other hand, deletions in the *srtB* locus ($\Delta lmo2185$, $\Delta lmo2186$ and $\Delta srtB$), the *fhu* locus ($\Delta lmo1959$, $\Delta lmo1960$) and the *feo* locus ($\Delta lmo2105$) displayed no impairment of their virulence in mice (Newton et al, 2005; Jin et al, 2006).

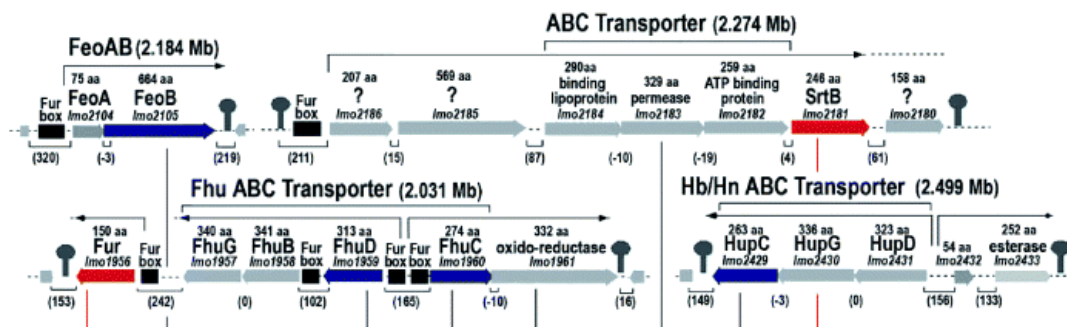


Figure 1.5 Putative and demonstrated iron transport loci in the genome of *L. monocytogenes* (adapted from: Jin et al, 2006)

1.7 Significance of this research

Listeria monocytogenes is an intracellular pathogen. Listeriosis, a serious infection caused by eating food contaminated with *L. monocytogenes*, has recently been recognized as an important public health problem in the United States. *L. monocytogenes* multiplies in a variety of mammalian cells and spreads from cell to cell. This suggests the bacterium readily acquires iron in the intracellular environment. Since the majority of intracellular iron source is heme iron, understanding the mechanism of heme utilization in *L. monocytogenes* is of great importance in both preventive and therapeutic aspects. During the past ten years, significant advances have been made to understand heme utilization in *S. aureus*, an important Gram-positive human pathogen and a close species of *L. monocytogenes*. Those studies are very suggestive to the understanding of heme utilization in *L. monocytogenes*. However, the research about heme utilization in *L. monocytogenes* is still indispensable, especially due to their fundamentally different pathogenic life cycle: intracellularly for *L. monocytogenes* and extracellularly for *S. aureus*. The overall goal of this research is to elucidate the mechanism of Hn/Hb transport in *L. monocytogenes*. The results will provide information about bacterial interactions with eukaryotic heme-containing proteins and define the mechanism for protein-mediated heme uptake through the listerial cell envelope. Lastly, the biochemical characterization of heme transporters in *L. monocytogenes* will provide a basis for comparison of their mechanisms, efficiencies, and specificities to that of other transport systems in Gram-positive and Gram-negative bacteria.

1.8 TonB in *E.coli*

As discussed previously, TonB or TonB-like proteins are essential for many iron transport systems in Gram-negative bacteria, potentially providing energy required for active iron transport across the outer membrane. In *E.coli*, two cytoplasmic proteins, ExbB and ExbD, form a complex with TonB (Letain et al, 1997). The TonB protein of *E.coli* consists of 239 amino acid residues. It is anchored to the inner membrane through its N-terminal domain with the bulk of the protein extending into the periplasm (Ködding et al, 2005; Chang et al, 2001). Four highly conserved residues of the N-terminal anchor domain, the so-called “SHLS motif”, was found to be essential for the interaction with ExbB (Larsen and Postle, 2001). The C-terminal domain of TonB may directly contact TonB-dependent receptors in the OM (Heller et al, 1988; Gunter and Braun, 1990). In between the 2 domains is an intermediate domain with high proline content. Both the intermediate domain and the C-terminal domain contain ~100 residues. Currently the exact roles of TonB, ExbB and ExbD are still unknown. It was proposed that ExbB and ExbD may function as proton translocators and TonB as an energy transducer.

Although much progress has been made during past decades, it still remains quite elusive about how TonB interacts with the TonB-dependent OM receptor. It has been reported that binding of ferrichrome to FhuA causes significant structural change in the region immediately C-terminal to the TonB box of FhuA from a helix packed against the β -barrel to an extended conformation, presumably making the TonB box available for interaction with TonB (Locher et al, 1998). It was proposed that TonB senses occupied OM receptor through its TonB box. This signaling cascade causes ExbB and ExbD

harvest the energy of proton motive force and promotes transfer of TonB from an unenergized form to energized form. TonB then transduces its stored energy to the OM receptors which then creates a channel for its cognate ligand to pass through. Currently there are two popular models for TonB-dependent energy transduction: the propeller model (Chang et al, 2001) and the shuttle model (Postle and Kadner, 2003). The propeller model was based on the crystal structure of the C-terminal domain of TonB (residues 164-239) which shows that this region forms a $\beta\beta\alpha\beta$ motif and dimerizes (Chang et al, 2001). According to this model, the TonB N-terminus remains associated with the IM at all times. It was proposed that the proton motive force might cause a torsional motion which could be transduced to the TonB C-terminal domain through its central proline-rich domain. TonB C-terminus thus could interact with the OM receptors and promote internalization of the substrates of the OM receptors. The shuttle model, on the other hand, hypothesizes that TonB shuttles between the IM and OM, switching between an unenergized conformation and an energized conformation. ExbB/D harvests the energy of the IM proton motive force and uses it to convert TonB from an unenergized conformation to an energized conformation. Energized TonB then dissociates from the IM. When the OM receptors bind their cognate substrates, energized TonB associates with the OM receptors to provide energy required for internalization of substrates. For both models, once substrate is transported across the OM, TonB dissociates from the OM receptors and reassociates with ExbB and ExbD.

Both the two models proposed for the action of TonB are still developing. A lot of related questions need to be addressed. For example, for the propeller model, how TonB/ExbB/ExbD harnesses the proton motive force? How the torsional motion is

propagated among TonB, ExbB, ExbD? Does the TonB/ExbB/ExbD complex keep rotating or only rotate when it senses the occupancy of the OM receptors by their cognate substrates? For the shuttle model, it was proposed based on the observation that TonB associated exclusively with the OM when both ExbB/ExbD and TolQ/TolR were absent (Letain and Postle, 1997). Then here comes a few questions: Is the TonB associated with the OM in an energized conformation? What is the energized conformation? Where does the energy come from? Undoubtedly, both models need lots of experimental data to address these questions. Based on structural homology between the TonB C-terminus and *E. coli* LysM (a lysin motif that confers affinity for peptidoglycan), Dr. Klebba proposed that TonB binds peptidoglycan. My experiments confirmed this idea: while purified peptidoglycan precipitated MalE-TonB69C, it did not precipitate MalE or FepB. Thus the affinity of TonB for peptidoglycan was not a general characteristic of periplasmic proteins, but a specific attribute of TonB itself. This result provides new perspective for understanding the mechanism of how TonB interacts with the outer membrane receptors and a membrane surveillance model of action was proposed (Kaserer et al, 2008).

Chapter 2 Materials and Methods

2.1 Bacteria strains and plasmids

All *E. coli* strains used in this study were *E. coli* k-12 derivatives. DH5 α and XL-1 Blue were used as hosts for plasmids. BL21 were used for protein expression. SM10 was used in the complementation of $\Delta hupD$ as a donor strain of pPL2. AN102 was used for purification of enterobactin. All listerial strains used in this study were *Listeria monocytogenes* EGD-e derivatives.

Table 2.1 Bacterial strains and plasmids used in this study

Strains, plasmids	Genotype and characterization	Source or reference
<i>E. coli</i>		
DH5 α	<i>supE44 ΔlacU169(Φ80lacZ ΔM15) hsdR17 recA1 endA1 gyra96 thi-1 relA1</i>	(Hanahan, 1983)
XL-1 Blue	<i>recA1 endA1 gyrA96 thi-1 hsdR17 supE44 relA1 lac</i>	Stratagene
BL21	<i>F dcm ompT hsdS(rB⁻ mB³) gal</i>	Stratagene
SM10	<i>F thi-1 thr-1 leuB6 recA tonA21 lacY1 supE44 (MuC⁺) λ Km^r Tra⁺</i>	(Lauer et al, 2002)
AN102	<i>thi trp fep proC leu tonA</i>	(Yeowell and White, 1982)
<i>L. monocytogenes</i>		
EGD-e	wild type	(Bierne et al, 2004)
Plasmids		
pKSV7	<i>E. coli-L. monocytogenes</i> shuttle vector	(Smith and Youngman, 1992)
pPL2	site-specific integration shuttle vector	(Lauer et al, 2002)
pET28a(+)	His-tag protein fusion vector	Novagen
pMAD	<i>E. coli-L. monocytogenes</i> shuttle vector	(Arnaud et al, 2004)
pKSV7 Δ hupD	encoding <i>hupD</i> deletion in <i>L. monocytogenes</i>	This study
pKSV7 Δ hupCDG	encoding <i>hupC</i> , <i>hupD</i> , <i>hupG</i> deletions in <i>L. monocytogenes</i>	This study
pKSV7 Δ 1960	encoding <i>lmo1960</i> deletion in <i>L. monocytogenes</i>	(Jin et al, 2006)

2.2 Growth media

Luria-Bertani (LB) broth (Difco) and Brain Heart Infusion (BHI) broth were the iron-rich media for regular growing of *E.coli* and *L.monocytogenes*, respectively. T medium was used as iron-deficient medium for purification of enterobactin. KRM medium was used as iron-deficient medium for overexpression of iron-regulated proteins in *Listeria*. Two kinds of MOPS medium were used in this study, one was for growing of *E.coli* and was designated as regular MOPS medium, the other was specifically modified by Dr. Xiaoxu Jiang for growing of *Listeria* and was designated as MOPS-L medium (Jiang's dissertation, 2009).

Table 2.2 Media used in this study

Media	References
Luria-Bertani (LB) Broth	(Miller, 1972)
Brain Heart Infusion (BHI) Broth	Difco
T medium	(Klebba et al 1982)
KRM medium	(Newton et al, 2005)
Regular MOPS medium	(Neidhart et al, 1974)
MOPS-L medium	(Jiang's Ph.D dissertation, 2009)

2.3 Oligonucleotides

Oligonucleotides were purchased from Invitrogen Corporation. Zymoclean™ Gel DNA Recovery Kit was purchased from Zymo Research Corporation. Plasmid purification kits, enzymatic reaction clean kits were purchased from QIAGEN. Taq 2x master mix, restriction enzymes and ligases were purchased from New England Biolabs.

Table 2.3 Primers used in this study

Primer Name Sequence (5'--3')

Primers for construction of $\Delta hupD$

DhupDHind1	TGTAAGCTTATTCGACAAACCGTGAAG
DhupDXho2	GGGGGGCTCGAGTTCATAATTCCCCTCCACAACAC
DhupDXho3	GGGCTCGAGCTAATGACAACCTGTGAAG
DhupDXba4	GGATCTAGACCAACTTCTAGCTGCTG
DhupD Int chk1	CCCGACCGTGAACCATGTTAGAGTAG
DhupD Int chk2	CTAATGCTGATTTTCATGAAGCAACCCTC
DhupDchk1	GACTGGGGGCATCGTTTCTTTGCA
DhupDchk2	CGTAAAGGAGAAACGCCGCGATCCC

Primers for construction of Δhup

DhupDHind1	TGTAAGCTTATTCGACAAACCGTGAAG
DhupDXho2	GGGGGGCTCGAGTTCATAATTCCCCTCCACAACAC
DhupXho3	GGGGGGCTCGAGTTAAAGAAAACAGAAAGAAG
DhupXba4	GGGGGGTCTAGATCCGTTTAAATTGGTACGG

DhupInt1 CCGACCGTGAACCATGTTAGAGTAG
DhupInt2 GCTGCATTCCGTCGCCAAGCGGAT
Dhupchk3 GACTGGGGGCATCGTTTCTTTGCA
Dhupchk5 GCAAGCTTCCAAGCGATCCGATACTAATCC

Primers for check EGD-e strain

LLOchk5 ATGAAAAAATAATGCTAGTTTTT
LLOchk3 ACGGCCATACGCCACACTTGAGAT

Primers for cloning of *hupD* into pET28a

hupDpET5(18) CCCCCGGATCCTCGTGTGGAAATGATACGACAACTG
hupDpET3 CCCCCCTCGAGTTAGTTATCCACCTTATTTATCTCATCTGTC
hupDpET5(20) CCCCCGGATCCGGAAATGATACGACAACTGATATGAAT

Primers for complementation of $\Delta hupD$

Primers for cloning *prohupD* into pKSV7

pKSVprohupD5 CCCCCGGATCCTTTTCATCGCCTCCTTAAGTTAATTATAAAG
pKSVhupD3 CCCCCCTGCAGTTAGTTATCCACCTTATTTATCTCATCTGTC

Primers for cloning *prohupD* into pPL2

prohupDBamH5 CCCCCGGATCCTTTTCATCGCCTCCTTAAGTTAATTATAAAG
hupDPst3 CCCCCCTGCAGTTAGTTATCCACCTTATTTATCTCATCTGTC
prohupDPst5 CCCCCCTGCAGTTTTTCATCGCCTCCTTAAGTTAATTATAAAG
hupDPst5 CCCCCCTGCAGATGAAGAAAATAACTATATTGATGTTAAGT
ATAACAGC
hupDKpn3 CCCCCGGTACCTTAGTTATCCACCTTATTTATCTCATCTGTC

Primers for cloning *prohupD* into pMAD

prohupDBamH5 CCCCCCGGATCCTTTTCATCGCCTCCTTAAGTTAATTATAAAG

hupDNco3 CCCCCCATGGTTAGTTATCCACCTTATTTATCTCATCTGTC

Primers for replacing the natural promoter of the *hup* operon with *clpB* promoter (*pclpB*)

pclpBBamH5 CCCCCCGGATCCGTCTAGTTAATGTGTAAACGTAACATTAGC

pclpBPst3 CCCCCCTGCAGGATCCTTAATTATATTATAGTCCCAAT

***Δlmo0641* check primers**

D0641chk5 CCAGCAAGCTTCCAAACAGTGGTT

D0641chk3 TAGAATTTTTGAACAGTACCAAGGTAAATCG

***Δlmo1960* check primers**

D1960chk5 CCCACAGGCTTCATTCCAAGCAAAC

D1960chk3 CGTACCACTACCTGTAGCAATGACAATTG

D1960Int5 GCGTAAGGAATTAACACAGTTGGCGC

D1960Int3 GCGAATTGTCGAATTTGGGATATG

***Δlmo2183* check primers**

D2183chk5 GATCAGGTGAAGTCGAATGTGG

FerDoCla ACAGCTAGATCATCCTCCTTCG

D2183Int1 GTGATGAGGAAAATGGCTGTCATATC

D2183Int2 CCACTTCATAATTCGTAAAGCCCG

***Δlmo2185* check primers**

D2185Int1 GGAATTTGAAGATGAAAGATTACTACGAG

D2185Int2 TTTCATCCAAATCATACACACGG

D2185Chk5 GGGAAATCAACTGTTAGCTTGCAAGTG

D2185Chk3 GGCTTCAACATCCGAATAATTTCC

Two primers for sequencing pPLprohupD

SeqhupDdir GTGCGTTCATTACTTGTTCTAGGAGC

SeqhupDrev CGACTTTTGGTCCTACCCCTTCC

2.4 Preparation of chromosomal DNA from *Listeria monocytogenes*

strain EGD-e

EGD-e was grown in 25 mL BHI broth overnight. The cells were harvested next morning and were spun down at 8000 g for 12 minutes. The pellet was resuspended in 1 mL ice cold distilled water and the resuspended cells were broken by Fast Prep Bead-beater at intensity of 6.5 for 30 seconds with 3 cycles. In between 2 cycles, the cell suspension was immediately chilled on ice for 30 seconds upon completion of each cycle. After 3 cycles, the resulting mixture was immediately chilled on ice and the unbroken cells were spin down. The supernatant was transferred to a 2 mL eppendorf tube and 5M NaCl was added to it to reach a final concentration of 100mM. 1 volume of buffered-phenol was added to the supernatant and well mixed. The mixture was spun down at 14,000 rpm for 1 minute and the supernatant was transferred to a fresh 2 mL eppendorf tube. The extraction with buffered-phenol was repeated once. The resulting supernatant was then extracted twice with chloroform/isoamyl-alcohol in the same way as with buffered-phenol. 2 volumes of ethanol were added to the supernatant. Precipitated DNA was spun down at 14,000 rpm for 30 minutes and the pellet was washed with 70% ethanol and then resuspended in 100 uL TE buffer with 2 uL RNase (0.5 mg/ml) added. All centrifugations were performed at 4⁰C.

2.5 Preparation of *E.coli* competent cells for electroporation

Cells were inoculated in 5 mL LB broth overnight. In the next morning, 500 mL prewarmed LB broth was inoculated with the 5 mL overnight culture. The cell culture was chilled on ice for 5 minutes when its optical density (OD) at 600 nm reached 0.5. The cell culture was then spun down at 8000 g for 15 minutes. The pellet was gently resuspended with 500 mL ice cold distilled water and the cell resuspension was recentrifuged under the same condition as above. After repeating distilled water suspension and centrifugation one more time, the pellet was resuspended in 100 mL ice cold 10% glycerol and then recentrifuged. The resulting pellet was then resuspended in 2 mL 10% glycerol and the suspension was aliquoted into microtubes with 40 uL for each.

2.6 Preparation of competent cells of *Listeria monocytogenes* for electroporation

Cells were inoculated in 25 mL BHI broth overnight. In the next morning, 500 mL BHI broth was inoculated with 10 mL overnight culture. Penicillin G was added to the culture to 0.12ug/mL when the OD at 600 nm reached 0.3. The cell culture was incubated around 2 more hours until the OD reached 0.8-0.9. Cells were spun down and washed with the buffer of 1 mM hepes/500 mM sucrose, firstly 100 mL, secondly 50 mL, lastly 25 mL with 3 repeats. After the last centrifugation the pellet was resuspended in a mixture of 500 uL 1 mM hepes/500 mM sucrose and 75uL glycerol. The resuspension was then aliquoted into microtubes with 100uL for each.

2.7 Site-directed chromosomal deletions in *L. monocytogenes*

Site-directed chromosomal deletions in *Listeria monocytogenes* EGD-e or its mutant derivatives were generated by *in vivo* recombinations (Newton et al, 2005; Jin et al, 2006). Two DNA fragments, upstream and downstream of the target gene to be deleted, were amplified by PCR using chromosomal DNA of *Listeria* as the template. Appropriate restriction digestion sites were added to both ends of the upstream and downstream DNA fragments. The upstream and downstream DNA fragments were then digested with appropriate restriction enzymes. At the same time, pKSV7, a thermosensitive and integrative *E. coli*-*L. monocytogenes* shuttle vector [pKSV7 (Ap^r, Cm^r), Ap^r stands for ampicillin resistant, Cm^r stands for chloramphenicol resistant] (Smith and Youngman, 1992), was also digested with appropriate restriction enzymes. The three fragments were then ligated together with T4 ligase. The ligations were purified and then electroporated into competent *E. coli* DH5 α cells. The transformants were plated out onto LB plus ampicillin plates which were additionally coated with IPTG and X-gal for blue-white screen. Colony PCR was performed by resuspension of a small portion of a colony into a 30 μ L PCR reaction containing appropriate primers. Colonies that gave positive PCR results were inoculated in LB plus ampicillin broth for purification of vectors. Purified vectors were then checked by PCR, restriction digestion and confirmed by DNA sequencing. A newly-constructed vector which contains a full deletion of the target gene(s) was then transferred into the competent EGD-e or its mutant derivatives. The transformants were grown at 30⁰C. Single colonies were picked and inoculated in BHI plus chloramphenicol broth at a non-permissive temperature (40⁰C) for pKSV7. Homologous recombination

took place because pKSV7 could not replicate by itself at temperatures above 30°C but had to integrate into EGD-e chromosomal DNA to confer resistance to chloramphenicol. After 2 times of inoculation at 40⁰C in BHI plus chloramphenicol broth, the transformants were then inoculated at 37⁰C in BHI broth without chloramphenicol for 8-10 passages. These successive passages in the absence of chloramphenicol allowed the rise of chloramphenicol sensitive derivatives resulting from another homologous recombination. These Cm sensitive derivatives were either the parental strain or the deletion mutant. Mutants were then identified by colony PCR test using two primers localized upstream and downstream of the target gene(s) and further confirmed by DNA sequencing.

2.8 Complementation of $\Delta hupD$

The gene *hupD* was amplified together with its natural promoter by PCR with BamHI and PstI restriction sites at extremities. Both the amplified PCR product and the vector pKSV7 were double-digested by restriction enzymes BamHI and PstI and then were ligated together. The ligations were then electroporated into competent *E. coli* DH5 α cells. Transformants were plated out onto LB plus ampicillin plates which were additionally coated with IPTG and X-gal for blue-white screen. Colony PCR was performed by resuspension of a small portion of a colony into a 30 uL PCR reaction containing appropriate primers. Colonies that gave positive PCR results were inoculated in LB plus ampicillin broth for purification of vectors. Purified vectors were then checked by PCR, restriction digestion and confirmed by DNA sequencing. A newly constructed

vector containing the DNA sequence of the gene *hupD* and its natural promoter was transferred to the *lmoΔhupD* mutant. The transformants were checked by PCR. The transformants were then grown at 40⁰C to allow intergration of the vector into *lmoΔhupD* chromosome. Integrants were picked from BHI plus chloramphenicol plates and verified by colony PCR. However, phenotype check with nutrition test showed both transformants (intergrated and non-intergrated) failed to complement the *lmoΔhupD*.

Another try of complementation was performed with pPL2, a *Listeria monocytogenes* site-specific phage integration vector (Lauer et al, 2002). The vector pPL2 can be directly conjugated from *E. coli* into *L. monocytogenes* and forms stable, single-copy integrants. It utilizes the listeriphage PSA integrase and attachment site within an arginine tRNA gene for chromosomal insertion. Just as the complementation with pKSV7, the gene *hupD* was PCR-amplified together with its natural promoter, double digested, and then ligated with pPL2. The ligations were then transferred into *E. coli* XL1-Blue competent cells. Transformants were picked and checked by PCR. A newly-constructed pPL2 derivative vector containing the insertion of *hupD* and its natural promoter was purified from the transformants, sequenced and electroporated into *E. coli* SM10 competent cells.

A streptomycin-resistant strain of *lmoΔhupD* was made for following conjugation. 5 mL of *ΔhupD* overnight culture was inoculated in 500 mL BHI. When OD at 600 nm was around 1, the culture was spun down and resuspended in 2.5 mL dH₂O. The resuspensions were plated out onto BHI plus streptomycin plates with 250 uL for each. The plates were incubated at 37⁰C and spontaneous streptomycin-resistant mutants arose. For conjugation experiments, the *E. coli* SM10 carrying pPL2 which contains the insertion of *hupD* and its natural promoter was the donor strain and the streptomycin-

resistant *lmoΔhupD* was the recipient strain. The SM10 donor strain was grown in LB plus 20 ug/mL chloramphenicol broth at 30⁰C and the *lmoΔhupD* strain was grown in BHI plus 100 ug/mL streptomycin broth at 30⁰C. The cells were grown until OD at 600 nm reached around 0.5. 2.5 mL donor culture was mixed with 1.5 mL recipient culture. The mixture was filtered with a Millipore 0.45 uM filter prewashed with 5 mL LB broth. The filter was then washed with 10 mL BHI broth and placed onto a fresh BHI plate at 30⁰C for 2 hours. Then the cells were gently resuspended in 2.5 mL BHI and portions (25 uL, 50 uL, 100 uL) were plated in LB soft agar on BHI plates containing 200 ug/mL streptomycin and 7.5 ug/mL chloramphenicol. The plates were incubated at 30⁰C overnight and then shifted to 37⁰C. New recombinant cells appeared and were picked. Colony PCR using appropriate primers was performed and the recombination was confirmed. However, phenotype check with nutrition test again showed this construction did not complement *lmoΔhupD*.

While I was trying to complement *lmoΔhupD*, the *lmoΔhupC* was complemented with the same bacterial conjugation method using the same vector pPL2 (Jiang's Ph.D dissertation, 2009). Similarly, the gene *hupC* and its natural promoter was inserted into the pPL2 vector. Because the gene *hupC* is not directly linked to its promoter, they were amplified separately and ligated together through the PstI restriction site. At the ends of the inserted fragment are the BamHI and KpnI restriction sites. Since this construction was reported to be functional, another similar construction of pPL2 derivative with the insertion of the gene *hupD* and its natural promoter was made: a PstI restriction site was deliberately introduced inbetween the gene *hupD* and its natural promoter while the BamHI and KpnI restriction sites were added to the ends. After having confirmed by

DNA sequencing, this construct was transferred to *lmoΔhupD* and integrated into the chromosomal DNA of *lmoΔhupD*. However, phenotype check with nutrition test again showed this construction did not complement *lmoΔhupD*. Another construction was made by replacing the natural promoter of the *hup* operon with *pclpB*, the promoter of the constitutively expressed *Staphylococcus aureus clpB* gene (Arnaud et al, 2004; Chastanet et al, 2003). Then this construction was transferred into *lmoΔhupD* but failed to complement it.

One more construction was made with *E.coli-L. monocytogenes* shuttle vector pMAD (Arnaud et al, 2004) in a similar way as described for the construction with pKSV7. That is, the gene *hupD* and its natural promoter was inserted into the pMAD vector in one step. This construction was also transferred into *lmoΔhupD*. Again, nutrition test showed that the complementation did not work.

2.9 Expression and purification of His-tagged HupD

A BamHI-XhoI DNA fragment containing the gene *hupD* was PCR-amplified using EGD-e chromosomal DNA as the template. The fragment was digested with BamHI and XhoI. A clone and expression vector, pET28a, was linearized by double digestion with BamHI and XhoI restriction enzymes. The enzyme-treated PCR fragment and pET28a were then ligated together and the ligations were transferred into *E.coli* DH5α. The transformants were plated out onto LB plus kanamycin plates. 20 transformants were picked and checked by colony PCR. Plasmids were purified from the cell cultures of the

transformants and one of them was sequenced. This sequence-verified vector was then transferred into *E.coli* BL21.

For protein expression and purification, cells of *E.coli* BL21 harboring the newly-constructed pET28a derivative were grown in LB plus kanamycin broth to mid-log phase ($OD_{600\text{ nm}} \sim 0.5$). IPTG was added to the culture and the growth continued for another 3-4 hours. The culture was harvested by centrifugation and pelleted cells were resuspended in lysis buffer (50 mM NaH_2PO_4 , 300 mM NaCl, 10 mM imidazole, pH 8.0) with 10ug/mL RNase and DNase. Cells were then lysed by passage through a French pressure cell at 14000 p.s.i. The lysate was subjected to centrifugation at 8000 g for 20 minutes. The resulting supernatant was transferred to another centrifuge tube and was spun at 30,000 rpm for 1 hour. The pellet (membrane) was saved at -20°C and the supernatant (cytoplasm) was passed through a Ni-NTA column (Qiagen) equilibrated with lysis buffer. The column was firstly washed by 10 volumes of lysis buffer and then by 10 volumes of wash buffer (50 mM NaH_2PO_4 , 300 mM NaCl, 20 mM imidazole, pH 8.0). Absorbed proteins were then eluted with a linear gradient of imidazole (40-250 mM) which was achieved by mixing the lysis buffer and elution buffer (50 mM NaH_2PO_4 , 300 mM NaCl, 250 mM imidazole, pH 8.0) in varying ratios. Collected fractions were then subjected to SDS-PAGE. The fractions of purified HupD were then pooled and dialyzed against TBS buffer (Tris Buffer Saline: 150 mM NaCl, 50 mM Tris, pH 7.4). Protein concentration was determined by Bradford assay.

Purified, pooled HupD fractions displayed colors varying from light yellow to brown: the more concentrated is the protein fraction, the darker is the color. Wavelength scan of the fractions from 200 nm to 700 nm displayed a Soret peak around 410 nm together with 2

Q bands, one around 530 nm and the other around 670 nm. This indicates HupD was purified bound with heme. Further dialysis did not remove heme from HupD. Gel filtration was then performed to separate HupD from its bound heme: The protein HupD was mixed with 1% SDS and 1% glycerol, boiled, and then applied to a Sephacryl S100 HR gel filtration column pre-washed with 6 volumes of Tris buffer (10 mM Tris-Cl, 1% SDS, pH 8.0). The same buffer was used to elute the protein and the elution was collected with each fraction around 1 mL. Collected fractions were then subjected to optical density check both at 280 nm and 405 nm. HupD was separated from hemin.

Although gel filtration separated HupD from its bound hemin, the protein was denatured. To separate HupD from hemin without denaturing HupD, anion-exchange was performed as following: HupD was loaded onto a DEAE Sepharose column prewashed with 10 volumes of 10 mM, pH 8.0 Tris-Cl. The column was then washed with 5 volumes of 10 mM, pH 8.0 Tris-Cl and eluted with a linear gradient of 0 to 1M NaCl. HupD eluted was dialyzed against Tris-HCl. OD check indicated that hemin dissociated from HupD. A pyridine hemochrome assay (Zhu H, Liu M, Lei B. 2008) was performed to measure the heme content for purified HupD. Briefly, HupD in 750 μ L of Tris-HCl was mixed with 175 μ L pyridine. 75 μ L of 1 M NaOH and 2 mg sodium hydrosulfite was then immediately added to the mixture. The OD₄₁₈ was then immediately recorded. The heme content was determined using the extinction coefficient $\epsilon_{418} = 191.5 \text{ mM}^{-1} \text{ cm}^{-1}$.

2.10 Nutrition test with *Listeria monocytogenes*

Cells were grown in BHI broth overnight. In the next morning, 2.5×10^7 cells from the overnight culture were inoculated in 20 mL BHI broth. Cells were grown until OD at 600 nm reached 0.12~0.15. 1.5 mM bipyridyl was then added to the culture and the cells were grown until OD at 600 nm reached 0.6~0.7. 200 uL cells were withdrawn from the culture and mixed with 8 mL molten BHI top agar and 20 uL bipyridyl. This mixture was poured onto a petri dish and allowed to solidify. Sterile paper disks were then placed on top of solidified agar and 10 uL siderophores or Hn/Hb of a certain concentration were loaded onto the center of the paper discs. The plates were incubated at 37⁰C overnight.

2.11 Synthesis of [⁵⁹Fe]-hemin

For the synthesis of [⁵⁹Fe]-hemin, ⁵⁹Fe was nonenzymatically incorporated into protoporphyrin IX (PPIX). The protocol reported by Babusiak et al (Babusiak et al, 2005) was strictly followed. 450 uL of glacial acetic acid was added to a 10 mL double-neck flask and nitrogen flowed through the flask at 60⁰C for 10 minutes. 50 uL of PPIX (Sigma-Aldrich) in a pyridine (Sigma-Aldrich) stock solution (6 mg/mL) was added to the glacial acetic acid. Thioglycolic acid (0.25 mL; Sigma-Aldrich) was added into the 0.5 M HCl solution containing 30 ug of ⁵⁹Fe and the resulting mixture was immediately injected into the prepared PPIX solution and held at 60⁰C for 30 min under a nitrogen atmosphere. Air was bubbled through the reaction mixture for 1.5 h at room temperature. The mixture was then transferred into 20 mL of ether and washed 6 times with 30 mL of

1 M HCl in order to remove the remaining protoporphyrin and iron. The ether fraction was dried overnight under a stream of gaseous nitrogen. Dried [⁵⁹Fe]-hemin was dissolved in 400 uL of DMSO and the solution was stored at 4⁰C.

The purity of the product was verified by thin layer chromatography on silica gel plates using 2,6-lutidine:H₂O (5:3.5) mobile phase at room temperature.

2.12 [⁵⁹Fe]-hemin uptake in *L. monocytogenes*

Listeria monocytogenes EGD-e and its mutant derivatives were inoculated in 10 mL BHI broth at 37⁰C overnight. In the next morning, 200 uL overnight BHI cultures were inoculated with 20 mL MOPS and were grown to stationary phase. 200 uL cell cultures were then reinoculated with 20 mL MOPS. Cultures were grown until OD at 600 nm reached around 0.8-1. Cells were then subjected to [⁵⁹Fe]-hemin uptake assay: 100 uL cell cultures were mixed with 10 mL MOPS media prewarmed to 37⁰C; 100 uL [⁵⁹Fe]-hemin of varying concentrations ranging from 10 nM to 2 uM were immediately added to the mixture. After incubation at 37⁰C for 5 seconds or 1 minute, the reaction was filtered through a 0.2 um Durapore or Acetate Plus filter and washed with 10 mL ice cold wash buffer (50 mM Tris, 0.05% Tween-20, PH=9). The radiation of the filters was counted in a Packard Cobra Gamma counter. At each concentration, data were collected in triplicate and averaged. The 5 seconds radiation was subtracted from the 1 minute radiation. The Km and Vmax of transport were determined by using the “Enzyme Kinetics” equation of Grafit 5.09 (Erithacus, Middlesex, UK).

For [⁵⁹Fe]-hemin uptake assay with the fixed concentration (200 nM), cells were prepared in the same way as described above. 1 mL cell culture and 1 mL [⁵⁹Fe]-hemin (20 uM) were sequentially added to 100 mL MOPS prewarmed to 37⁰C. The resulting mixture was immediately incubated at 37⁰C. At indicated time points varying from 5 minutes to 1 hour, 10 mL cell culture was withdrawn, filtered through an Acetate Plus filter and washed with 10 mL ice cold wash buffer (50 mM Tris, 0.05% Tween-20, PH=9). The radiation of the filters was counted in a Packard Cobra Gamma counter. For every strain at each time point, data were collected in triplicate and averaged. The 5 minutes radiation served as the background and was subtracted. The uptake rate was determined with cpm/10⁹ cells/min.

2.13 Generation of polyclonal mouse anti-HupD antibody

1 mL HupD of 0.37 mg/mL was mixed with 110 uL 10% SDS. The mixture was boiled for 5 minutes. 7.7 mL ice-cold acetone was then added to the boiled mixture. The resulting mixture was frozen at -20⁰C for 2 hours and then was spun at 7000g for 20 minutes. The pellet was resuspended with 1 mL distilled water. 7 mL ice-cold acetone was added to the resuspension and then was frozen at -20⁰C for 30 minutes. The frozen was then spun at 7000g for 20 minutes. The resulting pellet was resuspended with 0.5 mL TBS. 0.5 mL native HupD of 0.37 mg/mL was mixed with the resuspension. 1 mL complete Freund's adjuvant was added to this 1 mL mixture, emulsified, and injected into mice with 200 uL for each. In the following 3 weeks, the mice were boosted on a weekly basis with the same amount of the mixture of native and denatured HupD. For the first

following week the mixture was emulsified with 1 mL incomplete Freund's adjuvant. For the next two weeks, 10 uL aluminum hydroxide gel adjuvant was added to the mixture, mixed through vortex, and then incubated on ice for 1 hour before injection. After 4 weeks injection, mice were bled and the blood was collected in a sterile eppendorf tube. The blood collections were kept at 4⁰C overnight and then spun at 12000 rpm for 5 minutes. The supernatants containing anti-HupD antibody were transferred to a clean eppendorf tube and stored at 4⁰C.

2.14 Immunoblots with cell fractions of *Listeria monocytogenes*

Listeria monocytogenes EGD-e and its derivatives were grown in BHI broth overnight. The overnight cultures were subcultured with a ratio of 1:100 in 500 mL BHI broth, BHI plus 1 mM bipyridyl broth (bipyridyl was added to the cultures when OD at 600 nm reached 0.1-0.2.), MOPS-L or KRM media and the cultures were grown to stationary phase. For the growth in MOPS-L or KRM media, cells were subcultured again and grown to stationary phase. The cells were then pelleted by centrifugation at 6000 g for 15 min. The cell pellets were resuspended in 25 mL distilled water with 10ug/mL RNase and DNase. Cells were then lysed by 5 passages through a French pressure cell at 14000 p.s.i. The lysate was subjected to centrifugation at 8000 g for 20 minutes. The resulting supernatant was transferred to another centrifuge tube and was spun at 30,000 rpm for 1 hour. The pellet (cell envelope fraction) was resuspended in 2mL Tris buffer (20 mM Tris-Cl, pH 8.0). Both the cell envelope fraction and the cytoplasm fraction (the supernatant) were then subjected to SDS-PAGE. After resolution by SDS-PAGE,

proteins were electrophoretically transferred to a nitrocellulose membrane (0.45 μ m, PROTRAN, Whatman) through a Semi-Dry Blotting Unit (FB-SDB-2020, Fisher Scientific). Upon completion of transfer, the membrane was soaked in the blocking buffer (TBS, 1% gelatin) for 15 minutes. The blocking buffer was poured off and the primary antibody (mouse anti-HupD antibody) was added to the membrane. The membrane was incubated with the primary antibody either at room temperature on a shaker for 3 hours or at 4⁰C overnight. The primary antibody was then poured off and saved. The membrane was washed 5 times with 0.05% Tween-20 in TBS. Secondary antibody (goat-anti-mouse-IgG-alkaline phosphatase) was added to the membrane and incubated at room temperature on a shaker for 2 hours or at 4⁰C overnight. After 5 times wash with 0.05% Tween-20 in TBS, the membrane was developed with bromochloroindoyl phosphate (BCIP) and nitroblue tetrazolium (NBT).

2.15 Growth of *Listeria monocytogenes* in MOPS-L media

Cells of *Listeria monocytogenes* EGD-e and its mutant derivatives were grown in BHI overnight. In the next morning, the overnight cultures were subcultured 1:100 into MOPS-L media. Cells were grown to stationary phase and then subcultured 1:100 again into MOPS-L with the addition of hemin of indicated concentrations. OD₆₀₀ was then read at indicated time points for 36 hours

2.16 Intrinsic tryptophan fluorescence quenching

The binding affinity of HupD for hemin was determined by intrinsic fluorescence quenching method using an SLM-AMINCO 8000 fluorimeter (Rochester, NY) upgraded to 8100 functionality. 33 nM apo-HupD in 3 mL TBS was added to a quartz cuvette and the fluorescence was recorded from 320 nm to 340 nm. A tiny stir bar was used to keep the solution well-mixed in the cuvette. Various concentrations of hemin solution in DMSO were added to the 3 mL HupD solution and the fluorescence was recorded for every addition of hemin. The background fluorescence (various concentrations of hemin in TBS) and volume changes were accounted and the data were analyzed with the bound $(1-F/F_0)$ versus total function of GraFit 5.09 (Erithacus Software Ltd., Middlesex, UK).

2.17 Synthesis of [⁵⁹Fe]-Ferric Citrate

3 mL of 0.1M sodium citrate (pH=7) was mixed with 15 uL of 10 mM ⁵⁹FeCl₃ (in 0.5 M HCl solution) at room temperature, incubated for 1 hour (Braun and Herrmann, 2007). [⁵⁹Fe]-Ferric Citrate was then ready for transport experiment.

2.18 [⁵⁹Fe]-Ferric Citrate uptake in *Listeria monocytogenes*

Cells were prepared in the same way as described for [⁵⁹Fe]-hemin uptake in *Listeria monocytogenes*. Briefly, cells were inoculated overnight in BHI, subcultured (1:100) twice in MOPS, and then subjected to [⁵⁹Fe]-ferric citrate uptake assay: 100 uL cell

cultures were mixed with 10 mL MOPS media prewarmed to 37⁰C; 100 uL [⁵⁹Fe]-ferric citrate of varying concentrations ranging from 100 nM to 20 uM were immediately added to the mixture. After incubation at 37⁰C for 5 seconds or 1 minute, the reaction was filtered and washed with 10 mL ice cold 0.9% LiCl. The radioactivity associated with the filters was counted in a Packard Cobra Gamma counter. At each concentration, data were collected in triplicate and averaged. The 5 seconds radiation was subtracted from the 1 minute radiation. The Km and Vmax of transport were determined by using the “Enzyme Kinetics” equation of Grafit 5.09 (Erithacus, Middlesex, UK).

2.19 Binding of peptidoglycan to TonB C-terminus

Aliquots of purified peptidoglycan were mixed with 30 ug aliquots of purified proteins (MalE, MalE-TonB69C, and FepB) in 20 mM Tris-Cl, pH 8 (final volume of 100 uL) at room temperature for 30 min. The mixture was then centrifuged at 100000 g for 45 min in a Beckman Optima TL ultracentrifuge. Both the supernatants and the resuspended pellets were subjected to SDS-PAGE. The gels were stained with Coomassie blue, photographed, and analyzed by Image-Quant (Molecular Dynamics) to determine the amount of protein in the pellets and supernatants.

Chapter 3 Site-directed Chromosomal Deletions in *Listeria*

3.1 Target genes for deletion

As mentioned in chapter 1, there are four potential or demonstrated Fur-regulated iron transport systems in *Listeria*. Two systems, the Hup system and the Fhu system, have been reported to be involved in Hn/Hb uptake and hydroxamate type siderophore uptake, respectively (Jin et al, 2006). However, it was not clear that whether *Listeria* has multiple Hn/Hb uptake systems until this study was conducted. Although the *srtB* locus of *Listeria* has been suspected to be involved in the uptake of Hn/Hb because of the high similarity between this locus and the *isd* locus of *S. aureus* (Newton et al, 2005; Shao's Ph.D dissertation, 2007), its involvement in Hn/Hb uptake has not been undoubtedly reported. The FhuB and FhuG proteins encoded by *fur-fhu* locus, on the other hand, show high similarity to the IM heme permease of the *phu* system in *Pseudomonas aeruginosa*, raising the possibility that *fur-fhu* locus plays a role in Hn/Hb uptake. To identify potential Hn/Hb uptake systems, I made a series of mutants as listed in the table below (Table 3.1).

Table 3.1 Chromosomal deletion mutants made for this study

Strain	Locus
<i>ΔhupD (lmo2431)</i>	<i>hupCDG</i>
<i>Δhup (lmo2429, lmo2430, lmo2431)</i>	<i>hupCDG</i>
<i>ΔsvpA/Δhup (lmo2185, lmo2429, lmo2430, lmo2431)</i>	<i>srtB, hupCDG</i>
<i>Δ2183/Δhup (lmo2183, lmo2429, lmo2430, lmo2431)</i>	<i>srtB, hupCDG</i>
<i>Δ0641/Δhup (lmo0641, lmo2429, lmo2430, lmo2431)</i>	<i>lmo0641, hupCDG</i>
<i>ΔfhuC/Δhup (lmo1960, lmo2429, lmo2430, lmo2431)</i>	<i>fur-fhu, hupCDG</i>
<i>Δ2183/Δhup/ΔfhuC (lmo2183, lmo2429, lmo2430, lmo2431, lmo1960)</i>	<i>srtB, hupCDG, fur-fhu</i>
<i>Δ2183/ΔfhuC (lmo2183, lmo1960)</i>	<i>srtB, hupCDG, fur-fhu</i>

3.2 Chromosomal deletions

3.2.1 Deletion of *hupD*

The *hup* operon in *L. monocytogenes* contains 3 genes. Its promoter contains a conserved “Fur box” (TGAAAATAATTCTCA). The $\Delta hupC$ (*lmo2429*) mutant has already been available and has been experimentally demonstrated to be involved in Hn/Hb uptake. Two other single deletion mutants in this operon were recently made and I created the $\Delta hupD$ mutant by allelic replacement *in vivo*.

As described in chapter 2, the deletion process began with the amplification of two PCR fragments. The two fragments, one upstream and the other downstream of the target gene, were ligated together. A new fragment was thus created and this fragment had two characteristics: 1). It was homologous to the region in the bacterial chromosome that contains the target gene for deletion; 2). the fragment itself doesn't contain the target gene. This fragment was then ligated into pKSV7, a thermo-sensitive vector that can shuttle between Gram-positive and Gram-negative bacteria. This construction (pKSV7 $\Delta hupD$) was then introduced into *Listeria* at permissive temperature 30°C. At nonpermissive temperature above 37°C and under the antibiotic pressure, it integrated into the chromosome of *Listeria* through homologous recombination. Successive passages at 37°C without the presence of the antibiotic allowed a second homologous recombination to occur, which gave rise to either the parental strain or the deletion derivative. A schematic representation of the detailed process of the construction of $\Delta hupD$ is given below (Figure 3.1)

Site-directed chromosomal deletion(Construction of $\Delta hupD$)

A. Construction of plasmid pKSV7 $\Delta hupD$

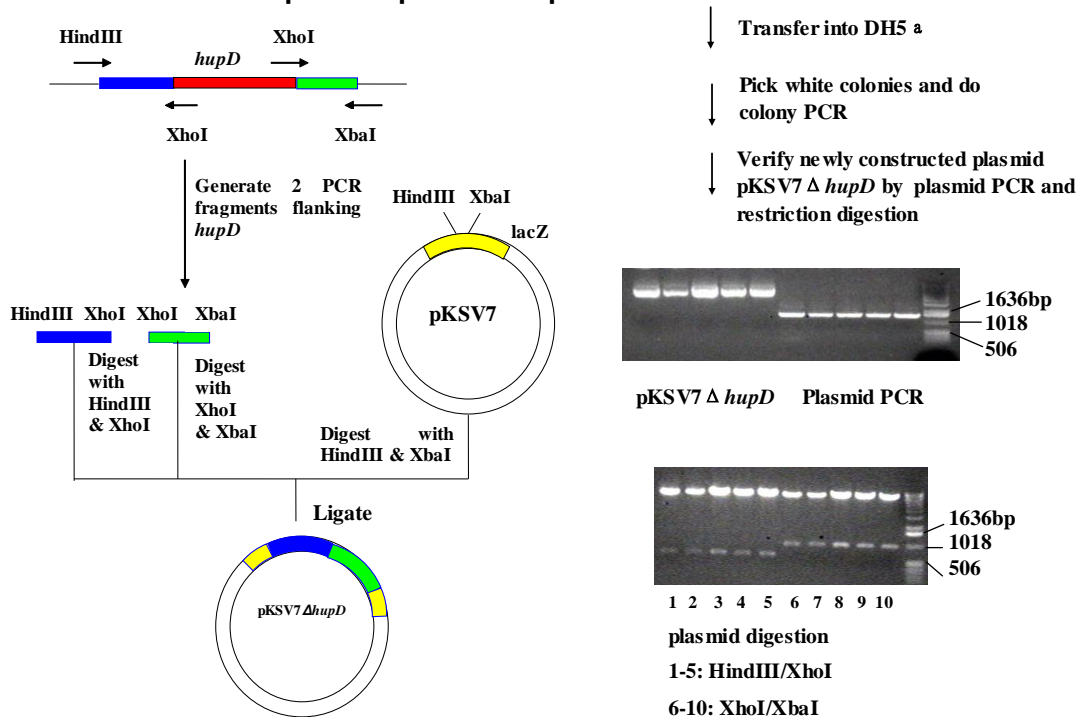


Figure 3.1 Schematic representation of the construction of $\Delta hupD$

A. The pictures of the two agarose gels on the right: the first 5 lanes of the top agarose gel are purified, newly-constructed pKSV7 $\Delta hupD$; lanes 6 to 10 are PCR products (~1.5 Kb) using the vector pKSV7 $\Delta hupD$ as the template and the primers DhupDHind1 and DhupDXho2 for PCR reaction; lane 11 is 1Kb DNA ladder (Gibco-BRL); the first 5 lanes of the bottom agarose gel are digestions of pKSV7 $\Delta hupD$ with restriction enzymes HindIII and XhoI (The size for the smaller fragment is ~600 bp); lanes 6 to 10 are digestions of pKSV7 $\Delta hupD$ with restriction enzymes XhoI and XbaI (The size for the smaller fragment is ~900 bp); lane 11 is 1Kb DNA ladder (Gibco-BRL).

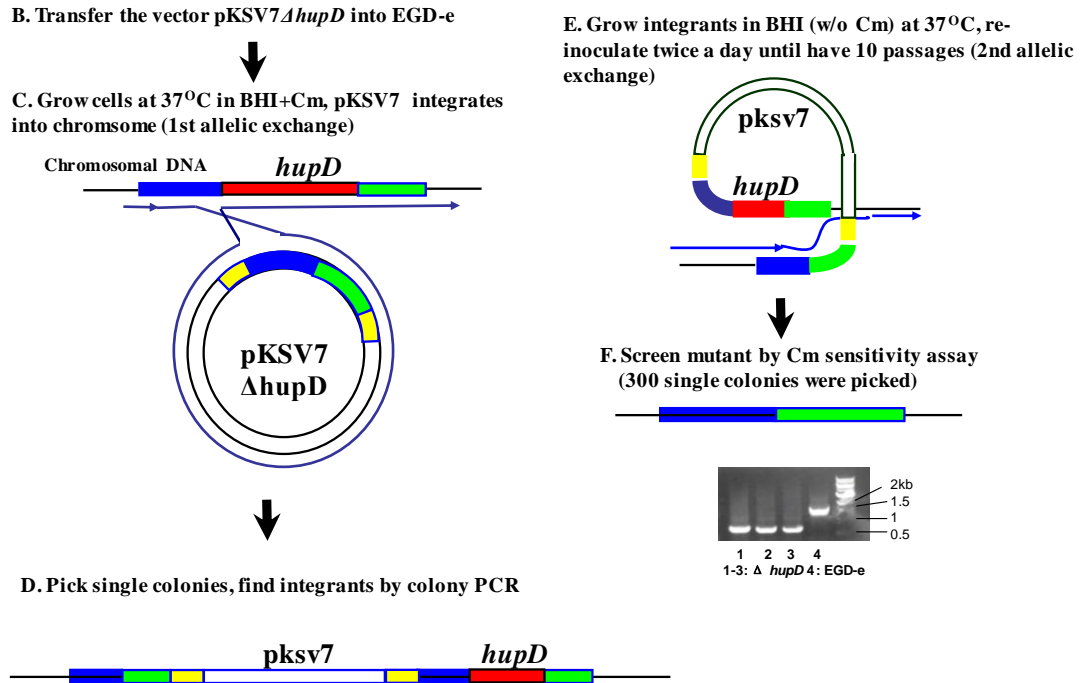


Figure 3.1 Schematic representation of the construction of Δ hupD (continued)

F. Agarose gel electrophoresis of the PCR products: the first 3 lanes are the reactions (0.7 Kb) with the primers DhupDchk1 and DhupDchk2 and using boiled Δ hupD mutant as the template; lane 4 is the control reaction (1.5 Kb) with the primers DhupDchk1 and DhupDchk2 and using boiled *EGD-e* as the template; lane 5 is 1Kb DNA ladder (Gibco-BRL).

3.2.2 Deletion of *hupCDG*

The four primers designed for making the *hupCDG* deletion mutant were DhupDHind1, DhupDXho2, DhupXho3 and DhupXba4. The strategy used in this deletion was the same as the one used in deleting *hupD*. The construction of pKSV7 Δ *hupCDG* needed to ligate two fragments, one upstream and the other downstream of *hupCDG*, into pKSV7. Since the vector pKSV7 Δ *hupD* already has the upstream fragment of *hupCDG* inserted into the vector pKSV7, I took advantage of it. That is: I PCR amplified the downstream fragment of *hupCDG*, digested the vector pKSV7 Δ *hupD* and the upstream fragment with the same restriction enzymes XhoI and XbaI, and ligated them together. The expected ligation product was pKSV7 Δ *hupCDG*. In other words, the successful construction should have eliminated the *hupCDG* but contain its upstream and downstream fragments that were ligated tail to head. The ligation product was then purified and electroporated into *E.coli* DH5 α . Host DH5 α strains potentially harboring the right construction were screened by colony PCR (Figure 3.2 A; for methods, see Chapter 2). The vector was then extracted and its construction was confirmed by plasmid PCR (Figure 3.2 B) and DNA sequencing. The newly-constructed vector was then transferred into EGD-e (Figure 3.2 C). The same procedure as the construction of the Δ *hupD* mutant was performed. Integration of the vector pKSV7 Δ *hupCDG* into EGD-e chromosome was checked by colony PCR (Figure 3.2 D) and the intergrants were grown for 10 successive passages. After two events of homologous recombination, the Δ *hup* mutant was generated (Figure 3.2 E).

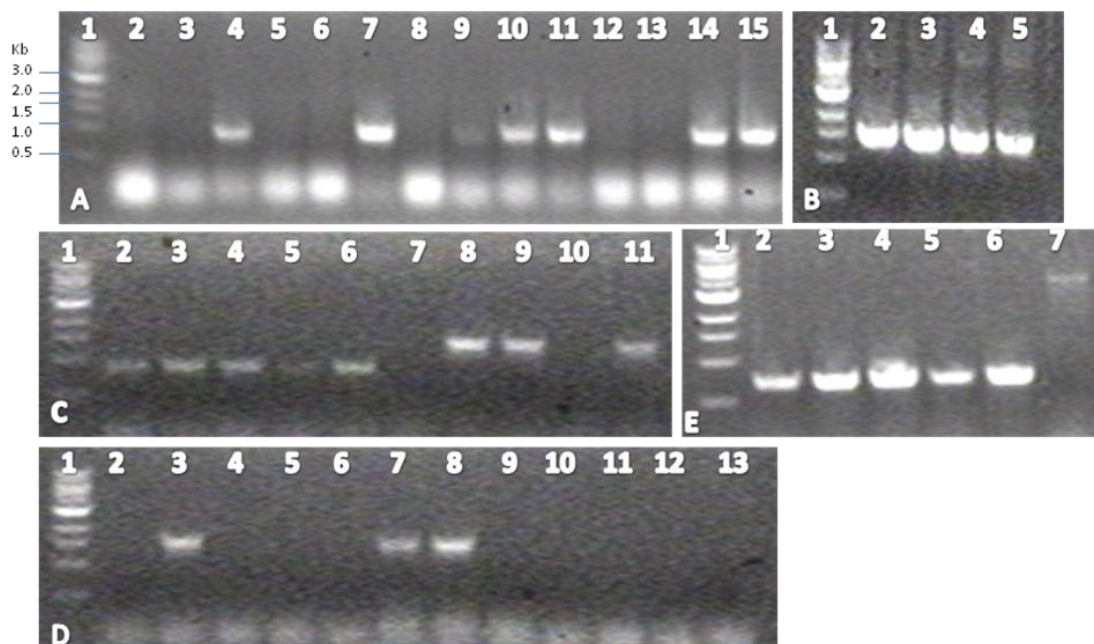


Figure 3.2 Construction of $\Delta hupCDG$

A. Colony PCR to screen host strains harboring the right construction. For all PCR reactions, DH5 α colonies picked from LB plus ampicillin plates were used as the template. The primers for all the 14 PCR reactions were DhupXho3 and DhupXba4. Lane 1 was the Quick-load 1 Kb DNA ladder from New England Biolabs; lanes 2-15 were the PCR reactions. The size of the expected PCR products was ~0.9 kb.

B. Plasmid PCR to verify the construction. For all the 4 PCR reactions, purified plasmids were used as the template and the primers were DhupDHind1 and DhupXba4. The size of the expected PCR products was ~1.5 kb. Lane 1 was the Quick-load 1 Kb DNA ladder from New England Biolabs; lanes 2-15 were the PCR reactions.

C. Colony PCR to verify transformation of EGD-e with pKSV7 $\Delta hupCDG$. 4 EGD-e transformants picked from BHI plus chloramphenicol plates were used as the template for all PCR reactions except the ones in lanes 2 and 7, which were the control PCR using EGD-e wild type as the template. Lane 1 was the Quick-load 1 Kb DNA ladder from

New England Biolabs; lanes 2-6 were the PCR reactions using the primers LLOchk3 and LLOchk5, the size of the expected PCR product was ~700 bp; lanes 7-11 were the PCR reactions using the primers DhupDHind1 and DhupXba4; the size of the expected PCR product in lane 7 was ~4.5 kb, which was too big to amplify; the size of the expected PCR products in lanes 8-11 was 1.5 kb.

D. Colony PCR to check intergration of pKSV7 Δ hupCDG into the chromosome of EGD-e. 4 Potential intergrants picked from BHI plus chloramphenicol plates were used as the template for PCR reactions. Lane 1 was Quick-load 1kb DNA ladder from New England Biolabs. The primers for the PCR reactions: lanes 2-5, DhupInt1 and DhupXba4; lanes 6-9, primers DhupDHind1 and DhupInt2; lanes 10-13, primers DhupInt1 and DhupInt2. Since for one single colony, the intergration could happen only in one place, between the two PCR reactions using the same colony as the template but using two different groups of primers (DhupInt1+DhupXba4 vesus DhupDHind1+DhupInt2) only one PCR reaction product is expected. Both lanes 2 and 7 gave right size PCR products, indicating that this colony was not pure enough. No product is expected for the PCR reactions using primers DhupInt1 and DhupInt2.

E. Colony PCR to verify the construction of Δ hupCDG. Lane 1 was the Quick-load 1 Kb DNA ladder from New England Biolabs; lanes 2-7 were the PCR reactions with the primers Dhupchk3 and Dhupchk5; the templates for the lanes 2-6 were the mutant Δ hupCDG which would give a PCR product with the size around 700 bp, the template for lane 7 was the wild type EGD-e which would give a PCR product with the size around 4.2 kb.

3.2.3 Construction of *lmo*Δ2183/Δ*hup*CDG

The construction of *lmo*Δ2183/Δ*hup*CDG took advantage of the existing mutant *lmo*Δ2183 and the newly constructed vector pKSV7Δ*hup*CDG. The approach that we employed to make site-directed chromosomal deletions in *L. monocytogenes* has a advantage of allowing facile construction of multiple mutants. Additional deletions can be introduced into the chromosome of existing mutant strains by transforming the existing mutant strains with corresponding plasmids encoding those additional deletions, followed by allelic exchange. This strategy was applied in the construction of *lmo*Δ2183/Δ*hup*CDG. The vector pKSV7Δ*hup*CDG was transferred into *lmo*Δ2183 (Figure 3.3 A) and then intergrated into its chromosome (Figure 3.3 B) through homologous recombination. The vector pKSV7 was excised from its chromosome in the second homologous recombination event and the double mutant was generated (Figure 3.3 C).

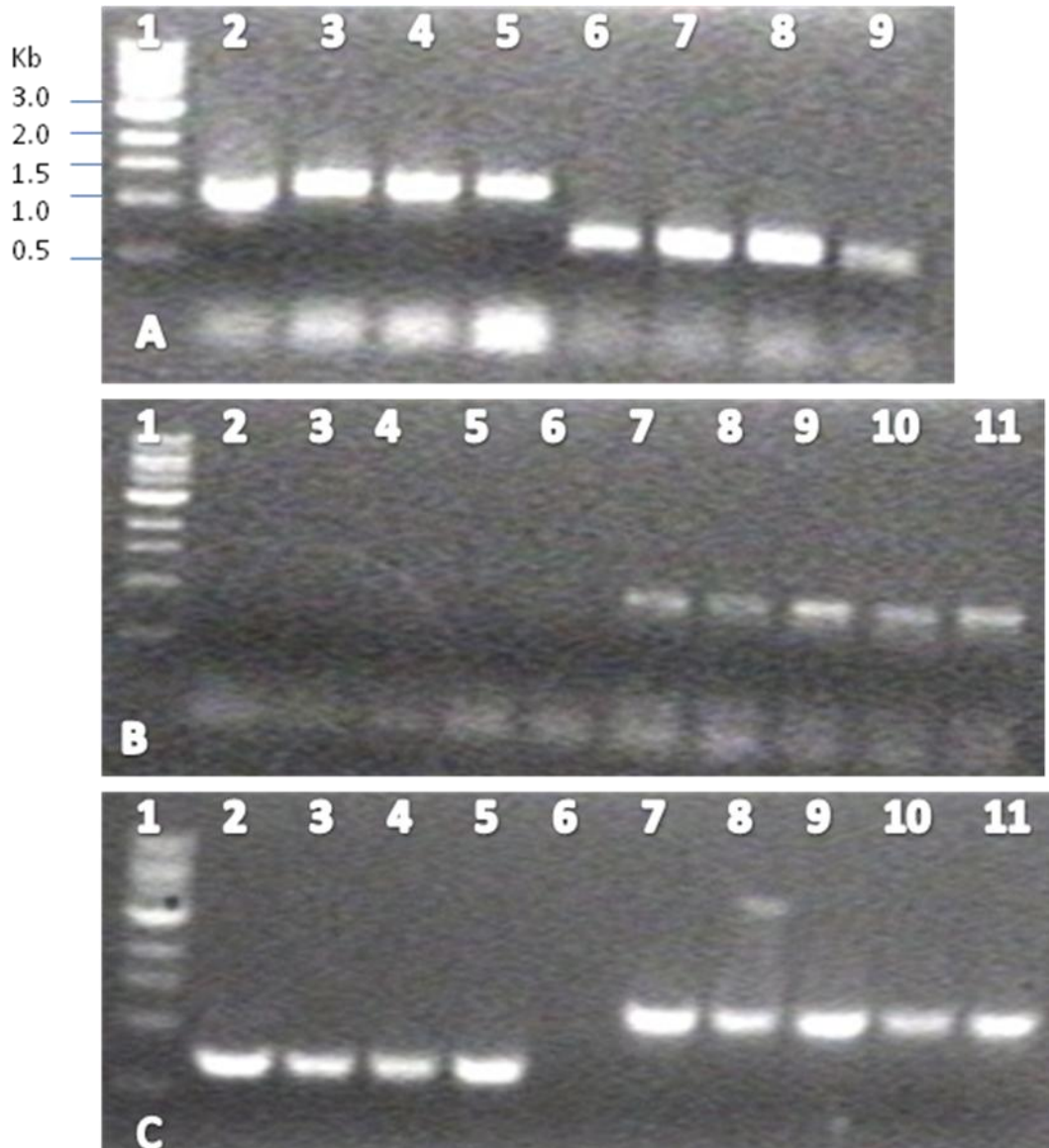


Figure 3.3 Construction of *lmo*Δ2183/Δ*hup*CDG

A. Colony PCR to verify transformation of *lmo*Δ2183 with pKSV7Δ*hup*CDG. 4 transformants picked from BHI plus chloramphenicol plates were used as the template for all PCR reactions. Lane 1 was the Quick-load 1 Kb DNA ladder from New England Biolabs; lanes 2-5 were the PCR reactions using the primers D2183Int1 and FerDoCla, the size of the expected PCR product was ~1.2 kb; lanes 6-9 were the PCR reactions

using the primers Dhupchk3 and Dhupchk5, the size of the expected PCR products was ~700 bp.

B. Colony PCR to check intergration of pKSV7 Δ hupCDG into the chromosome of *lmo* Δ 2183. 5 Potential intergrants picked from BHI plus chloramphenicol plates were used as the template for PCR reactions. Lane 1 was Quick-load 1kb DNA ladder from New England Biolabs. The primers for the PCR reactions: lanes 2-6, DhupInt1 and DhupXba4; lanes 7-11, primers Dhupchk3 and DhupInt2.

C. Colony PCR to verify the construction of *lmo* Δ 2183/ Δ hupCDG. Lane 1 was the Quick-load 1 Kb DNA ladder from New England Biolabs; lanes 2-6 were the PCR reactions with the primers Dhupchk3 and Dhupchk5; the templates for the lanes 2-5 were the double mutant *lmo* Δ 2183/ Δ hupCDG, the template for lane 6 was the single mutant *lmo* Δ 2183; the size of the expected PCR products in lanes 2-5 was ~700 bp and 4.2 kb in lane 6, which was too big to amplify. Lanes 7-11 were the PCR reactions using the primers D2183Int1 and FerDoCla, the templates for the lanes 7-10 were the double mutant *lmo* Δ 2183/ Δ hupCDG, the template for lane 11 was the single mutant *lmo* Δ 2183; the size of the expected PCR products in lanes 7-11 was ~1.2 kb.

3.2.4 Construction of *lmo*Δ2185/Δ*hup*CDG

Just as the construction of *lmo*Δ2183/Δ*hup*CDG, I took advantage of the existing mutant *lmo*Δ2185 and the newly constructed vector pKSV7Δ*hup*CDG to make *lmo*Δ2185/Δ*hup*CDG. Briefly, the vector pKSV7Δ*hup*CDG was transferred into *lmo*Δ2185 (Figure 3.4 A) and then integrated into its chromosome (Figure 3.4 B) through homologous recombination. The vector pKSV7 was excised from its chromosome in the second homologous recombination event and the double mutant *lmo*Δ2185/Δ*hup*CDG was generated (Figure 3.4 C).

3.2.5 Construction of *lmo*Δ0641/Δ*hup*CDG

This construction took advantage of the existing mutant *lmo*Δ0641 (provided by Dr. Cormac). The vector pKSV7Δ*hup*CDG was transferred into *lmo*Δ0641 (Figure 3.5 A) and then integrated into its chromosome (Figure 3.5 B). The double mutant *lmo*Δ0641/Δ*hup*CDG was generated (Figure 3.5 C) through a second homologous recombination.

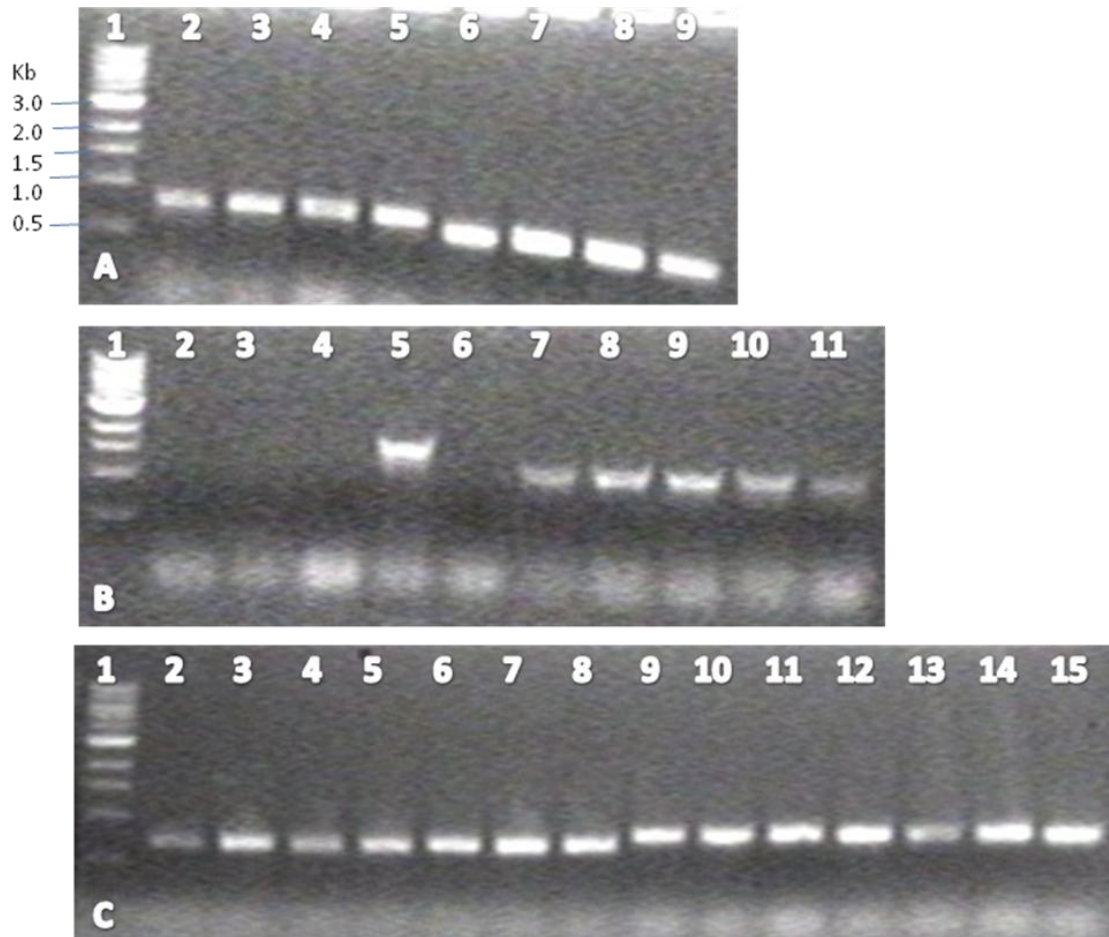


Figure 3.4 Construction of *lmo* Δ 2185/ Δ *hup*CDG

A. Colony PCR to verify transformation of *lmo* Δ 2185 with pKSV7 Δ *hup*CDG. 4 transformants picked from BHI plus chloramphenicol plates were used as the template for all PCR reactions. Lane 1 was the Quick-load 1 Kb DNA ladder from New England Biolabs; lanes 2-5 were the PCR reactions using the primers D2185chk3 and D2185chk5, the size of the expected PCR product was ~800 bp; lanes 6-9 were the PCR reactions using the primers Dhupchk3 and Dhupchk5, the size of the expected PCR products was ~700 bp.

B. Colony PCR to check intergration of pKSV7 Δ hupCDG into the chromosome of *lmo* Δ 2185. 5 Potential intergrants picked from BHI plus chloramphenicol plates were used as the template for PCR reactions. Lane 1 was Quick-load 1kb DNA ladder from New England Biolabs. The primers for the PCR reactions: lanes 2-6, DhupInt1 and DhupXba4; lanes 7-11, primers Dhupchk3 and DhupInt2.

C. Colony PCR to verify the construction of *lmo* Δ 2185/ Δ hupCDG. The templates for all PCR are the double mutant *lmo* Δ 2185/ Δ hupCDG. Lane 1 was the Quick-load 1 Kb DNA ladder from New England Biolabs; lanes 2-8 were the PCR reactions with the primers Dhupchk3 and Dhupchk5; the size of the expected PCR products in lanes 2-8 was ~700 bp; lanes 9-15 were the PCR reactions using the primers D2185chk3 and D2185chk5; the size of the expected PCR products in lanes 9-15 was ~800 bp.

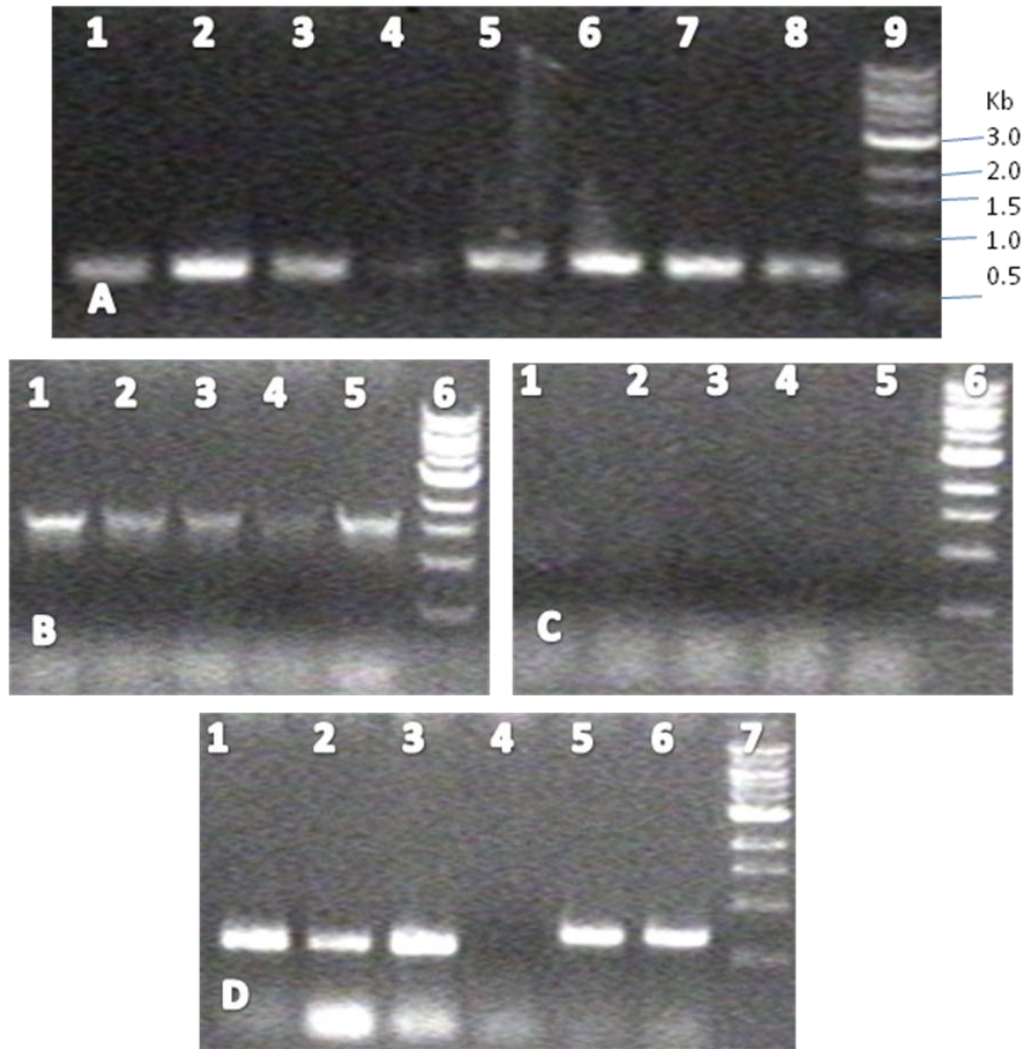


Figure 3.5 Construction of *lmo*Δ0641/Δ*hup*CDG

A. Colony PCR to verify transformation of *lmo*Δ0641 with pKSV7Δ*hup*CDG. 4 transformants picked from BHI plus chloramphenicol plates were used as the template for all PCR reactions. Lane 9 was the Quick-load 1 Kb DNA ladder from New England Biolabs; lanes 1-4 were the PCR reactions using the primers D0641chk3 and D0641chk5, the size of the expected PCR product was ~650 bp; lanes 5-8 were the PCR reactions using the primers Dhupchk3 and Dhupchk5, the size of the expected PCR products was ~700 bp.

B. Colony PCR to check intergration of pKSV7 Δ hupCDG into the chromosome of *lmo* Δ 0641. 5 Potential intergrants picked from BHI plus chloramphenicol plates were used as the template for PCR reactions. Lane 6 was Quick-load 1kb DNA ladder from New England Biolabs. The primers for the PCR reactions were DhupInt1 and DhupXba4.

C. Also colony PCR to check intergration of pKSV7 Δ hupCDG into the chromosome of *lmo* Δ 0641, but with different primers: Dhupchk3 and DhupInt2. The templates for the PCR reactions were the same as used in B. Lane 6 was Quick-load 1kb DNA ladder from New England Biolabs.

D. Colony PCR to verify the construction of *lmo* Δ 0641/ Δ hupCDG. Lane 7 was the Quick-load 1 Kb DNA ladder from New England Biolabs; lanes 1-3 were the PCR reactions with the primers D0641chk3 and D0641chk5; the template for the PCR in lane 1 was *lmo* Δ 0641; the templates for the PCRs in lanes 2 and 3 were *lmo* Δ 0641/ Δ hupCDG; the size of the expected PCR products in lanes 1-3 was ~650 bp; lanes 4-6 were the PCR reactions using the primers Dhupchk3 and Dhupchk5; the template for the PCR in lane 4 was *lmo* Δ 0641; the templates for the PCRs in lanes 5 and 6 were *lmo* Δ 0641/ Δ hupCDG; the size of the expected PCR products in lanes 5 and 6 was ~700 bp ; the size of the expected PCR product in lane 4 was 4.2 kb (failed to amplify).

3.2.6 Construction of *lmo*Δ1960/Δ*hup*CDG

This construction took advantage of the existing mutant *lmo*Δ1960. The vector pKSV7Δ*hup*CDG was transferred into *lmo*Δ1960 (Figure 3.6 A) and then intergrated into its chromosome. The double mutant *lmo*Δ1960/Δ*hup*CDG was generated (Figure 3.6 B) through a second homologous recombination.

3.2.7 Construction of *lmo*Δ2183/Δ*hup*CDG/Δ1960

This construction took advantage of the newly constructed mutant *lmo*Δ2183/Δ*hup*CDG and the existing construction pKSV7Δ1960. The vector pKSV7Δ1960 was transferred into *lmo*Δ2183/Δ*hup*CDG (Figure 3.7 A) and then intergrated into its chromosome (Figure 3.7 B). The triple mutant *lmo*Δ2183/Δ*hup*CDG/Δ1960 was generated (Figure 3.7 C) through a second homologous recombination.

3.2.8 Construction of *lmo*Δ2183/Δ1960

This construction took advantage of the existing mutant *lmo*Δ2183 and the existing construction pKSV7Δ1960. The vector pKSV7Δ1960 was transferred into *lmo*Δ2183 (Figure 3.8 A) and then intergrated into its chromosome (Figure 3.8 B). The double mutant *lmo*Δ218/Δ1960 was generated (Figure 3.8 C) through a second homologous recombination.

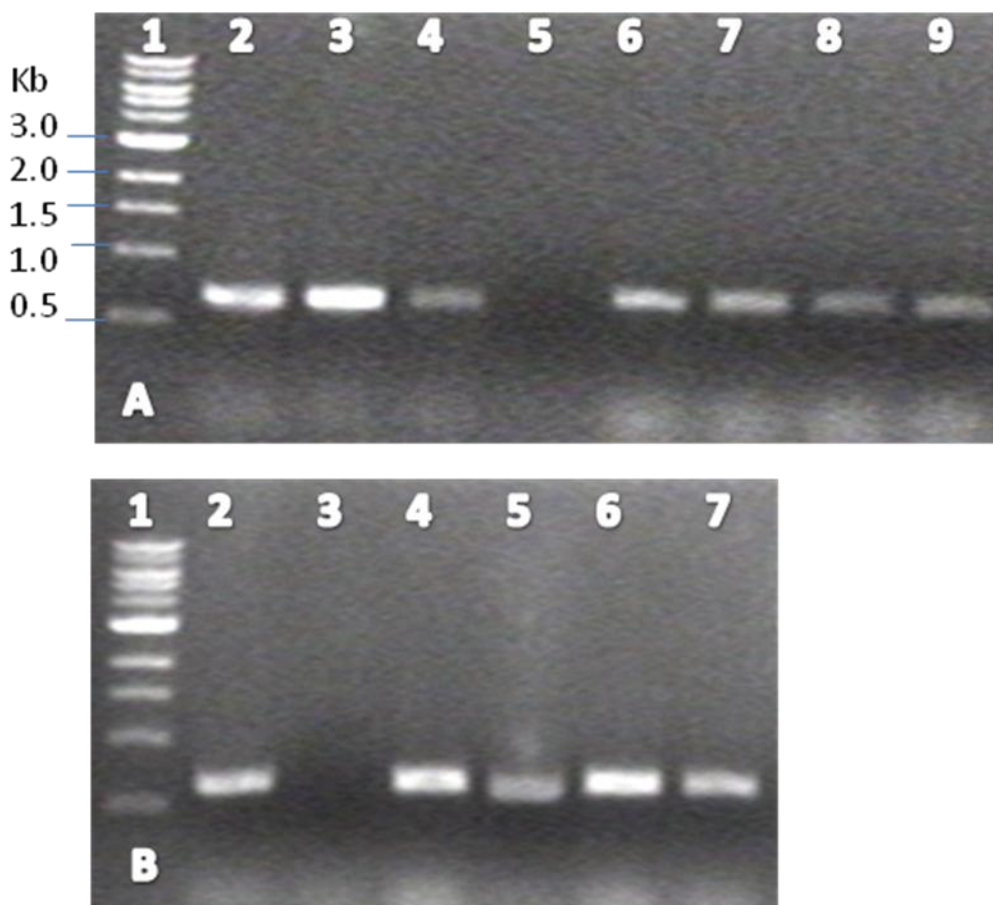


Figure 3.6 Construction of *lmo*Δ1960/Δ*hup*CDG

A. Colony PCR to verify transformation of *lmo*Δ1960 with pKSV7Δ*hup*CDG. The templates for the PCR reactions were 3 transformants (lanes 2-4 and lanes 6-8) picked from BHI plus chloramphenicol plates and the mutant *lmo*Δ1960 (lanes 5 and 9). Lane 1 was the Quick-load 1 Kb DNA ladder from New England Biolabs; lanes 2-5 were the PCR reactions using the primers Dhupchk3 and Dhupchk5, the size of the expected PCR products in lanes 2-4 was ~700 bp and ~4.2 kb in lane 5 (too big to amplify); lanes 6-9 were the PCR reactions using the primers D1960chk3 and D1960chk5, the size of the expected PCR products was ~700 bp.

B. Colony PCR to verify the construction of *lmo* Δ 1960/ Δ *hup*CDG. The templates for the PCRs were 6 chloramphenicol sensitive colonies. Lane 1 was the Quick-load 1 Kb DNA ladder from New England Biolabs; lanes 2-7 were the PCR reactions with the primers Dhupchk3 and Dhupchk5; the size of the expected PCR products in lanes 2-7 was ~700 bp (lane 3 did not show PCR product and it turned out later that colony was the single mutant *lmo* Δ 1960).

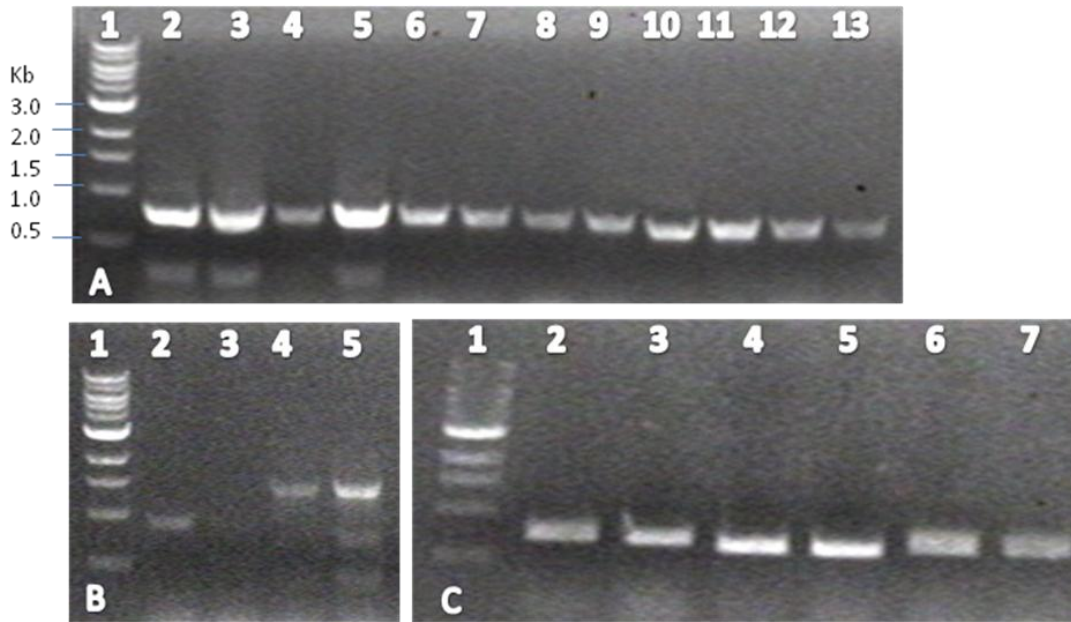


Figure 3.7 Construction of *lmo*Δ2183/Δ*hup*CDG/Δ1960

A. Colony PCR to verify transformation of *lmo*Δ2183/Δ*hup*CDG with pKSV7Δ1960. 4 transformants picked from BHI plus chloramphenicol plates were used as the template for all PCR reactions. Lane 1 was the Quick-load 1 Kb DNA ladder from New England Biolabs; lanes 2-5 were the PCR reactions using the primers D1960chk3 and D1960chk5, the size of the expected PCR product was ~700 bp; lanes 6-9 were the PCR reactions using the primers D2183chk5 and FerDoCla, the size of the expected PCR product was ~700 bp; lanes 10-13 were the PCR reactions using the primers Dhupchk3 and Dhupchk5, the size of the expected PCR products was ~700 bp.

B. Colony PCR to check intergration of pKSV7Δ1960 into the chromosome of *lmo*Δ2183/Δ*hup*CDG. 2 Potential intergrants picked from BHI plus chloramphenicol plates were used as the template for PCR reactions. Lane 1 was Quick-load 1kb DNA ladder from New England Biolabs. The primers for the PCR reactions: lanes 2-3, D1960Int5 and D1960chk3; lanes 4-5, primers D1960chk5 and D1960Int3.

C. Colony PCR to verify the construction of *lmo* Δ 2183/*hup*CDG/*lmo* Δ 1960. The templates for all PCRs were 2 colonies of the triple mutant *lmo* Δ 2183/*hup*CDG/*lmo* Δ 1960. Lane 1 was the Quick-load 1 Kb DNA ladder from New England Biolabs; lanes 2-3 were the PCR reactions with the primers D2183chk5 and FerDoCla; the size of the expected PCR products in lanes 2-3 was ~700 bp; lanes 4-5 were the PCR reactions using the primers Dhupchk3 and Dhupchk5; the size of the expected PCR products in lanes 4-5 was ~700 bp; lanes 6-7 were the PCR reactions using the primers D1960chk3 and D1960chk5; the size of the expected PCR products in lanes 6-7 was ~700 bp.

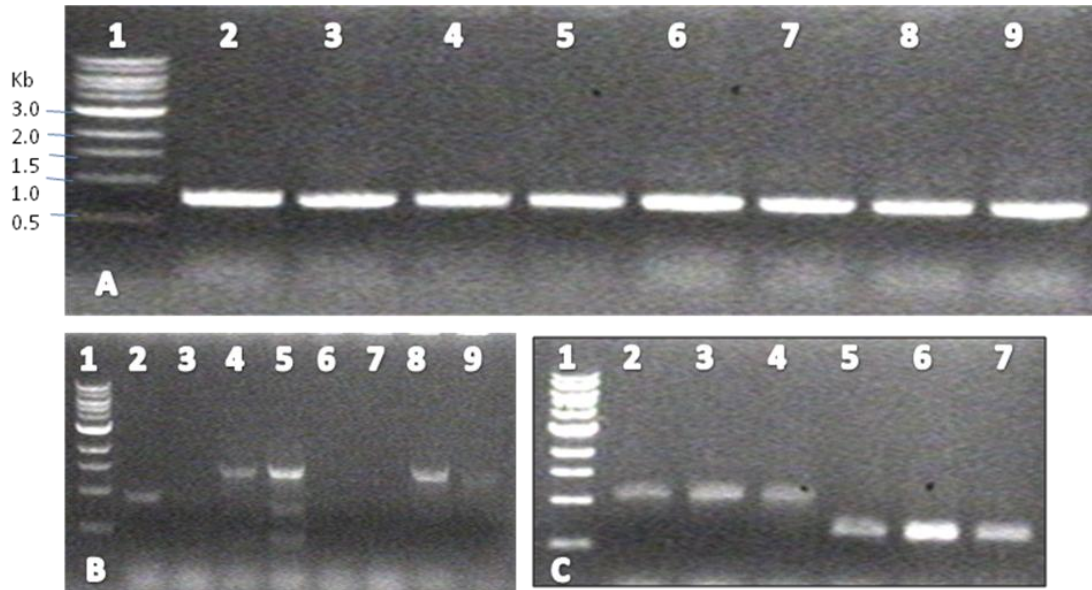


Figure 3.8 Construction of *lmo*Δ2183/Δ1960

A. Colony PCR to verify transformation of *lmo*Δ2183 with pKSV7Δ1960. 4 transformants picked from BHI plus chloramphenicol plates were used as the template for all PCR reactions. Lane 1 was the Quick-load 1 Kb DNA ladder from New England Biolabs; lanes 2-5 were the PCR reactions using the primers D1960chk3 and D1960chk5, the size of the expected PCR product was ~700 bp; lanes 6-9 were the PCR reactions using the primers D2183chk5 and FerDoCla, the size of the expected PCR product was ~700 bp.

B. Colony PCR to check intergration of pKSV7Δ1960 into the chromosome of *lmo*Δ2183. 2 Potential intergrants picked from BHI plus chloramphenicol plates were used as the template for PCR reactions in lanes 6-9 (lanes 2-5 were PCRs to check intergration of pKSV7Δ1960 into the chromosome of *lmo*Δ2183/Δ*hup*CDG, see Figure 3.7 B). Lane 1 was Quick-load 1kb DNA ladder from New England Biolabs. The primers for the PCR reactions: lanes 6-7, D1960Int5and D1960chk3; lanes 8-9, primers D1960chk5 and D1960Int3.

C. Colony PCR to verify the construction of *lmo* Δ 2183/ Δ 1960. The templates for all PCRs were 3 colonies of the double mutant *lmo* Δ 2183/ Δ 1960. Lane 1 was the Quick-load 1 Kb DNA ladder from New England Biolabs; lanes 2-4 were the PCR reactions with the primers D2183Int1 and FerDoCla; the size of the expected PCR products in lanes 2-4 was ~1200 bp; lanes 5-7 were the PCR reactions using the primers D1960chk3 and D1960chk5; the size of the expected PCR products in lanes 5-7 was ~700 bp.

3.3 Complementation of $\Delta hupD$

To follow Koch's postulates, I tried to confirm the role of *hupD* in Hn/Hb uptake by introducing the wild type gene into the mutant $\Delta hupD$ to see whether the wild type ability to transport Hn/Hb could be restored.

First I tried to clone the gene *hupD* together with its native promoter into the vector pKSV7 (Figure 3.9A-D). Then I transferred the newly constructed vector pKSV*hupD* into the mutant $\Delta hupD$ (Figure 3.9 E). However nutrition test with the transformants showed this construction failed to complement $\Delta hupD$ (data not shown). I then switched to another vector, pPL2, for the complementation clone. pPL2 is an *E.coli-Listeria* shuttle vector (Figure 3.10) and successful complementation with pPL2 has been reported (Riedel CU et al, 2007). As I did for the complementation clone of *hupD* with pKSV7, I cloned the gene *hupD* and its native promoter together into pPL2 (Figure 3.11 A-C), transferred this new construction to *E.coli* SM10 (Figure 3.11 D). Through conjugation, pPL2 was transferred from SM10 (donor cell) to *Listeria* (acceptor cell). pPL2 then integrated into the listerial chromosome at the PSA prophage attachment site (Figure 3.11 E). Once integrated, it remains one copy and is highly stable even without the antibiotic pressure. Although the construction of pPL2-pro-*hupD* was confirmed by DNA sequencing (100% matched the original DNA sequence), nutrition tests showed that integration of pPL2-pro-*hupD* into the chromosome of $\Delta hupD$ still failed to restore the ability to uptake Hn/Hb (data not shown). While I was trying to complement $\Delta hupD$ with pPL2, a former graduate student, Dr. Xiaoxu Jiang, succeeded in complementing $\Delta hupC$ and $\Delta hupG$. He cloned the native promoter into the vector pPL2 (we designated this new

construction pPro) and then inserted the gene *hupC* (or *hupG*) right after the native promoter. I utilized this new construction of pPro by inserting the gene *hupD* into the vector at the site right after the promoter of the *hup* operon (Figure 3.12 A). The vector pPro-hupD was then purified, transferred to SM10 strain. However, integration of pPro-hupD into the chromosome of $\Delta hupD$ still failed to complement the mutant (data not shown). I then replaced the native promoter of the *hup* operon by *pclpB* (Figure 3.12 B-C). Again, this construction failed to complement the mutant $\Delta hupD$.

In addition to the complementation clone with pKSV7 and pPL2, I also cloned the gene *hupD* and its native promoter together into another temperature sensitive E.coli-Listeria shuttle vector pMAD (Figure 3.13). Still, this construction did not complement the mutant $\Delta hupD$.

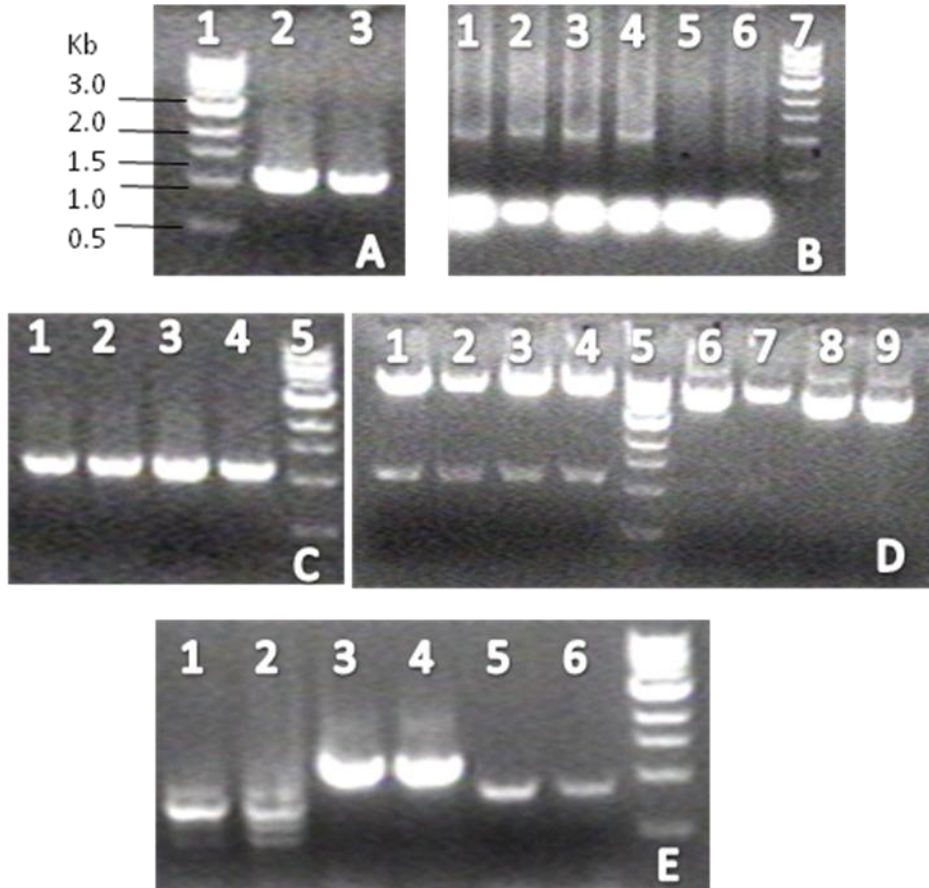


Figure 3.9 Complementation clone of *hupD* with pKSV7

Note: All markers are Quick-load 1 Kb DNA ladder from New England Biolabs.

A. Lane 1, 1 kb DNA ladder; lanes 2 and 3, purified *pro-hupD* fragment with BamHI and PstI restriction sites added to its extremities.

B. Colony PCR to screen potential DH5 α strains harboring the construction of pKSV7-*pro-hupD* with primers pKSVprohupD5 and pKSVhupD3. Lanes 1-4 show right size PCR products.

C. Plasmid PCR using purified vector pKSV7-*pro-hupD* as the template, the primers were pKSVprohupD5 and pKSVhupD3. All show right size PCR product.

D. Lanes 1-4 are digestions of purified pKSV7-pro-hupD with BamHI and PstI restriction enzymes. Lanes 6-9 are purified pPL2-pro-hupD.

E. Colony PCR to verify transformation. 2 transformants picked from BHI plus chloramphenicol plate were used as the template; lanes 1-2 are PCRs with primers DhupDchk1 and DhupDchk2; lanes 3-4 are PCRs with primers pKSVprohupD5 and pKSVhupD3; lanes 5-6 are PCRs with primers LLOchk5 and LLOchk3.

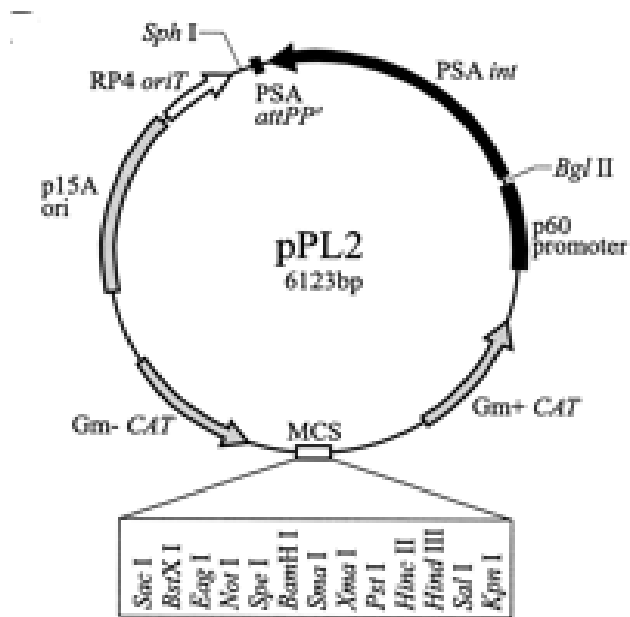


Figure 3.10 Plasmid map of pPL2 (Lauer et al, 2002)

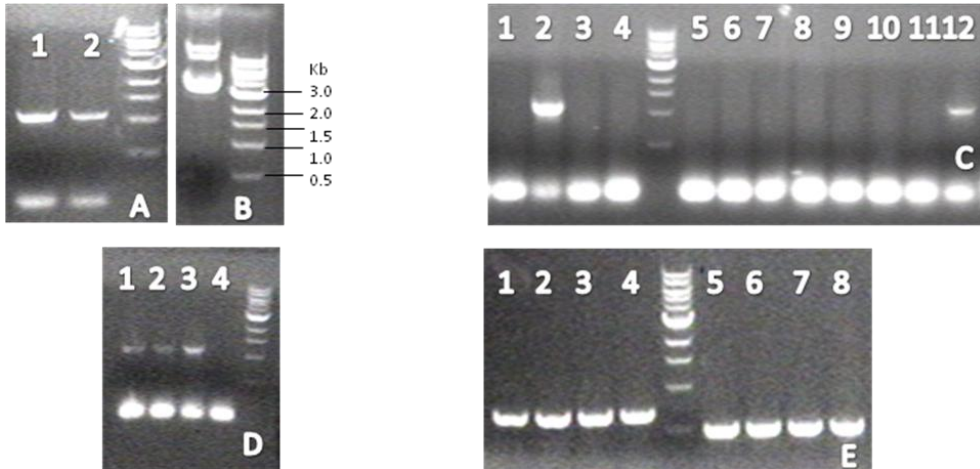


Figure 3.11 Complementation clone with pPL2

A.Lanes 1-2 , purified PCR fragment pro-2431 with BamHI and PstI restriction sites added to the extremities

B.Sample lane, purified vector pPL2

C.Colony PCR to screen potential XL1-Blue colonies harboring the construction of pPL2-pro-2431. 12 colonies were picked from LB plus chloramphenicol plates and served as templates for PCRs. The primers used for PCRs were pro-hupDBamH5 and hupDPst3. Lanes 2 and 12 showed PCR products with right size.

D.Colony PCR to verify transformation of E.coli SM10 with pPL2-pro-2431. Four SM10 colonies were picked from LB plus chloramphenicol plates to be used as the template for PCRS. The same primers as C were used. Lanes 1-3 gave right size PCR products.

E.Colony PCR to check integration of pPL2-pro-2431 into the chromosome of $\Delta hupD$. 4 integrants were picked from BHI plus chloramphenicol and streptomycin plates, boiled and aliquoted to two different groups of PCR reactions. Lanes 1-4 were PCRS with primers DhupDchk1 and DhupDchk2 and lanes 5-9 were PCRS with primers NC16 and PL95. All lanes showed PCR products with right size.

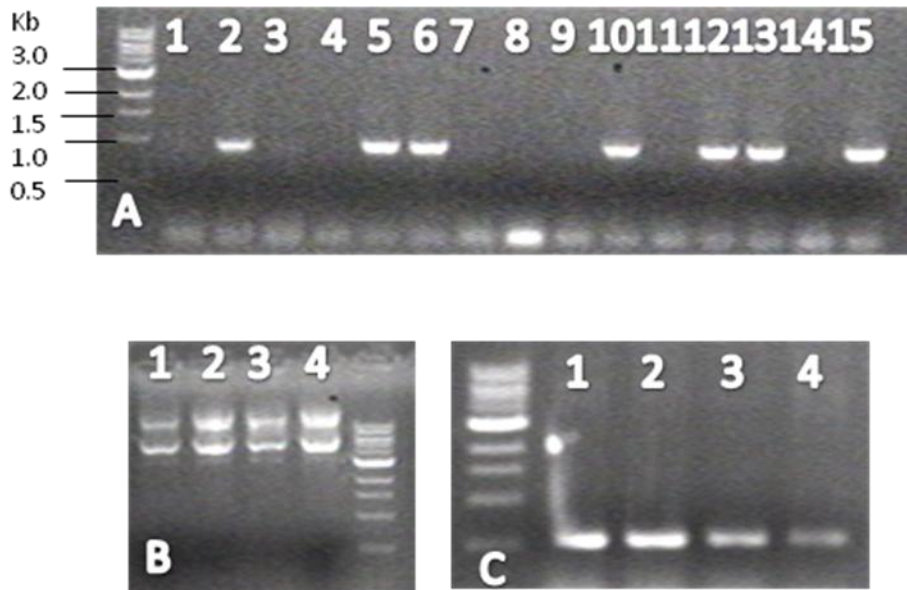


Figure 3.12 Cloning of *hupD* into pPro and replacement of the native promoter

A. Colony PCR to screen potential XL1-Blue colonies harboring pPro-*hupD*. 15 colonies picked from LB plus chloramphenicol plates were used as templates. The primers were *hupDPst5* and *hupDKpn3*. Lanes 2,5,6,10,12,13,15 showed PCR products of right size.

B. Lanes 1-4, purified pPL2-*pclpB-hupD*.

C. Colony PCR to verify transformation of SM10 with pPL2-*pclpB-hupD*. Templates were SM10 colonies picked from LB plus chloramphenicol plates. The primers were *pclpBBamH5* and *Seq2431rev*. All lanes showed right size PCR products.

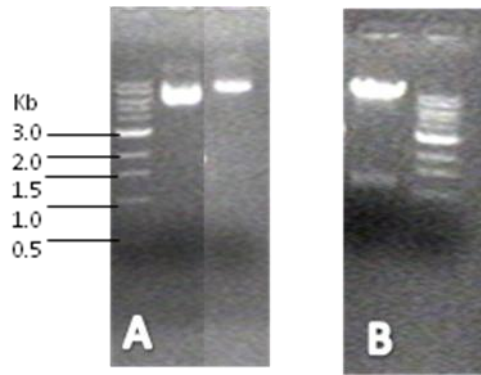


Figure 3.13 Cloning *hupD* and its native promoter into pMAD

Note: The DNA marker in both gels were Quick Load 1 kb DNA ladder from New England Biolabs.

A. The left sample lane was the vector pMAD, the right sample lane was the newly constructed vector pMAD-prohupD.

B. Verify the construction of pMAD-prohupD by digestion with restriction enzymes BamHI and NcoI.

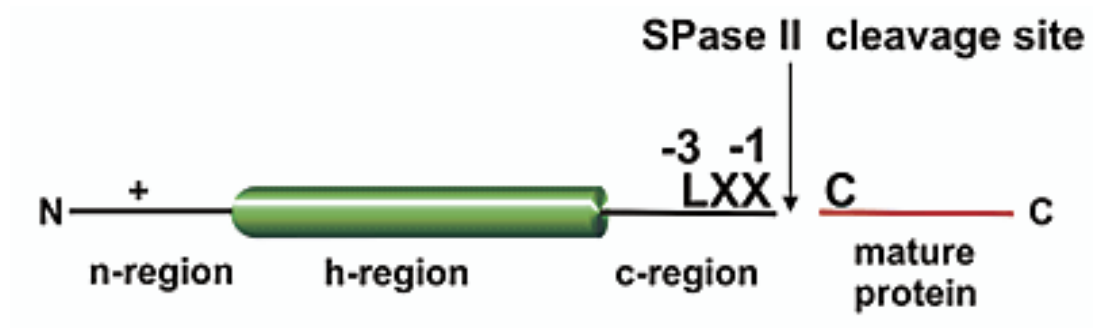
Chapter 4 Characterization of Binding Specificity of HupD

4.1 Expression and purification of HupD

The N-terminus of HupD contains a signal peptidase II recognition sequence (Figure 4.1). In our lab, we previously overexpressed a hydroxymate siderophore binding protein by removing its N terminal signal peptide (Shao's Ph.D dissertation, 2007). I followed this strategy and removed the first eighteen residues of the N-terminus of HupD (MKKITILMLSITAALLLASC, the sequence underlined was removed). As described in "Materials and Methods" section, I used the vector pET28a for cloning and expression (Figure 4.2). Appropriate primers were designed for PCR and the resulting PCR product is a DNA fragment without the sequence encoding those eighteen residues (Figure 4.3A). The fragment was inserted into pET28a (Figure 4.3B, Figure 4.2) and the purified pETHupD Δ 18 was transferred into *E.coli* BL21 cells (Figure 4.3C). However, from the SDS-PAGE we did not see obvious expression of HupD when the cell culture of BL21/pETHupD Δ 18 was exposed to IPTG (data not shown). So I checked its expression by Western immunoblot with anti-Histag antibody and the immunoblot showed expression of HupD (Figure 4.4). We suspected the fact that HupD was not overexpressed was because of the Cys residue at position 20 of the N-terminus. HupD may be anchored to the cytoplasmic membrane through this Cys residue. When HupD was expressed in *E.coli*, anchoring of HupD to the cytoplasmic membrane of *E.coli* may damage the membrane. Thus makes HupD toxic to *E.coli*. To avoid this problem, I further removed 2 more residues (Figure 4.5). This resulted in high-level expression of

HupD as a soluble protein, which facilitated its Ni⁺⁺-NTA chromatographic purification (Figure 4.6).

A. Lipoprotein signal peptide



(Chem Rev.2002. 102(12):4549-80)

B.N-terminus of HupD in EGD-e

MKKITILMLSITAALLLASCGND.....

Figure 4.1 Signal peptidase II recognition sequence of HupD in EGD-e

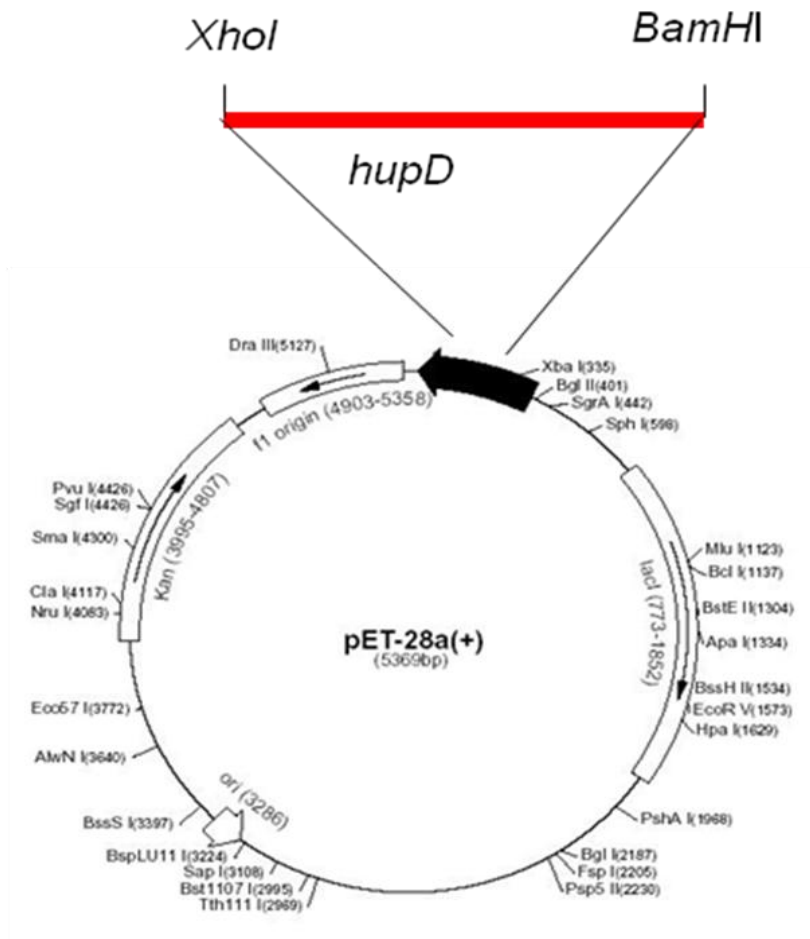


Figure 4.2 Schematic depiction of insertion of the *hupD* fragment into pET28a

(The plasmid map is from Novagen)

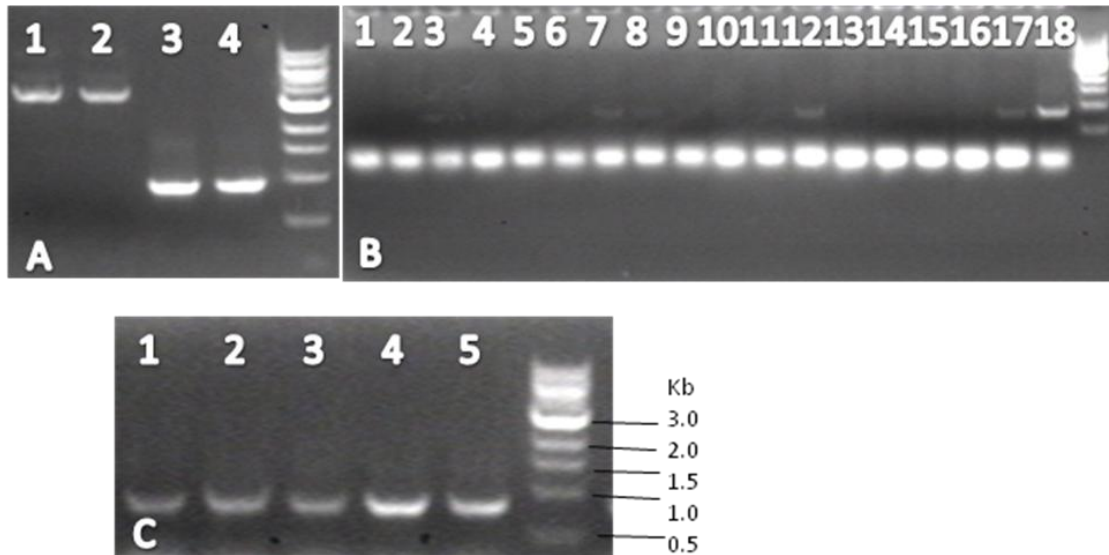


Figure 4.3 Cloning of hupD into pET28a and transformation of BL21 with pETHupDΔ18

Note: all DNA markers are Quick Load 1 Kb DNA ladder from New England Biolabs

A. Lanes 1-2, purified pET28a; lanes 3-4, purified PCR fragment hupDΔ18.

B. Colony PCR with primers hupDpET5(18) and hupDpET3; Templates were DH5α colonies picked from LB plus kanamycin plates; lanes 7,12,17,18 show right size PCR products

C. Colony PCR to verify transformation of BL21 with pETHupDΔ18. Primers were hupDpET5(18) and hupDpET3; Templates were BL21 colonies picked from LB plus kanamycin plates; all lanes show right size PCR products.

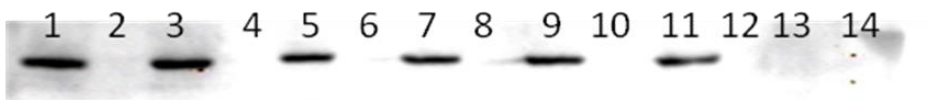


Figure 4.4 HupD expression check by Western Immunoblot with anti-Histag antibody

(Lanes 1-12 were from cell lysates of BL21 harboring pETHupD Δ 18; lanes 13-14 were from cell lysates of BL21 harboring the empty vector pET28a; cells in odd number lanes were exposed to IPTG while cells in even number lanes were not.)

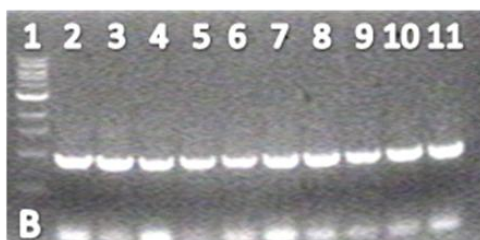


Figure 4.5 Cloning of hupD into pET28a and transformation of BL21 with pETHupD Δ 20

Note: all DNA markers are Quick Load 1 Kb DNA ladder from New England Biolabs

A.Colony PCR with primers hupDpET5(20) and hupDpET3; Templates were DH5 α colonies picked from LB plus kanamycin plates; lanes 11,15,20,21 show right size PCR products

B.Colony PCR to verify transnsformation of BL21 with pETHupD Δ 20. Primers were hupDpET5(20) and hupDpET3; Templates were BL21 colonies picked from LB plus kanamycin plates; all lanes show right size PCR products.

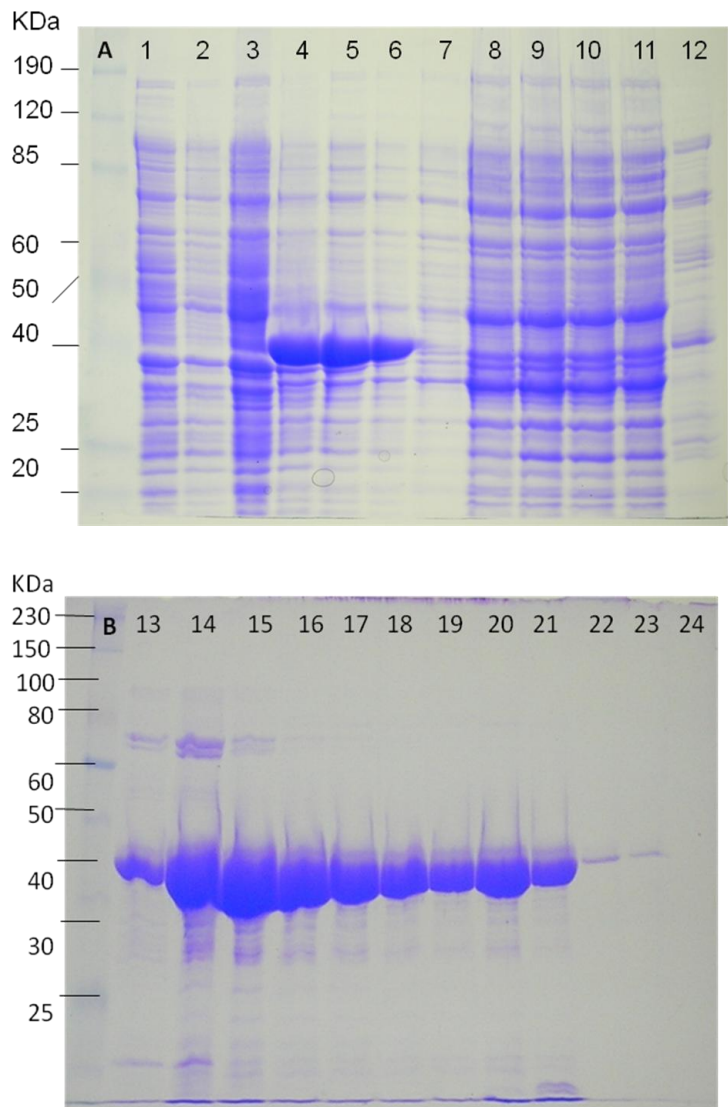


Figure 4.6 Expression and purification of HupD

A. Lanes 1-2 were cell lysates of BL21 harboring the empty vector pET28a, cells from lane 2 were exposed to IPTG while cells from lane 1 were not; lanes 3-5 were cell lysates of BL21 harboring pETHupDΔ20, cells from lanes 4-5 were exposed to IPTG while cells from lane 3 were not, cells from lane 4 were lysed by boiling while cells from lane 5 were lysed by French Press, lane 6 was cytoplasmic extract of BL21/pETHupDΔ20 exposed to IPTG; lanes 7-8 were flow through of the cytoplasmic extract from Ni⁺⁺-NTA agarose; lanes 9-11, elution by 10 mM imidazole; lanes 12, elution by 50 mM imidazole.

B. lanes 13-21, elution by 50 mM imidazole; lanes 22-24, elution by 100-250 mM imidazole.

4.2 Binding specificity of HupD

Listeria HupD is related to *E. coli* FhuD [EcoFhuD; PDB 1ESZ (Clarke *et al.*, 2002)]: they are 17% identical and 57% similar. Both *E. coli* FhuD and Listeria HupD contain Trp: LmoHupD at residue 280; EcoFhuD at residues 43, 68, 102, 210, 217, 255 and 273. EcoFhuD W273, which is situated in the solute binding site, aligns with W280 in LmoHupD.

The presence of Trp in proximity to the binding cavity permitted fluorescence spectroscopic measurements of solute adsorption to purified LmoHupD. As demonstrated from Figure 4.8 B, purified LmoHupD was virtually monospecific: it bound Hn with high affinity ($K_d = 40$ nM), but did not measurably adsorb any of the other iron complexes that we tested (Fc, ferrichrome; FcA, ferrichrome A; FxB, ferrioxamine B; FeEnt, ferric enterobactin). Only PPIX also bound to LmoHupD, but with 30-fold lower affinity ($K_d=1120$ nM), indicating the importance of iron in the recognition reaction. To exclude the possibility that the high affinity of HupD for Hn resulted from the Histag, I also studied the binding specificity of another His-tagged listerial binding protein (LmoFhuD) for Hn. LmoFhuD is the listerial hydroxamate siderophore binding protein. Dr. Yi Shao, a former graduate student, characterized the binding specificity of LmoFhuD and found that the protein recognizes a variety of iron complexes, including Fc, FcA, FxB and FeEnt (Shao's dissertation, 2007; Figure 4.8 A). LmoFhuD showed recognition of Hn, but with a much lower affinity ($K_d=2.9$ μ M) (Figure 4.8 A). Thus the high affinity of LmoHupD for Hn was not due to the Histag.

The high affinity of LmoHupD for Hn was apparent even during its purification. When expressed in *E. coli* DH5 α and purified by Ni⁺⁺-NTA chromatography, solutions of LmoHupD were yellow, red or brown, and their visible spectra showed a Soret peak and other two peaks characteristic of Hn (Figure 4.9). Removal of Hn from LmoHupD required either anion exchange chromatography or SDS-denaturation of the protein (Materials and Methods; Figure 4.7).

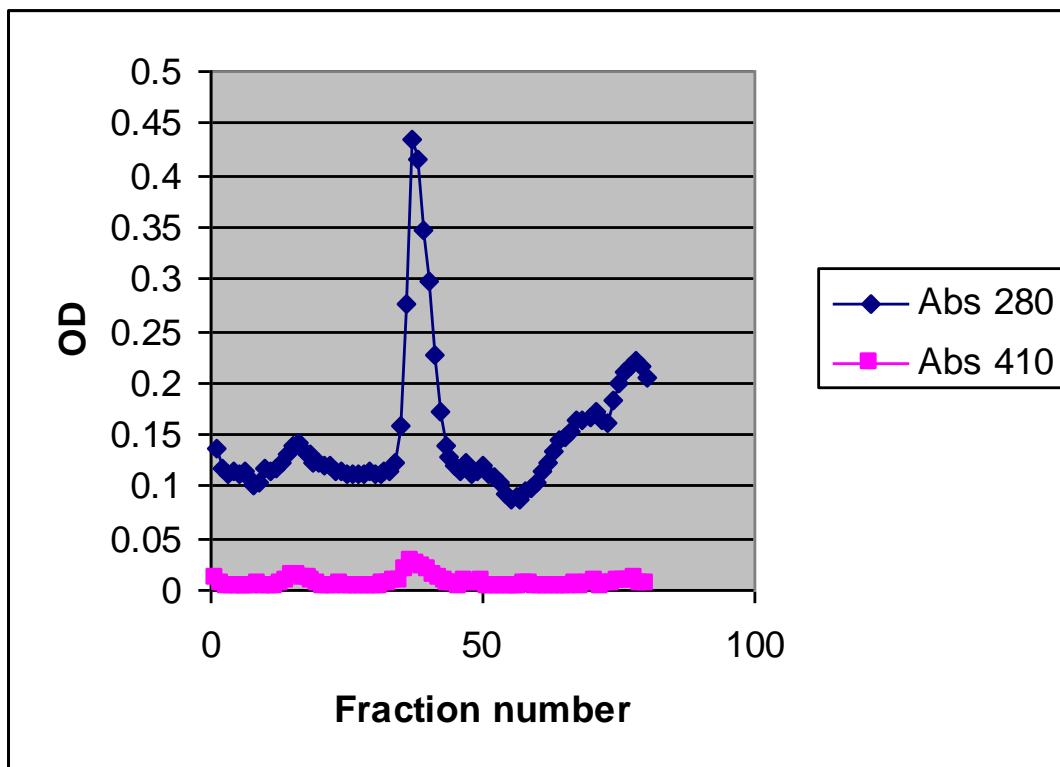


Figure 4.7 Separation of Hn from HupD by SDS-denaturation

HupD fractions purified from Ni⁺⁺-NTA agarose column were colored from yellow to brown. UV-visible wavelength scan indicated HupD purified with bound Hn (Figure 4.8). Removal of Hn from HupD required either anion exchange chromatography (data not shown) or SDS-denaturation of the protein (Materials and Methods).

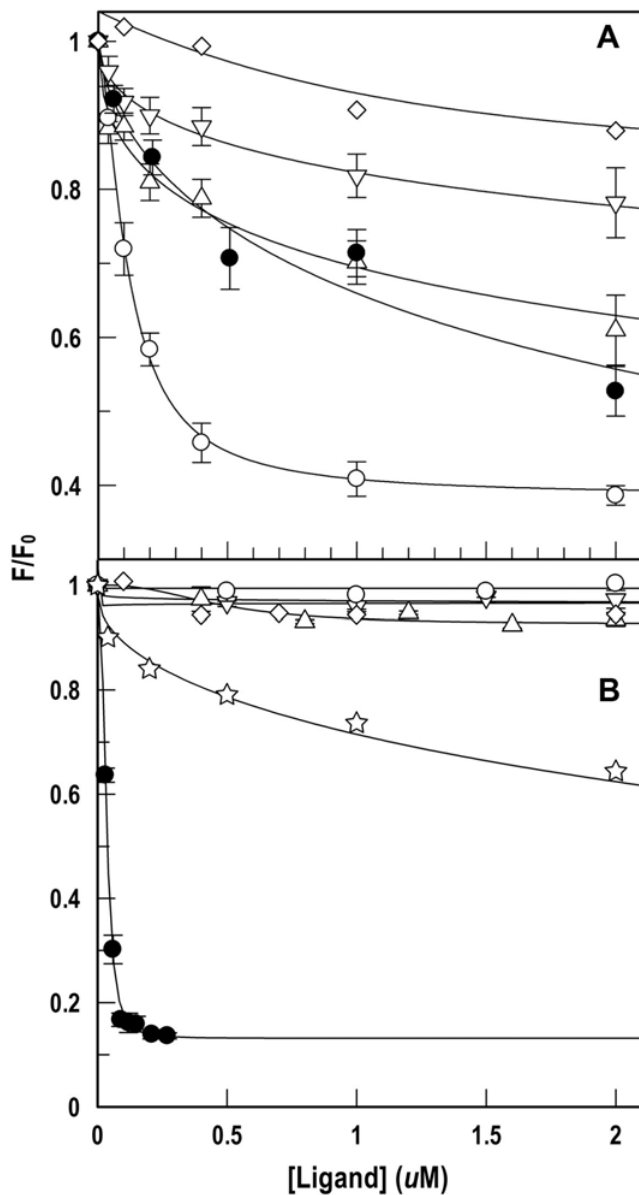


Figure 4.8 Binding specificity of HupD

L. monocytogenes FhuD (Histagged; Shao's dissertation, 2007) and HupD (Histagged) were tested for their ability to bind ferric siderophores and Hn, by monitoring quenching of Trp fluorescence. (Top panel)

FhuD, the ferric hydroxamate binding protein, showed broad recognition of a variety of iron complexes, including Hn, whereas (bottom panel) HupD, the Hn binding protein, was virtually specific for its ligand to the exclusion of all other siderophores [(○) FxB; (Δ) Fc; (▽) FcA; (◇) FeEnt; (●) Hn; (☆) PPIX]. K_d values of the binding interactions for HupD are provided in the text.

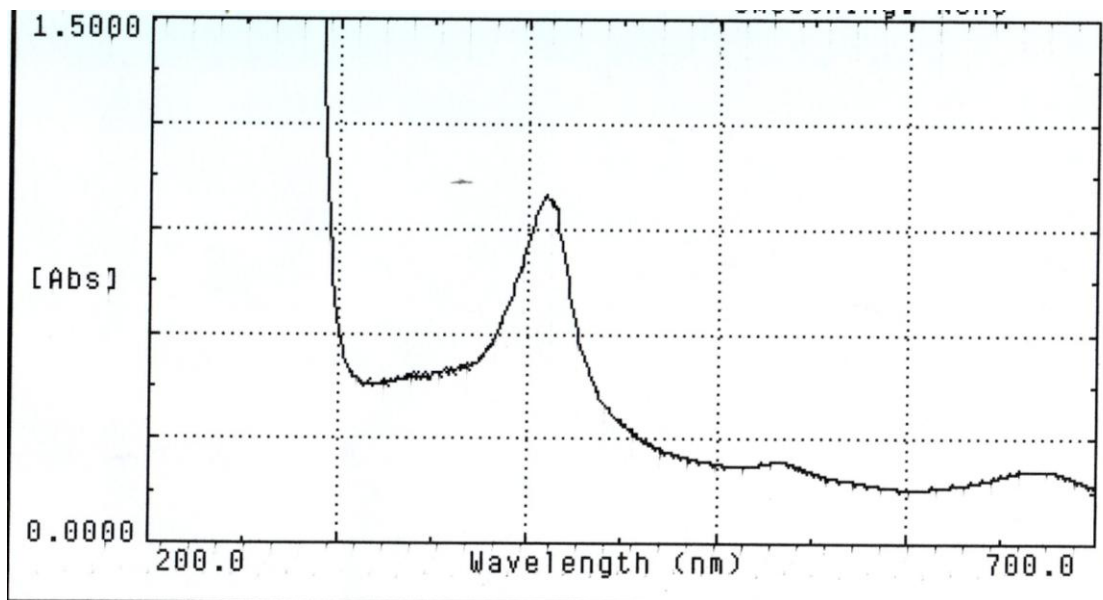


Figure 4.9 UV-visible wavelength scan of purified HupD

Purified solutions of HupD were yellow, red or brown, and their visible spectra showed a Soret peak (~410 nm) and other two peaks (~530 nm and ~670 nm). Together these peaks suggested that the pigment was Hn.

Chapter 5 Hemin Binding and Uptake by *Listeria monocytogenes*

5.1 Putative or demonstrated Hemin uptake systems in *Listeria monocytogenes*

L. monocytogenes actively utilizes both Hn and Hb, and their transport system contributes to its virulence (Jin et al., 2005). Putative or demonstrated Hn uptake systems exist in *S. aureus* (Grigg et al., 2010), *Streptococcus pyogenes* (Lei et al., 2002) and *Bacillus anthracis* (Tarlovsky et al., 2010). In *S. aureus* the *isd* locus has been demonstrated to be involved in Hn/Hb uptake (Mazmanian et al., 2003). It encodes sortase B, a sortase B dependent protein (IsdC), an ABC transporter and other sortase A-dependent PG-associated proteins. The *srtB* locus of *L. monocytogenes* is very similar to the *isd* locus of *S. aureus*, but deletion within this locus did not noticeably influence either Hn or Hb uptake (Jin et al., 2005). For instance, elimination of the sortase B-dependent IsdC homolog Lmo2185 did not impair the ability of *L. monocytogenes* to utilize iron from Hn. Nor did it reduce the virulence of *L. monocytogenes* in a mouse model (Jin et al., 2005). Deletion of *hupC* within *hup* locus, on the other hand, impaired both Hn and Hb uptake and decreased virulence (Jin et al., 2005).

The ambiguities in Hn transport pathway of Gram-positive bacteria necessitates further studies of Hn and Hb uptake by *L. monocytogenes*. We improved the sensitivity of nutrition test, developed protocols to quantitatively characterize the Hn binding and uptake by *L. monocytogenes*. All these efforts finally led to the identification of the

function of the *srtB* locus and the first report of the biochemical parameters of Hn utilization by bacteria.

5.2 Nutrition tests

Although nutrition test is just a qualitative assay, a nice nutrition test can provide us very useful information. We optimized the conditions for nutrition test and developed a new protocol. Comparing to the old protocol of nutrition test (Newton et al, 2005; Jin et al, 2006), the new protocol has two major changes (See Materials and Methods). One is that I added more 2,2-bipyridyl to the media to render the media more iron-deficient. This creates a clean background for the nutrition test and makes the halos much more clear. The other change is about the solvent system for dissolving Hn. Instead of using 50 mM NaOH to dissolve Hn, we adapted to DMSO (Collier *et al*, 1979; Jiang's dissertation, 2009). While in our previous studies only nutrition tests with relatively high concentrations of Hn [200 μ M; (Newton et al, 2005; Jin et al., 2006)] displayed stimulation of the growth of EGD-e, the addition of more bipyridyl to the media and the adaptation to DMSO as the solvent allowed detection of growth stimulation at much lower concentrations (as low as 0.5 μ M for EGD-e). The solubility of Hn in aqueous buffers is poor because Hn may dimerize and precipitate in aqueous solution (Collier *et al.*, 1979, de Villiers *et al.*, 2007, Asher *et al*, 2009). The use of a solvent/buffer system containing DMSO minimized dimerization of Hn, which improved its dissolution in culture media. The higher sensitivity of the nutrition tests made it possible to see the defects of some of EGD-e derivatives in the utilization of Hn.

5.2.1 Nutrition tests with $\Delta hupD$ and Δhup

Once I constructed $\Delta hupD$, I did nutrition test to check whether it has defects in utilization of iron complexes. I tested its ability to utilize ferrichrome (Fc), ferrichrome A (FcA), ferrioxamine B (FxB), Hn and Hb (Figure 5.1). Comparing to the wild type EGD-e, the mutant did not show any defects in utilization of hydroxamate type siderophores (Fc, FcA or FxB) but was severely impaired in Hn/Hb utilization. However, residual Hn/Hb utilization still remained for the mutant. Nutrition tests with the full *hup* operon deletion mutant, Δhup , showed almost exactly the same phenotype with $\Delta hupD$ (Figure 5.1). Together these data suggested a central role the *hup* operon plays in Hn/Hb uptake and the existence of secondary Hn/Hb uptake system(s).

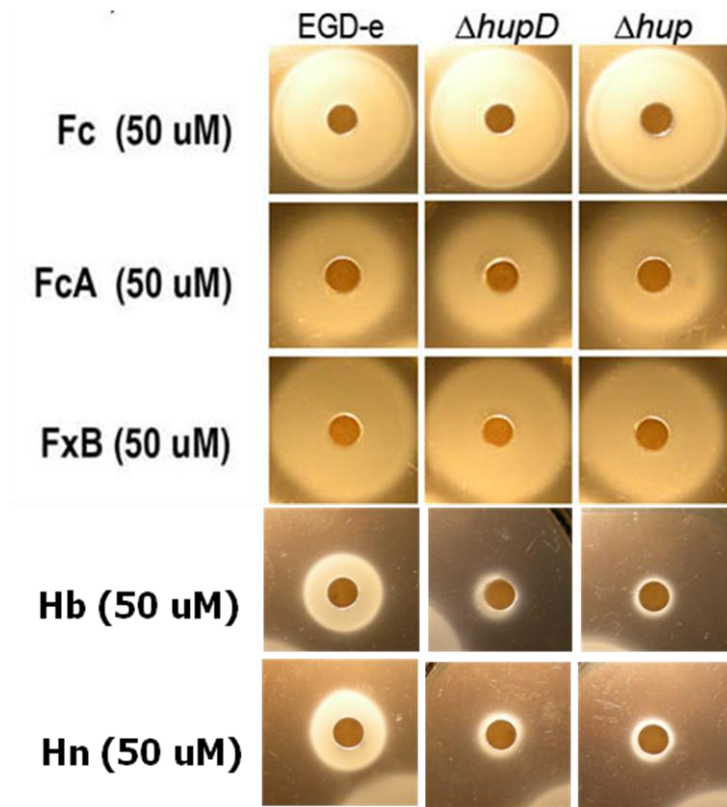


Figure 5.1 Nutrition tests of EGD-e, $\Delta hupD$ and Δhup

EGD-e and mutant strains were grown in BHI, subjected to iron deprivation at mid-log by addition of 1.5 mM bipyridyl, and plated on BHI agar containing 0.25 mM bipyridyl (Materials and Methods). Paper discs were placed on the agar, and 10 μ L of various iron compounds were applied to the discs. $\Delta hupD$ and Δhup was severely impaired in their utilization of Hn and Hb but normally utilized the hydroxamate type siderophores Fc, FcA, FxB.

5.2.2 Nutrition tests with deletion mutants in *srtB* locus and *fhu* locus

The improved sensitivity in nutrition tests provided an opportunity to characterize the deletion mutants that we were not be able to characterize before. Because of the similarity between the *srtB* locus of *L. monocytogenes* and *isd* locus of *S.aureus* and the sequence homology between FhuB/FhuG of *L. monocytogenes* and PhuU (Hn permease) of *Pseudomonas aeruginosa*, I further tested Hn/Hb uptake by deletion mutants in both *srtB* locus ($\Delta 2183$, $\Delta sypA$, $\Delta srtB$) and *fhu* locus ($\Delta 1959$, $\Delta 1960$) with nutrition tests (Figure 5.2). All these deletion mutants and $\Delta 2183/\Delta 1960$, the double mutant across the two locus, displayed obvious impairment in Hn/Hb utilization at 15 uM. While the growth of the wild type EGD-e was still stimulated by addition of either 1.5 uM or 0.5 uM Hn/Hb to BHI top agar, I did not observe any growth stimulation for all these mutants under the same condition. Another mutant strain, $\Delta srtA$ (*srtA* is located outside the *srtB* and *fhu* locus), displayed wild type phenotype in Hn/Hb uptake. This suggests a role of *srtB* and *fhu* locus in Hn/Hb uptake by *L. monocytogenes* and the role of *srtB* locus was further confirmed by [⁵⁹Fe]-Hn binding and uptake assays.

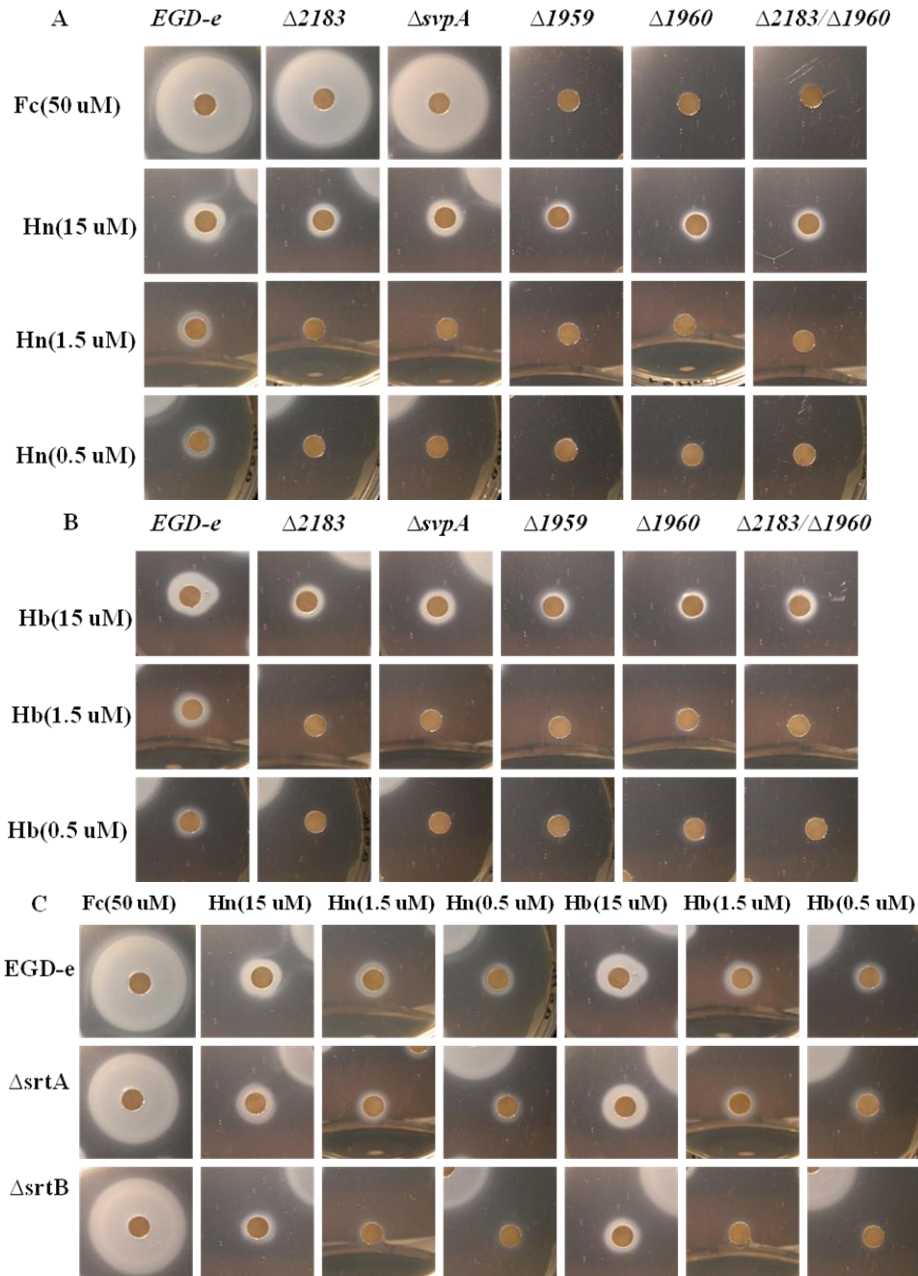


Figure 5.2 Nutrition tests with mutants in *srtB* and *fhu* loci

EGD-e and mutant strains were grown in BHI, subjected to iron deprivation at mid-log by addition of 1.5 mM bipyridyl, and plated on BHI agar containing 0.25 mM bipyridyl (Materials and Methods). Paper discs were placed on the agar, and 10 μ L of various iron compounds were applied to the discs. Mutants in the *fhu* and *srtB* operon had reduced iron supply from Hn and Hb, whereas $\Delta srtA$ showed no reduction in this assay.

5.3 [⁵⁹Fe]-Hn binding and uptake

5.3.1 Development of the [⁵⁹Fe]-Hn uptake protocol

We followed Babusiak's protocol (Babusiak *et al*, 2005; Jiang's dissertation, 2009) for synthesis of [⁵⁹Fe]-Hn. The specific activity of [⁵⁹Fe]-Hn synthesized with this protocol ranged from 250 to 350 cpm/pico mole. This high specific activity of [⁵⁹Fe]-Hn made it possible to quantitatively characterize [⁵⁹Fe]-Hn binding and uptake by *L. monocytogenes*.

I developed the [⁵⁹Fe]-Hn uptake protocol. It was based on the protocol that Dr. Xiaoxu Jiang developed and used (Jiang's dissertation, 2009). There are two main differences between my protocol and Xiaoxu's protocol: one is the time allowed for bacteria to transport [⁵⁹Fe]-Hn and the other is the concentrations of [⁵⁹Fe]-Hn used for [⁵⁹Fe]-Hn uptake assay. The deduction of transport time from 1 hour or 30 minutes to 1 minute eliminated the problem of substrate depletion which occurred at very low concentrations of [⁵⁹Fe]-Hn. This allowed me to observe substrate saturation at very low concentrations (< 5 nM). With 30 minutes or 1 hour transport, it is impossible to see this because the substrate depleted quickly and the transport rates dropped off dramatically as transport proceeded. As a result, the calculated transport rate is no longer the initial transport rate but is much less. The other change is that I did the uptake assay with [⁵⁹Fe]-Hn concentrations ranging from 0.1 nM to 20 nM while Xiaoxu performed the experiments with [⁵⁹Fe]-Hn concentrations ranging from 1 nM to 5000 nM. This change led to the identification of the role of *srtB* locus in Hn uptake by *L. monocytogenes*. Because Hn can diffuse through the peptidoglycan, at higher concentrations (>50 nM) of [⁵⁹Fe]-Hn,

the role of SrtB-anchored Hn binding proteins was obscured because the amount of [⁵⁹Fe]-Hn that diffused through peptidoglycan might be sufficient to saturate CM permease to transport it across the CM. At high concentrations of Hn, it is also possible that a lot of Hn could just intercalate into the CM because of the hydrophobicity and small size (~600 Da) of Hn. All these could obscure the active transport of Hn across the cell envelope.

5.3.2 The *hup* operon in Hn binding and uptake

I synthesized [⁵⁹Fe]-Hn (Materials and Methods) and measured its binding and uptake by EGD-e and its derivatives with deletions in the *hup* operon (Figure 5.3; Table 3.1). When grown in MOPS-L the binding capacity of EGD-e for [⁵⁹Fe]-Hn was 130 pMol/10⁹ cells and the K_d of the binding interaction was 2.4 nM. Complete deletion of the *hup* operon did not eliminate Hn adsorption, but decreased binding capacity by ~20%, to 105 pMol/10⁹ cells. This result suggested the presence of secondary Hn/Hb uptake system(s), and [⁵⁹Fe]-Hn uptake assay confirmed it. For EGD-e the V_{max} of [⁵⁹Fe]-Hn uptake was 23 pMol/10⁹ cells, and its overall uptake K_M was ~1 nM (Fig. 5.3; Table 3.1). As in [⁵⁹Fe]-Hn binding assay, deletion of the *hup* operon did not eliminate [⁵⁹Fe]-Hn uptake. Residual Hn uptake remained when the Hup system was destroyed, but V_{max} decreased to 7.5 pMol/10⁹ cells/min, 27% of the wild type rate. Nevertheless, the overall kinetic and thermodynamic properties of the residual system were similar to those of the wild-type: V_{max} was lower, but K_M was the same (~1 nM). Thus, Hup is not the only Hn uptake system in *L. monocytogenes*. Subtraction of the residual accumulation in Δhup from that of the wild-type gave an estimate of the Hup-dependent uptake rate: V_{max} was 15.5 pMol/10⁹ cells/min.

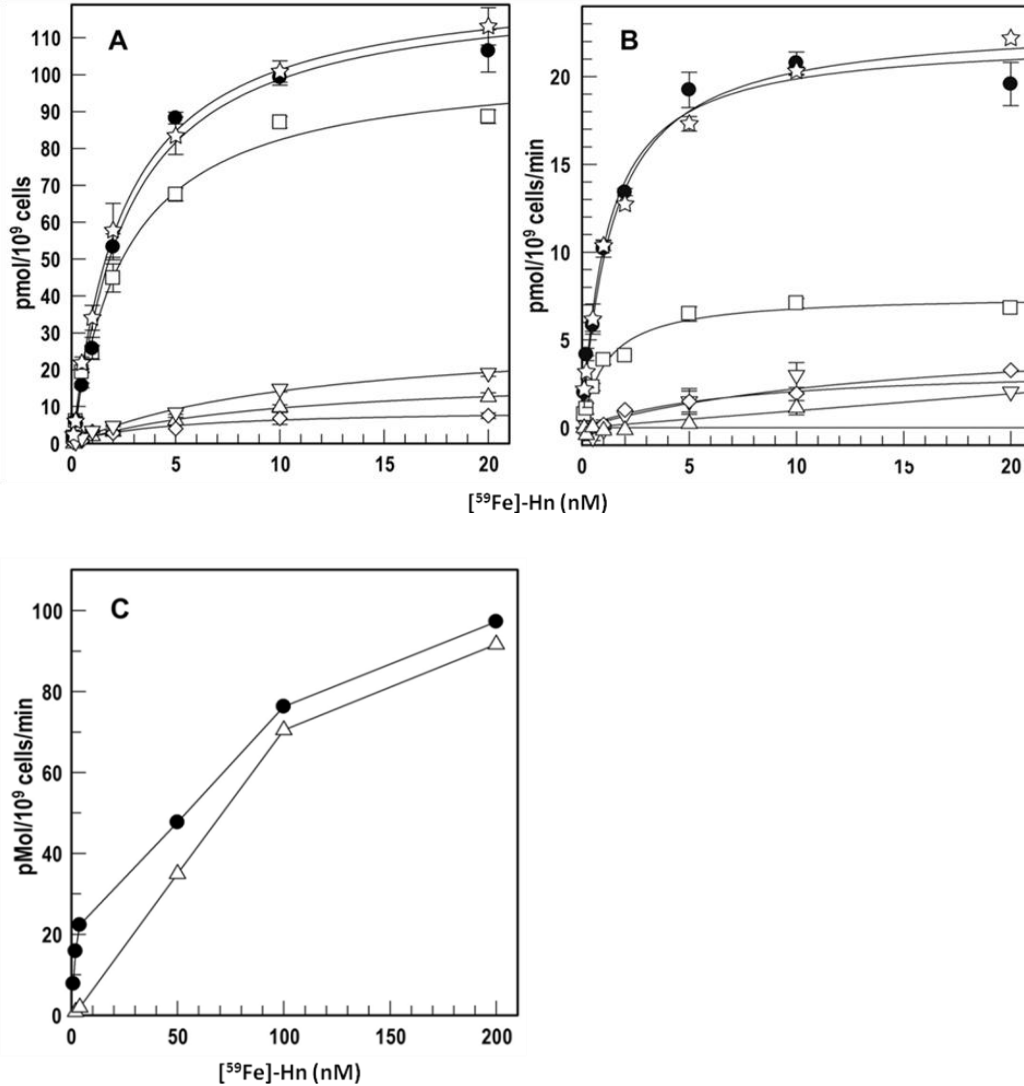


Figure 5.3 $[^{59}\text{Fe}]\text{-Hn}$ binding and uptake by EGD-e and its derivatives

In panels A-C, wild type strain EGD-e (●) or its derivatives carrying the individual mutations Δhup (□), $\Delta srtA$ (☆), $\Delta lmo2185$ (Δ), $\Delta srtB$ (▽) and $\Delta srtAB$ (◇) were grown in BHI, subcultured twice in MOPS-L, and tested for their ability to bind or uptake (Materials & Methods). $[^{59}\text{Fe}]\text{-Hn}$ binding (A) and uptake (B) assays of *L. monocytogenes* revealed impaired Hn acquisition by Δhup , $\Delta srtB$, and $\Delta lmo2185$ at low concentrations of the iron porphyrin, but no obvious effect of $\Delta lmo2185$ at Hn concentrations ≥ 50 nM (C).

Table 5.1 Binding and transport properties of EGD-e and its mutant derivatives

Strain	Binding		Transport	
	K _d (nM)	Capacity (pMol/10 ⁹ cells)	K _M (nM)	V _{max} (pMol/10 ⁹ cells/min)
EGD-e	2.4±0.47	129.5±5.6	1.2±0.2	22.2±0.9
<i>Δhup</i>	2.5±0.45	105±4.2	1.1±0.2	7.5±0.3
<i>ΔsrtA</i>	2.3±0.16	129±1.9	1.4±0.2	23.1±0.6
<i>ΔsrtB</i>	9.9±1.3	18.7±0.9	NS	NS
<i>ΔsrtAB</i>	5.1±3	9±1.5	NS	NS
<i>Δlmo2185</i>	11.4±2.6	30.1±2.9	NS	NS

NS: non-saturation uptake process

5.3.3 Sortase B and Lmo2185 in Hn binding and uptake

The high specific activity of [⁵⁹Fe]-Hn and the successful development of [⁵⁹Fe]-Hn uptake protocol allowed further study of sortase-dependent proteins in Hn acquisition. The product of *lmo2185* (formerly known as SvpA) is secreted into the extracellular environment, but a portion remains anchored to peptidoglycan by sortase B (Newton et al., 2005). Hn associates with Lmo2185 (Newton et al, 2005), so we determined the effect of the $\Delta lmo2185$ and $\Delta srtB$ mutations on utilization of Hn. Their impact was unambiguous in quantitative binding and uptake assays (Figure 5.3; Table 3.1). $\Delta lmo2185$ and $\Delta srtB$ reduced the Hn binding capacity to levels that were about 20% of those seen in EGD-e. At Hn concentrations ≤ 20 nM, both $\Delta lmo2185$ and $\Delta srtB$ displayed no obvious uptake of Hn. However, at Hn concentrations ≥ 50 nM, no obvious defect in [⁵⁹Fe]-Hn uptake was observed for $\Delta lmo2185$ (Figure 5.3 C). In the same tests $\Delta srtA$ did not affect [⁵⁹Fe]-Hn binding K_d nor capacity, nor its transport K_M nor V_{max} . The double mutant $\Delta srtAB$ was indistinguishable from $\Delta srtB$ alone (Figure 5.3; Table 3). Thus, at low concentrations Hn uptake in *L. monocytogenes* was *srtA*-independent, but *srtB*-dependent. At higher concentrations (≥ 50 nM) Hn uptake is *srtB*-independent.

5.4 Expression and localization of HupD in *Listeria monocytogenes*

I cloned HupD into pET28a, overexpressed it in *Escherichia coli* strain BL21, and purified it by Ni⁺⁺-NTA chromatography (Materials and Methods). Mice were immunized with purified HupD and anti-HupD antibody was generated (Materials and Methods).

I then performed Western immunoblots with anti-HupD antibody to evaluate HupD expression under different media conditions (Materials and Methods). The media used in this study included BHI broth, BHI broth plus 1 mM 2,2-bipyridyl, KRM and MOPS-L. Comparing to its expression in BHI broth, HupD was not overexpressed when EGD-e was grown in either KRM or MOPS (Figure 5.4 A). One slight difference observed is that when 1 mM 2,2-bipyridyl was added to BHI broth, the expression of HupD in cytoplasm doubled (Figure 5.4 A). This result also suggested that HupD was very likely localized in the cell envelope of *L. monocytogenes*. The appearance of HupD in the cytoplasmic extract of EGD-e was very likely due to the fact that proteins are synthesized in the cytoplasm.

I also further confirmed deletion of *hupD* and *hup* operon by Western immunoblot (Figure 5.4 B). In agreement with the result of Figure 5.4 A, this result also showed that addition of 2,2-bipyridyl to BHI broth promoted HupD expression. Again, most of the protein HupD was found in the cell envelope extract. As expected, deletion of *hupD* or the *hup* operon eliminated HupD expression from both mutant strains.

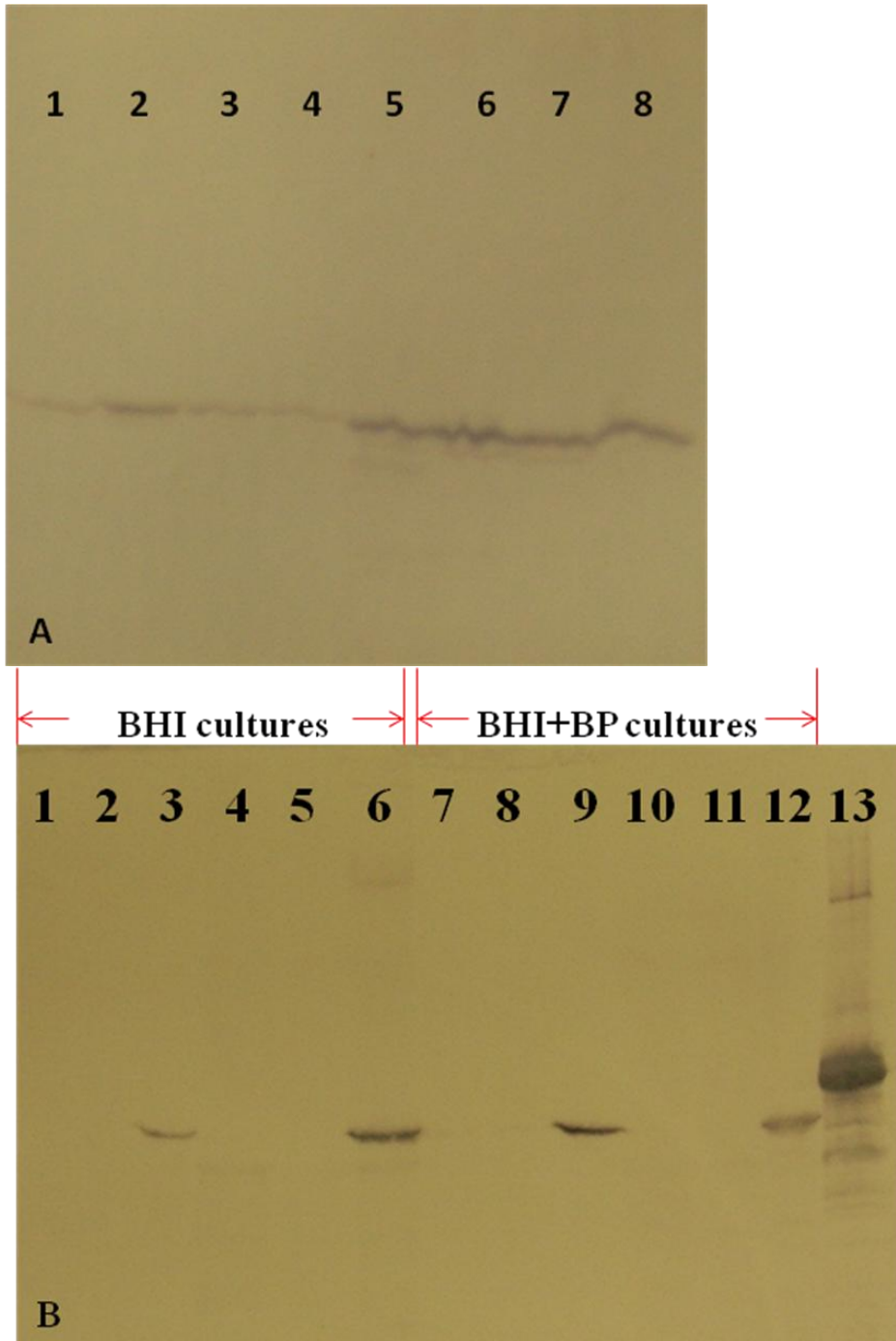


Figure 5.4 Expression and localization of HupD in *L. monocytogenes*

A. Cytoplasmic extracts (lanes 1-4) or cell envelope extracts (lanes 5-8) from EGD-e grown in BHI broth (lanes 1 and 5), BHI broth plus 2,2-bipyridyl (lanes 2 and 6), MOPS-L (lanes 3 and 7) or KRM (lanes 4 and 8) were boiled, loaded to SDS-PAGE (Materials

and Methods). HupD expression was checked by Western immunoblot with anti-HupD antibody (Materials and Methods).

B. Cells were grown either in BHI broth or BHI broth plus 2,2-bipyridyl, as indicated by the picture; cytoplasmic extracts or cell envelope extracts were prepared and subjected to Western immunoblot in the same way as A; lanes 1-3 and lanes 7-9 were cytoplasmic extracts; lanes 4-6 and lanes 10-12 were cell envelope extracts; lane 13 was purified HupD; materials in lane 1,4,7,10 were from Δhup ; materials in lanes 2,5,8,11 were from $\Delta hupD$; materials in lanes 3,6,9,12 were from EGD-e.

Chapter 6 Heme export by *Listeria monocytogenes*

6.1 Potential function of *lmo0641*

According to its annotation, *lmo0641* encodes a protein similar to heavy metal-transporting ATPase (<http://genolist.pasteur.fr/ListiList/>). A research group led by Dr. Cormac Gahan at University College Cork in Ireland was interested in the function of *lmo0641*. They found a “Fur box” preceding the gene *lmo0641*. So they suspected that *Lmo0641* may be involved in iron transport. They made precise, clear deletion of *lmo0641* ($\Delta lmo0641$) using site-directed chromosomal deletion approach (Materials and Methods). They also complemented the deletion ($\Delta lmo0641/comp$) with the vector pPL2 (Materials and Methods). However, after a long time working on this project they still could not identify the function of *Lmo0641*. So they turned to us for help and I started to work on this project.

6.2 Nutrition tests

I did nutrition tests with the strains they provided to search potential defects in iron transport (Figure 6.1). Comparing to the wild type EGD-e, the mutant $\Delta lmo0641$ displayed no defect in the utilization of all iron complexes I tested, including Fc, FcA, FxB, Hn and Hb. However, we noticed that the halos from utilization of Hn and Hb were brighter in the complemented mutant than those in EGD-e. Thus we suspected that *lmo0641* may encode a secondary Hn/Hb uptake system in EGD-e. To test this

hypothesis, I went ahead and made the double mutant $\Delta lmo0641/\Delta hup$. However, nutrition tests with Hn/Hb displayed no difference between the single mutant Δhup and the double mutant $\Delta lmo0641/\Delta hup$ (data not shown).

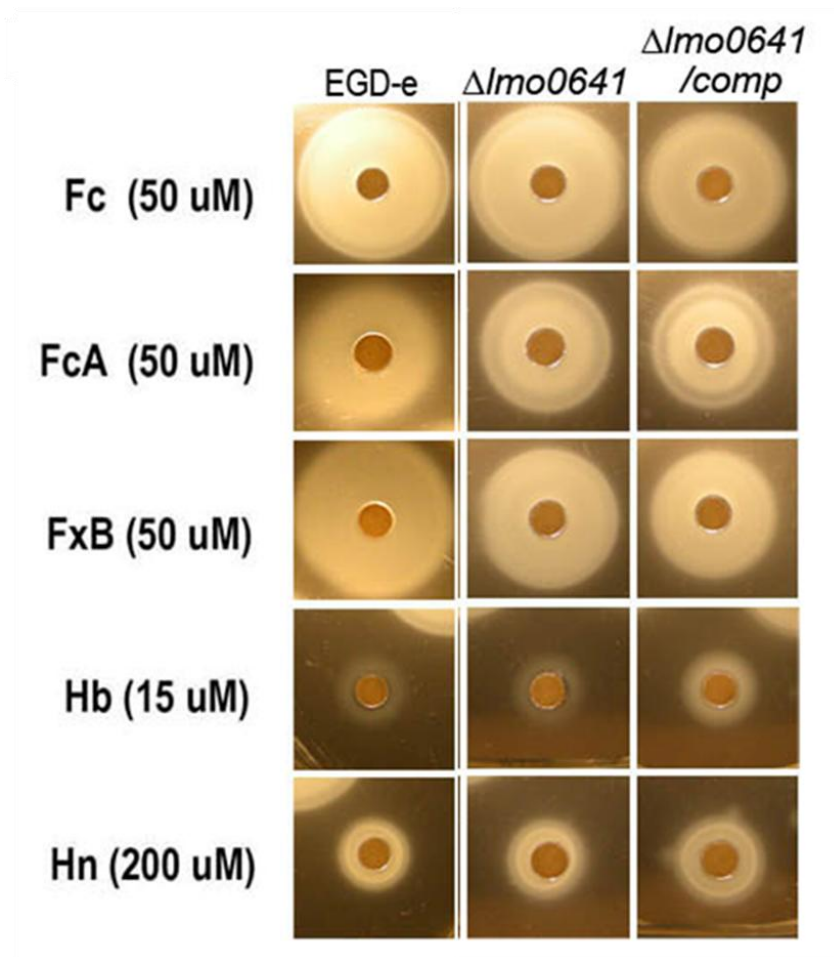


Figure 6.1 Nutrition tests with EGD-e, $\Delta 0641$ and $\Delta 0641/comp$

EGD-e and its derivatives were grown in BHI, subjected to iron deprivation at mid-log by addition of 1.5 mM bipyridyl, and plated on BHI agar containing 0.25 mM bipyridyl (Materials and Methods). Paper discs were placed on the agar, and 10 μ L of various iron compounds were applied to the discs. $\Delta lmo0641$ was indistinguishable from EGD-e, but its complemented strain showed brighter halo for Hn/Hb.

6.3 Growth assays

I also tested the growth of those strains in liquid media, including BHI broth and MOPS-L. Comparing to EGD-e and its complemented strain (*Δlmo0641/comp*), *Δlmo0641* displayed minor defect in growth with BHI broth (Figure 6.2 D). When grown in the iron-deficient medium MOPS-L, the mutant behaved differently from EGD-e: while addition of all tested concentrations of Hn (0.2 uM, 2 uM) or Hb (0.02 uM, 2 uM) to the medium MOPS-L stimulated the growth of EGD-e, growth of *Δlmo0641* was promoted in BHI broth supplemented with 0.2 uM Hn or 0.02 uM Hb but was severely inhibited when the medium was supplemented with 2 uM Hn/Hb (Figure 6.2). On the other hand, under all the conditions tested, *Δlmo0641/comp* behaved almost exactly the same as EGD-e did (Figure 6.2). This indicated defect of *Δlmo0641* in its detoxification of Hn.

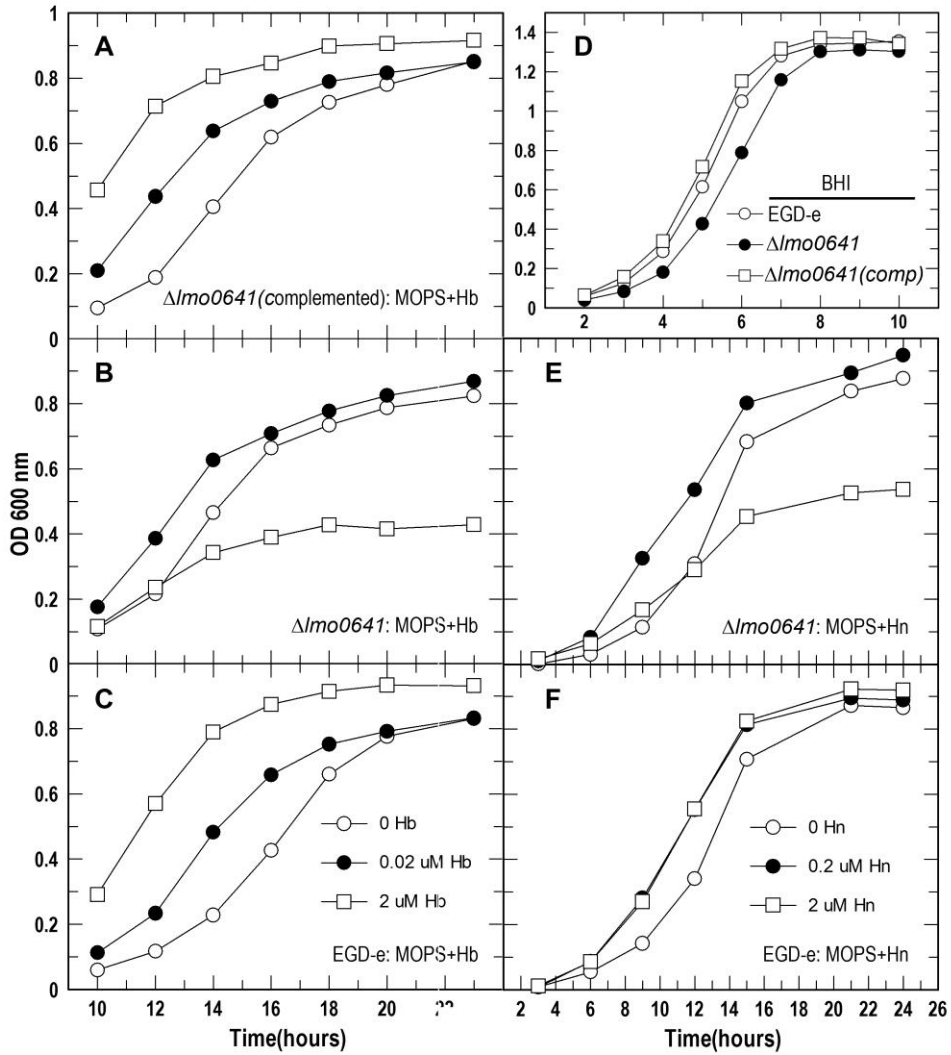


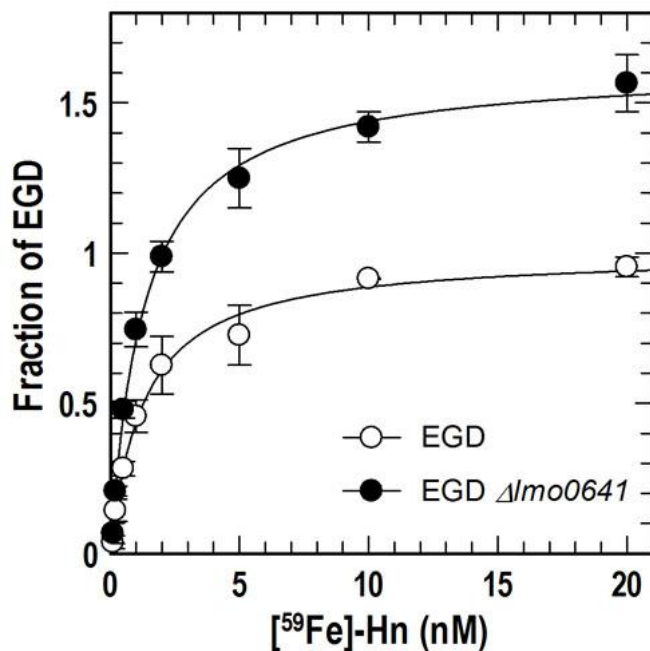
Figure 6.2 Growth of EGD-e and its derivatives in BHI broth and MOPS-L

Cells were grown in BHI overnight, subcultured (1%) into MOPS-L and grown to $OD_{600}=0.9-1$, then subcultured (1%) again into MOPS-L in the presence Hn or Hb at the indicated concentrations. Growth was monitored by optical density at 600 nm.

6.4 Hn uptake

Δlmo0641 was poisoned when grown in MOPS-L supplemented with 2 μM Hn or Hb. This could be due to defects in Hn degradation, Hn storage or active efflux of Hn. Since *Lmo0641* has been annotated as a likely heavy metal-transporting ATPase, we suspected that *lmo0641* may encode a heme exporter. To test this hypothesis, I synthesized [⁵⁹Fe]-Hn and performed [⁵⁹Fe]-Hn uptake assay (Materials and Methods). As expected, the mutant *Δlmo0641* retained more [⁵⁹Fe]-Hn than EGD-e did (Figure 6.3). This 1.6 fold increase in the Vmax of [⁵⁹Fe]-Hn uptake for *Δlmo0641* is very likely resulting from the mutant's defect to actively pump out Hn. The rationale for this is that if *Lmo0641* is a heme oxygenase or heme storage protein, there should be either no difference in the Vmax of [⁵⁹Fe]-Hn uptake between EGD-e and *Δlmo0641* (given the fact that the [⁵⁹Fe]-Hn uptake assay was performed in a way that only allowed 1 minute uptake to occur (Materials and Methods)) or a smaller Vmax for the mutant *Δlmo0641* (if the mutant senses the toxicity of [⁵⁹Fe]-Hn and actively pumps it out of the cell).

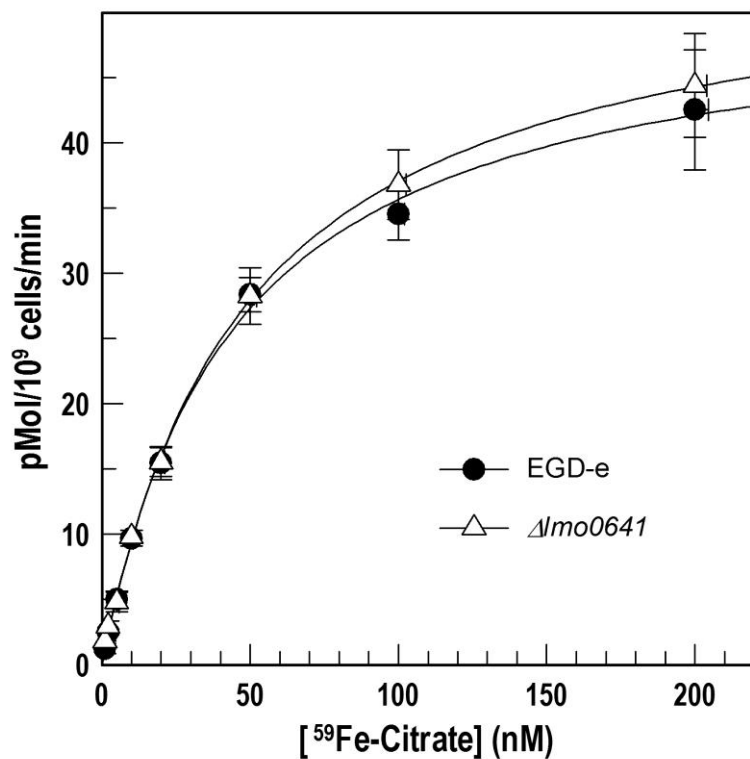
As a control, I also synthesized [⁵⁹Fe]-citrate and performed its uptake experiments (Materials and Methods). As shown in Figure 6.4, the mutant *Δ0641* was indistinguishable from EGD-e: the Vmax of [⁵⁹Fe]-citrate uptake for EGD-e was 51.4 pmol/10⁹ cells/min and 55 pmol/10⁹ cells/min for *Δ0641*; the K_M was 44.2 nM for EGD-e and 48.4 nM for *Δ0641*.



Normalized Data			
EGDe	Parameter	Value	Std. Error
	Vmax	1.0005	0.0314
	Km	1.2829	0.1473
$\Delta 0641$	Parameter	Value	Std. Error
	Vmax	1.6221	0.0324
	Km	1.2730	0.0942

Figure 6.3 [⁵⁹Fe]-Hn uptake by EGD-e and $\Delta lmo0641$

Wild type strain EGD-e or the mutant $\Delta 0641$ were grown in BHI, subcultured twice in MOPS-L, and tested for their uptake [⁵⁹Fe]-Hn (Materials & Methods). The normalized data were from three separate experiments. The Vmaxs of the three experiments for EGD-e were 15.4, 21.2, 19.9 pmol/10⁹ cells/min and 27, 34.9, 29.9 pmol/10⁹ cells/min for $\Delta 0641$. The average of the 3 Vmaxs for EGD-e was 18.8 p mol/10⁹ cells/min and 30.6 p mol/10⁹ cells/min for $\Delta 0641$.



Parameter	Value	Std. Error	
Vmax	51.4230	1.2136	EGD-e
Km	44.2087	2.8661	
Parameter	Value	Std. Error	
Vmax	55.0013	1.0054	Δlmo0641
Km	48.3983	2.3662	

Figure 6.4 [⁵⁹Fe]-citrate uptake by EGD-e and Δlmo0641

Wild type strain EGD-e or the mutant Δlmo0641 were grown in BHI, subcultured twice in MOPS-L, and tested for their uptake of [⁵⁹Fe]-citrate (Materials & Methods). The data presented here were from the average of three separate experiments. The mutant Δlmo0641 was indistinguishable from EGD-e.

Chapter 7 Discussion

The comparative biochemistry of iron uptake through the Gram-positive and Gram-negative cell envelopes is a question of interest. Toward that end the experiments quantitatively characterized, for the first time, the envelope Hn/Hb acquisition systems of *L. monocytogenes*.

In the wild type strain the uptake process was similar to ferric siderophore transport. The steady state Hn uptake rate was nearly identical to that of the listerial CM Fc transporter (FhuDGC: $V_{max}=24 \text{ pMol}/10^9 \text{ cells}/\text{min}$; Jin et al., 2005), which is half the rate of enteric bacterial Fc transport (*E. coli* FhuA: $V_{max}=45 \text{ pMol}/10^9 \text{ cells}/\text{min}$; Newton et al., 2010). The main mechanistic distinction of listerial iron acquisition was lower affinity. For Hn or Fc transport, $K_d \approx K_M \approx 1 \text{ nM}$, 10-fold less than the affinity of ferric siderophore transport systems of *E. coli* [for ferric enterobactin or Fc, $K_d \approx K_M \approx 0.1 \text{ nM}$ (Newton et al., 1999; Scott et al., 2001; Annamalai et al., 2004)]. The latter mechanisms begin with tight binding of metal complexes to the external surfaces of the OM proteins that transport them. My findings and other data (Lei et al., 2002, 2003; Mazmanian et al., 2002, 2003) demonstrate that despite their lack of an OM, Gram-positive cells also employ high-affinity cell surface binding sites for adsorption of iron-containing compounds. The role of Lmo2185 in iron transport was previously in doubt, but the data reported here show that the sortase B-anchored protein adsorbs Hn during the uptake reaction. Therefore, we propose renaming Lmo2185 as Hbp (Hn/Hb binding protein). Nevertheless, the uptake process typified by Hbp is not all-inclusive in Gram-positive bacteria, as TonB-dependent

OM iron (III) transport systems are universal in Gram-negative bacteria. In *L. monocytogenes* ferric siderophores directly adsorb to their CM ABC-transporters (Jin et al., 2005), with about the same affinity as Hn binding to Hbp.

In Gram-positive bacteria the PG matrix forms the biochemical interface with the environment. In *S. aureus*, *B. anthracis*, and *S. pyogenes* sortase-anchored proteins bind Hb in this framework, presumably increasing the efficiency of its capture and subsequent extraction of Hn for delivery to CM transporters. Sortases A and B assemble products of the *isd* locus in the staphylococcal cell envelope (Maresso et al., 2006, Mazmanian et al., 2003). IsdB binds Hb, extracts Hn and transfers it to IsdC, which subsequently passes it to the CM ABC transporter IsdDEF (Mazmanian et al., 2003; Torres et al, 2006; Reniere et al., 2007). The LPXTG sorting signals of IsdA and IsdB make their attachment to PG sortase A-dependent, whereas the NPQTN motif of IsdC dictates its processing by sortase B. According to this scheme the Hn/Hb uptake system of *S. aureus* requires participation of both classes of sortase-anchored proteins. In the *srtB* locus of *L. monocytogenes*, *lmo2186* and *hbp* encode proteins with the NPQTN SrtB sorting motif, that have sequence homology to IsdC (Bierne et al, 2004). Hbp is overproduced in iron-deficient environments and largely excreted, but a fraction becomes anchored to PG (Newton et al., 2005). Both Δhbp and $\Delta srtB$ reduced Hn/Hb utilization in nutrition tests. Quantitative assay further determined that at lower concentrations $\Delta srtB$ and Δhbp reduced the [^{59}Fe]-Hn binding capacity and uptake rate more than Δhup . The Δhbp mutant decreased capacity from 130 pMol/10⁹ cells to 30 pMol/10⁹ cells, while Δhup only dropped it to 105 pMol/10⁹ cells. Thus, at low external concentrations Hbp is the primary Hn adsorption site, responsible for about 80% of Hn binding to *L. monocytogenes*. Direct Hn binding to

Hup accounts for the remaining 20%. Secondly, *Δhbp* caused a 5-fold reduction in Hn binding affinity (K_d increased from 2 nM to ~10 nM), whereas (likely because of its lower abundance) *Δhup* caused no observable change in affinity. So besides being the predominant cell envelope Hn binding constituent, Hbp is also the highest affinity component. Hup is 4-fold less abundant and manifests 5-fold lower affinity for Hn. The estimation of the amounts of Hbp and Hup from [^{59}Fe]-Hn binding capacities agreed with immunoblots (Figure 5.4; Newton et al, 2005) and proteomics data (Ledala et al., 2010). The [^{59}Fe]-Hn uptake results also corroborated our main conclusions from binding studies: when the external concentration of Hn was less than 20 nM, both *ΔsrtB* and *Δhbp* resulted in a non-saturable uptake process and only showed negligible Hn uptake. These data concur with postulates about the SrtB-dependence of Hn/Hb acquisition in *S. aureus* (Maresso et al., 2006, Mazmanian et al., 2003). Additionally, the *ΔsrtA* mutation did not influence listerial Hn/Hb uptake at any concentration in either nutrition tests or [^{59}Fe]-Hn binding and transport measurements, demonstrating that sortase A-anchored proteins play no role in Hn acquisition.

The fact that deletion of the *hup* operon or its individual membrane permease components decreased but did not eliminate Hn uptake implied the existence of secondary CM Hn uptake systems in *L. monocytogenes*. [^{59}Fe]-Hn uptake assays showed residual uptake, for which V_{max} was 7 pMol/ 10^9 cells/min and $K_M \approx 1$ nM. Subtraction of the uptake rates of *Δhup* from those of EGD-e allowed estimation of the kinetic and thermodynamic parameters of the *hup* system itself: $V_{\text{max}} = 16$ pMol/ 10^9 cells/min, and $K_M \approx 1$ nM. Therefore, the Hup permease is the primary CM Hn transporter, in the sense that its steady-state uptake rate is double that of the other system. A secondary CM

transporter exists, whose overall affinity for Hn is similar to that of HupDGC. A second carrier also exists in *S. aureus*, where both Isd and Hts Hn/Hb ABC transporters are thought to function (Skaar et al., 2004). In this sense it's relevant that HupD was monospecific for Hn, while FhuD was promiscuous for iron complexes, including Hn, raising the possibility that the CM ferric hydroxamate transporter (FhuBCDG) provides an auxiliary pathway for Hn uptake.

HupD displayed high affinity for Hn: it was purified with bound Hn. Fluorescence titration assay further quantized the Hn-HupD interaction: the K_d was 40 nM. This affinity is very close to that of *S. aureus* FhuD1 and FhuD2 for ferrichrome ($K_d=50$ nM for FhuD1 and $K_d=20$ nM for FhuD2; Sebulsky et al, 2003, 2004) but significantly higher than that of *E.coli* periplasmic binding protein FhuD for ferrichrome ($K_d=1$ μ M; Rohrbach et al, 1995). The similarity and difference in the affinity of these binding proteins for their cognate ligands suggest that Gram-positive bacteria and Gram-negative bacteria may employ different mechanisms of nutrients uptake, given the fundamentally different architecture of their cell envelope. In general, periplasmic binding proteins of Gram-negative bacteria do not have to evolve high affinity for their cognate ligands because they don't directly serve as surface receptors. On the other hand, the surface receptors anchored on the OM generally have high affinity for their substrates (FepA: $K_d=0.1$ nM; Newton et al,1999; FhuA: $K_d=50$ nM; Locher and Rosenbush, 1997). In the periplasm, the substrates are generally enriched. However, Gram-positive bacteria don't have a periplasm and their CM-anchored proteins may directly serve as surface receptors (Sebulsky et al, 2001, 2003, 2004). Therefore, it may be necessary for Gram-positive bacteria to have high affinity substrate binding proteins anchored on the CM to serve as

surface receptors. Due to high toxicity of Hn, in animal body fluids free Hn concentration has always been maintained at a low level (Wandersman and Delepelaire, 2004; Tong and Guo, 2009). This entails the high affinity of listerial HupD for Hn, if it serves as a surface receptor. Interestingly, both FhuD1 and FhuD2 are covalently attached to the CM of *S.aureus* (Sebulsky et al, 2001, 2003, 2004) through the Cys residue at the very end of their N-termini, which is likely also the case for HupD of *L. monocytogenes*. Taken together, the high affinity of these demonstrated or potentially CM-anchored binding proteins for their cognate ligands suggests that they may directly serve as surface receptors. In supporting this hypothesis, my binding and uptake data showed that when external Hn concentration is above 50 nM, $\Delta lmo2185$ imported Hn as efficiently as the wild type EGD-e (Figure 5.3). Additionally, previous reports demonstrated that in *L. monocytogenes* and *S.aureus* ferrichrome directly adsorbed to its CM ABC-transporters (Jin et al., 2005; Sebulsky et al, 2003, 2004).

While Hn is an indispensable cofactor for many enzymes, it is also highly toxic. Intracellular Hn concentration is thus tightly regulated. As an intracellular pathogen, *L. monocytogenes* may be exposed to high concentrations of heme iron sources, for example, upon erythrocyte lysis at the infection site. This could lead to rapid accumulation of intracellular Hn, necessitating its detoxification. While exposure of *S. aureus* $\Delta hrtA$ (or $\Delta hrtB$) to 10 μ M Hn *in vitro* severely inhibited its growth (Torres et al, 2007), the growth of EGD-e $\Delta 0641$ was greatly inhibited when it was exposed to 2 μ M Hn/Hb, suggesting its relatively higher sensitivity to Hn toxicity. Under the same conditions, $\Delta 0641$ accumulated 1.6 fold higher amount of [59 Fe]-Hn (Figure 6.3) than that accumulated by the wild type EGD-e, suggesting deficiency in Hn export by $\Delta 0641$. The

identification of a potential Hn export in *L. monocytogenes* together with other findings in this study, including the demonstration of the role of the *srtB* locus in Hn/Hb uptake, and the primary cytoplasmic membrane Hn transport system (Hup system), suggested a conserved Hn utilization mechanism between *L. monocytogenes* and *S.aureus*.

Chapter 8 Binding of peptidoglycan to TonB

8.1 Sequence relationship between TonB and YcfS

Dr. Klebba made analysis of the sequence of the TonB C terminus and found homology to *E. coli ycfS*, which encodes a 320-amino-acid, proline-rich (8.4%) protein with a calculated mass of 34.6 kDa. YcfS is a member of a family of putative periplasmic proteins (Bateman and Bycroft, 2000) of unknown function that contains a signal peptide (residues 1 to 23) followed by a hydrophobic, potential IM anchor, a lysin (LysM) motif (residues 45 to 91) that confers affinity for PG (Bateman and Bycroft, 2000; Steen et al, 2003), and a central proline-rich sequence. YcfS and its *E. coli* paralogs YnhG, YbiS, and ErfK form a family of cell envelope proteins. Each one, composed of approximately 320 amino acids, has an N-terminal hydrophobic region (putative transmembrane helix), a PG-binding domain (LysM) in the first third of primary structure, and a high percentage of proline residues (8 to 10%, roughly twice that of most proteins and half as much as TonB). These attributes bear similarities to those of TonB, another proline-rich (16.7%) periplasmic protein that contains a hydrophobic N-terminal sequence, postulated to act as an IM anchor. CLUSTALW comparison of the *E. coli* LysM motif and the primary structure of TonB mapped a homologous region in the C terminus of TonB (residues 175 to 231; Figure 8.1). Although the sequences of the 48-residue LysM motif and the C-terminal 69 amino acids of TonB are not highly conserved (19% identity, 77% homology), low overall identity is typical among LysM-containing, PG-binding cell envelope proteins (Parsons et al, 2006; Steen et al, 2003). In this alignment, it was noteworthy that D11 in LysM, at the center of the PG-binding surface (Bateman and

Bycroft, 2000), corresponded with D189, on the exterior surface of the TonB C terminus. The structural homology between the LysM motif and regions of the TonB C terminus raised the possibility of an affiliation between TonB and the murein sacculus.

8.2 Peptidoglycan precipitated MalE-TonB69C

To test this prediction, we purified sacculi from *E. coli* by SDS extraction (Kaserer et al, 2008) and evaluated their ability to adsorb MalE-TonB69C. The purified PG fraction was free of cell envelope proteins, including the major proteins and iron-regulated LGP, as indicated by SDS-PAGE (Figure 8.2) and by its transparency at 280 nm (data not shown). The purified sacculi precipitated MalE-TonB69C from solution, but not MalE nor FepB (Figure 8.2). The binding reaction manifested saturation behavior: increasing amounts of PG bound and precipitated increasing amounts of MalE-TonB69C to a plateau value. The control proteins were themselves biologically active: maltose-binding protein was purified by amylase affinity columns, and chromatographically purified FepB (Sprenzel et al, 2000) bound FeEnt (data not shown). Therefore, the affinity of TonB for PG was not a general characteristic of periplasmic proteins, but a specific attribute of TonB itself.



Figure 8.1 CLUSTALW analysis of YcfS homologs (adapted from: Kaserer et al, 2008)

CLUSTALW was used to align the sequence of the LysM motif from the *E. coli* membrane-bound lytic murein transglycosylase D (MltD), which is structurally solved as an $\alpha\beta$ domain (Bateman and Bycroft, 2000), to the *E. coli* proteins YcfS, YbiS, YnhG, ErfK, and to the TonB C terminus. The figure shows the alignment of the relevant regions of the four proteins, and the consensus sequence (Cons) from the analysis. Hydrophilic residues are colored green, acidic residues are blue, basic residues are magenta, and hydrophobic residues are red. The consensus is also aligned to the sequence of the crystallized LysM domain of MltD. LysM alignment to TonB identified a sequence relationship at the C terminus of TonB. Asp 11 in LysM (blue), which denotes the PG-binding surface in its structure (Bateman and Bycroft, 2000), aligns with TonB residue Asp 189.

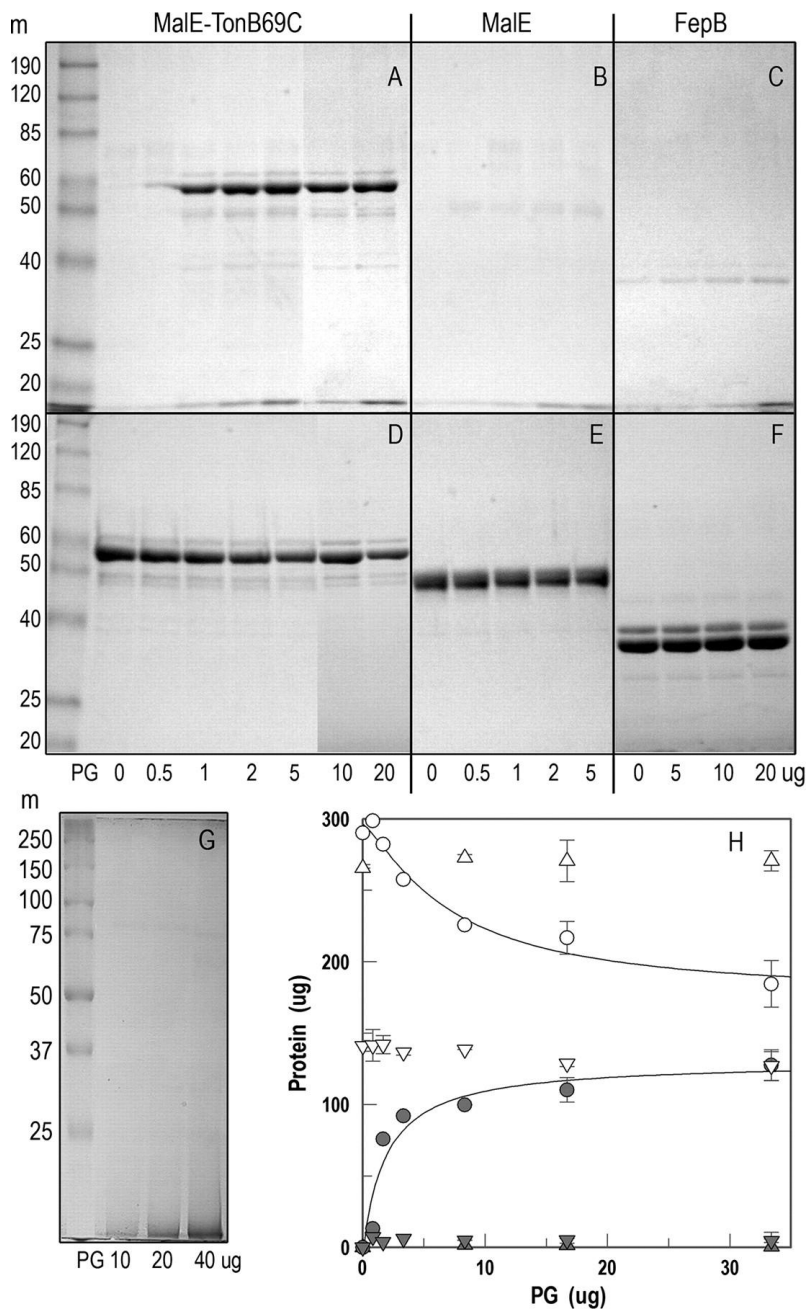


Figure 8.2 Affinity of the TonB C terminus for PG

(A to F) Purified *E coli* PG was suspended in distilled water at 1.7 mg/ml. Increasing amounts of the PG solution were mixed with 30 μ g of purified proteins MalETonB69C, MalE, and FepB in a final volume of 100 μ L, incubated for 30 min at room temperature, and subjected to ultracentrifugation (100,000 g , 45 min). The pellets (A to C) and

supernatants (D to F) were resolved by SDS-PAGE, and the gels were stained with Coomassie blue. The positions of molecular size markers (m) (in kilodaltons), the BenchMark prestained protein ladder (Invitrogen), are shown to the left of the gels. Panels A and D are composite pictures from two separate experiments; the amount of added PG (in micrograms) is denoted beneath each lane. (G) SDS-PAGE of purified PG. Aliquots of the solution of purified sacculi were subjected to SDS-PAGE, and the gel was stained with Coomassie blue. The positions of molecular weight markers (m) (in kilodaltons), Precision Plus protein standards (Bio-Rad), are shown to the left of the gel. (H) Quantification of MalE-TonB69C precipitation in pellets and depletion from supernatants by PG. SDS-polyacrylamide gels were photographed, and the images were quantified using ImageQuant (Molecular Dynamics). Filled symbols are derived from analysis of pellets, while open symbols are derived from analysis of supernatants: MalE-TonB69C (circles) was precipitated, while MalE (inverted triangles) and FepB (triangles) were not precipitated by PG. The quantities of protein and PG (in micrograms) are shown on the y and x axes. The graph depicts the means standard errors (error bars) from two experiments.

References

- Aiba H.** 2007. Mechanism of RNA silencing by Hfq-binding small RNAs. *Curr Opin Microbiol* **10**:134-139.
- Andrade M.A, F.D. Ciccarelli, C. Perez-Iratxeta, P. Bork.** 2002. NEAT: a domain duplicated in genes near the components of a putative Fe³⁺ siderophore transporter from Gram-positive pathogenic bacteria. *Genome Biol* **3**:1–9 (Research 0047.).
- Annamalai, R., B. Jin, Z. Cao, S. M. Newton & P. E. Klebba.** 2004. Recognition of ferric catecholates by FepA. *J Bacteriol* **186**: 3578-3589.
- Arnoux P, Haser R, Izadi N, Lecroisey A, Delepierre M, Wandersman C, Czjzek M.** 1999. The crystal structure of HasA, a hemophore secreted by *Serratia marcescens*. *Nat Struct Biol* **6**:516–520.
- Arnoux P, Haser R, Izadi-Pruneyre N, Lecroisey A, Czjzek M.** 2000 Functional aspects of the heme bound hemophore HasA by structural analysis of various crystal forms. *Proteins* **41**:202–210.
- Arnaud M, Chastanet A, Débarbouillé M.** 2004. New vector for efficient allelic replacement in naturally nontransformable, low-GC-content, gram-positive bacteria. *Appl Environ Microbiol.* **70**(11):6887-91.
- Asher, C., K. A. de Villiers, et al.** 2009. Speciation of ferriprotoporphyrin IX in aqueous and mixed aqueous solution is controlled by solvent identity, pH, and salt concentration. *Inorg Chem* **48**: 7994-8003
- Babusiak M, Man P, Sutak R, Petrak J, Vyoral D.** 2005. Identification of heme binding protein complexes in murine erythroleukemic cells: study by a novel two-dimensional native separation -- liquid chromatography and electrophoresis. *Proteomics* **5**(2):340-50.
- Bateman, A., and M. Bycroft.** 2000. The structure of a LysM domain from *E. coli* membrane-bound lytic murein transglycosylase D (MltD). *J. Mol. Biol.* **299**:1113–1119.
- Bates C.S., G.E. Montanez, C.R. Woods, R.M. Vincent, Z. Eichenbaum.** 2003. Identification and characterization of a *Streptococcus pyogenes* operon involved in binding of hemoproteins and acquisition of iron. *Infect. Immun.* **71**: 1042–1055
- Bearden S.W., Staggs T.M., Perry R.D.** 1998 An ABC transporter system of *Yersinia pestis* allows utilization of chelated iron by *Escherichia coli* SAB11. *J Bacteriol* **180**: 1135–1147

- Bergmann B., Raffelsbauer D., Kuhn M., Goetz M., Hom S., Goebel W.** 2002 InlA-but not InlB-mediated internalization of *Listeria monocytogenes* by non-phagocytic mammalian cells needs the support of other internalins. *Mol Microbiol* **43**: 557–570.
- Bierne, H., S. K. Mazmanian, M. Trost, M. G. Pucciarelli, P. Dehoux, L.Jansch, F. G. Portillo, L. G., O. Schneewind, and P. Cossart.** 2002a. Inactivation of the *srtA* gene in *Listeria monocytogenes* inhibits anchoring of surface proteins and affects virulence. *Mol. Microbiol.* **43**:869–881.
- Bierne H., Cossart P.** 2002b. InlB, a surface protein of *Listeria monocytogenes* that behaves as an invasin and a growth factor. *J Cell Sci* **115**: 3357–3367.
- Bierne, H., C. Garandeau, M. G. Pucciarelli, C. Sabet, S. Newton, F. Garcia-del Portillo, P. Cossart, and A. Charbit.** 2004. Sortase B, a new class of sortase in *Listeria monocytogenes*. *J. Bacteriol.* **186**:1972–1982
- Borths EL, Locher KP, Lee AT, Rees DC.** 2002. The structure of *Escherichia coli* BtuF and binding to its cognate ATP binding cassette transporter. *Proc Natl Acad Sci U S A.* **99**(26):16642-7.
- Bracken CS, Baer MT, Abdur-Rashid A, Helms W, Stojiljkovic I.** 1999. Use of heme-protein complexes by the *Yersinia enterocolitica* HemR receptor: histidine residues are essential for receptor function. *J Bacteriol.* **181**(19):6063-72
- Braun, V., H. Killmann.** 1999. Bacterial solutions to the iron-supply problem. *Trends Biochem Sci* **24**:104-9.
- Braun V, Mahren S, Ogierman M.** 2003. Regulation of the FecI-type ECF sigma factor by transmembrane signalling. *Curr Opin Microbiol* **6**:173–80.
- Braun V.** 2005 Bacterial iron transport related to virulence. *Contrib Microbiol* **12**: 210–233
- Braun V, Herrmann C.** 2007. Docking of the periplasmic FecB binding protein to the FecCD transmembrane proteins in the ferric citrate transport system of *Escherichia coli*. *J Bacteriol* **189**(19):6913-8.
- Brett PJ, M.N. Burtnick, J.C. Fenno, F.C. Gherardini.** 2008. *Treponema denticola* TroR is a manganese- and iron-dependent transcriptional repressor. *Mol. Microbiol* **70**:396–409
- Brickman TJ, Anderson MT, Armstrong SK.** 2007. *Bordetella* iron transport and virulence. *Biomaterials* **20**(3-4):303-22

Buchanan SK, Smith BS, Venkatramani L, Xia D, Esser L, Palnitkar M, Chakraborty R, van der Helm D, Deisenhofer J.1999 Crystal structure of the outer membrane active transporter FepA from *Escherichia coli*. *Nat Struct Biol.* **6**(1):56-63.

Burkhard K.A., A. Wilks. 2008. Functional characterization of the *Shigella dysenteriae* heme ABC transporter. *Biochemistry* **47**: 7977–7979

Caillet-Saguy C, Delepierre M, Lecroisey A, Bertini I, Piccioli M, Turano P.2006 Direct-detected ¹³C NMR to investigate the iron(III) hemophore HasA. *J Am Chem Soc.* **128**(1):150-8

Caillet-Saguy C, Piccioli M, Turano P, Izadi-Pruneyre N, Delepierre M, Bertini I, Lecroisey A. 2009. Mapping the interaction between the hemophore HasA and its outer membrane receptor HasR using CRINEPT-TROSY NMR spectroscopy. *J Am Chem Soc.* **131**(5):1736-44

Carrano, Carl J., Kenneth N. Raymond. 1979. Ferric Ion Sequestering Agents. 2. Kinetics and Mechanism of Iron Removal From Transferrin by Enterobactin and Synthetic Triccatechols. *J. Am. Chem. Soc.***101**: 5401–5404.

Cartron ML, Maddocks S, Gillingham P, Craven CJ, Andrews SC. 2006. Feo--transport of ferrous iron into bacteria. *Biometals* **19**(2):143-57.

Chang C, Mooser A, Plückthun A, Wlodawer A. 2001 Crystal structure of the dimeric C-terminal domain of TonB reveals a novel fold. *J Biol Chem.* **276**(29):27535-40.

Chastanet, A., J. Fert, T. Msadek. 2003. Comparative genomics reveal novel heat-shock regulatory mechanisms in *Staphylococcus aureus* and other Gram-positive bacteria. *Mol. Microbiol.* **47**:1061–1073.

Clarke TE, Ku SY, Dougan DR, Vogel HJ, Tari LW. 2000. The structure of the ferric siderophore binding protein FhuD complexed with gallichrome. *Nat Struct Biol.* **7**(4):287-91.

Clarke TE, Braun V, Winkelmann G, Tari LW, Vogel HJ. 2002. X-ray crystallographic structures of the *Escherichia coli* periplasmic protein FhuD bound to hydroxamate-type siderophores and the antibiotic albomycin. *J Biol Chem.* **277**:13966-13972.

Collier G. S., J. M. Pratt, C. R. De Wet, C. F. Tshabalala. 1979. Studies on haemin in dimethyl sulphoxide/water mixtures. *Biochem J* **179**: 281-289.

Cope L.D., R. Yogev, U. Muller-Eberhard and E.J. Hansen.1995. A gene cluster involved in the utilization of both free heme and heme:hempoxin by *Haemophilus influenzae* type b. *J Bacteriol.* **177** :2644–2653

- Cope L.D., S.E. Thomas, Z. Hrkal and E.J. Hansen.** 1998. Binding of heme-hemopexin complexes by soluble HxuA protein allows utilization of this complexed heme by *Haemophilus influenzae*. *Infect. Immun.* **66**:4511–4516
- Cornelissen C.N., Sparling P.F.** 1994. Iron piracy: acquisition of transferrin-bound iron by bacterial pathogens. *Mol Microbiol* **14**:843-50
- Cornelis P, Matthijs S, Van Oeffelen L.** 2009. Iron uptake regulation in *Pseudomonas aeruginosa*. *Biometals* **22**(1):15-22.
- Cossart P.** 2002 Molecular and cellular basis of the infection by *Listeria monocytogenes*: an overview. *Int J Med Microbiol* **291**: 401–409.
- Deneer HG, Healey V, Boychuk I.** 1995. Reduction of exogenous ferric iron by a surface-associated ferric reductase of *Listeria* spp. *Microbiology.* **141**(Pt 8):1985-92
- Deniau C, Gilli R, Izadi-Pruneyre N, Letoffe S, Delepierre M, Wandersman C, Briand C, Lecroisey A.** 2003. Thermodynamics of heme binding to the HasA(SM) hemophore: effect of mutations at three key residues for heme uptake. *Biochemistry* **42**:10627–10633
- de Villiers, K. A., C. H. Kaschula, et al.** 2007. Speciation and structure of ferriprotoporphyrin IX in aqueous solution: spectroscopic and diffusion measurements demonstrate dimerization, but not μ -oxo dimer formation. *J Biol Inorg Chem* **12**: 101-117.
- Dharmarha Vaishali.** 2008. The majority of deaths from *Listeria* food poisoning are in individuals with compromised immune systems: pregnant women, newborns, the elderly, and the immunosuppressed. "A Focus on *Listeria Monocytogenes*" National Agricultural Library
- Dmireiev B.A., S. Ehlers, E.T. Rietschel.** 1999. Layered murein revisited: a fundamentally new concepts of bacterial cell wall structure, biogenesis and functions, *Med. Microbiol. Immunol (Berl)* **187**:173-81.
- Dramsi S., Biswas I., Maguin E., Braun L., Mastroeni P., Cossart P..** 1995. Entry of *Listeria monocytogenes* into hepatocytes requires expression of inIB, a surface protein of the internalin multigene family. *Mol. Microbiol.* **16**:251-261.
- Drazek ES, Hammack CA, Schmitt MP.** 2000. *Corynebacterium diphtheriae* genes required for acquisition of iron from haemin and haemoglobin are homologous to ABC haemin transporters. *Mol Microbiol* **36**:68–84

- Dryla, A., Gelbmann, D., von Gabain, A., and Nagy, E.** 2003. Identification of a novel iron regulated staphylococcal surface protein with haptoglobin-haemoglobin binding activity. *Mol Microbiol.* **49**, 37–53.
- Ernst J, Bennett R, Rothfield L.** 1978. Constitutive expression of the ironenterochelin and ferrichrome uptake systems in a mutant strain of *Salmonella typhimurium*. *J. Bacteriol.* **135**:928–34
- Everse J, Hsia N.** 1997. The toxicities of native and modified hemoglobins. *Free Radic Biol Med* **22**:1075–1099.
- Frankenberg-Dinkel N.** 2004. Bacterial heme oxygenases. *Antioxid Redox Signal* **6**:825–834.
- Friedman DB, Stauff DL, Pishchany G, Whitwell CW, Torres VJ, Skaar EP.** 2006 Staphylococcus aureus redirects central metabolism to increase iron availability. *PLOS Pathogens* **2**(8):e87
- Furman M., Fica A., Saxena M., Di Fabio J.L., Cabello F.C.** 1994. *Salmonella typhi* iron uptake mutants are attenuated in mice. *Infect Immun* **62**: 4091–4094
- Ghigo JM, Letoffe S, Wandersman C.** 1997. A new type of hemophore-dependent heme acquisition system of *Serratia marcescens* reconstituted in *Escherichia coli*. *J Bacteriol* **179**:3572–3579
- Glaser P, Frangeul L, Buchrieser C, Rusniok C, Amend A, Baquero F, Berche P, Bloecker H, Brandt P, Chakraborty T, Charbit A, Chetouani F, Couvé E, de Daruvar A, Dehoux P, Domann E, Domínguez-Bernal G, Duchaud E, Durant L, Dussurget O, Entian KD, Fsihi H, García-del Portillo F, Garrido P, Gautier L, Goebel W, Gómez-López N, Hain T, Hauf J, Jackson D, Jones LM, Kaerst U, Kreft J, Kuhn M, Kunst F, Kurapkat G, Madueno E, Maitournam A, Vicente JM, Ng E, Nedjari H, Nordziek G, Novella S, de Pablos B, Pérez-Díaz JC, Purcell R, Rimmel B, Rose M, Schlueter T, Simoes N, Tierrez A, Vázquez-Boland JA, Voss H, Wehland J, Cossart P.** 2001. Comparative genomics of *Listeria* species. *Science* **294**(5543):849-52.
- Gray, M. L., and A. H. Killinger.** 1966. *Listeria monocytogenes* and listeric infection. *Bacteriol. Rev.* **30**:309-382.
- Grigg J.C, C.L. Vermeiren, D.E. Heinrichs, M.E. Murphy.** 2007a. Haem recognition by a *Staphylococcus aureus* NEAT domain. *Mol. Microbiol.* **63**:139–149.
- Grigg JC, Vermeiren CL, Heinrichs DE, Murphy ME.** 2007b. Heme coordination by *Staphylococcus aureus* IsdE. *J Biol Chem* **282**:28815–28822.
- Grigg JC, Ukpabi G, Gaudin CF, Murphy ME.** 2010. Structural biology of heme binding in the *Staphylococcus aureus* Isd system. *J Inorg Biochem.* **104**(3):341-8.

- Gunter, K., and Braun, V.** 1990. In vivo evidence for FhuA outer membrane receptor interaction with the TonB inner membrane protein of *Escherichia coli*. *FEBS Lett.* **274**, 85–88
- Hanahan, D.** 1983. Studies on transformation of *Escherichia coli* with plasmids. *J Mol Biol* **166**:557-80.
- Hanson MS, Pelzel SE, Latimer J, Muller-Eberhard U, Hansen EJ.** 1992. Identification of a genetic locus of *Haemophilus influenzae* type b necessary for the binding and utilization of heme bound to human hemopexin. *Proc Natl Acad Sci U S A* **89**:1973–1977
- Hantke K.** 1981. Regulation of ferric iron transport in *Escherichia coli* K12: isolation of a constitutive mutant. *Mol. Gen.Genet.* **182**:288–92
- Hantke K.** 1987 Ferrous iron transport mutants in *Escherichia coli* K-12. *FEMS Microbiol Lett* **44**:53–57.
- Hantke K.** 2001. Iron and metal regulation in bacteria. *Curr Opin Microbiol* **4**:172-177.
- Heller, K., Kadner, R. J., and Gunter, K.** 1988. *Gene (Amst.)* **64**, 147–153
- Henderson D.P. and S.M. Payne.** 1994. *Vibrio cholerae* iron transport systems: roles of heme and siderophore iron transport in virulence and identification of a gene associated with multiple iron transport systems. *Infect Immun* **62**:5120–5125.
- Hill PJ, A. Cockayne, P. Landers, J.A. Morrissey, C.M. Sims and P. Williams.** 1998. SirR, a novel iron-dependent repressor in *Staphylococcus epidermidis*. *Infect. Immun.* **66**:4123–4129.
- Ho WW, Li H, Eakanunkul S, Tong Y, Wilks A, Guo M, Poulos TL.** 2007. Holo- and apo-bound structures of bacterial periplasmic heme-binding proteins. *J Biol Chem* **282**:35796–35802.
- Huang, X., A. Aulabaugh, W. Ding, B. Kapoor, L. Alksne, K. Tabei, and G. Ellestad.** 2003. Kinetic mechanism of *Staphylococcus aureus* sortase SrtA. *Biochemistry* **42**:11307–11315.
- Idei A, Kawai E, Akatsuka H, Omori K.** 1999. Cloning and characterization of the *Pseudomonas fluorescens* ATP-binding cassette exporter, HasDEF, for the heme acquisition protein HasA. *J Bacteriol* **181**:7545–7551.
- Izadi N, Henry Y, Haladjian J, Goldberg ME, Wandersman C, Delepierre M, Lecroisey A.** 1997. Purification and characterization of an extracellular heme-binding protein, HasA, involved in heme iron acquisition. *Biochemistry* **36**:7050–7057

- Jiang XX.** 2009. Biochemistry of hemin uptake in *Listeria monocytogenes* and the function of TonB in *Escherichia coli*. Ph.D dissertation
- Jin B, Newton SM, Shao Y, Jiang X, Charbit A, Klebba PE.** 2006 Iron acquisition systems for ferric hydroxamates, haemin and haemoglobin in *Listeria monocytogenes*. *Mol Microbiol.* **59**(4):1185-98
- Karpowich NK, Huang HH, Smith PC, Hunt JF.** 2003. Crystal structures of the BtuF periplasmic-binding protein for vitamin B12 suggest a functionally important reduction in protein mobility upon ligand binding. *J Biol Chem.* **278**(10):8429-34.
- Kaserer WA, Jiang X, Xiao Q, Scott DC, Bauler M, Copeland D, Newton SM, Klebba PE.** 2008. Insight from TonB hybrid proteins into the mechanism of iron transport through the outer membrane. *J Bacteriol.* **190**(11):4001-16.
- Khun, H.H., S.D.Kirby, B.C.lee.** 1998. A *Neisseria meningitidis* fbpABC mutant is incapable of using nonheme iron for growth. *Infect.Immun.* **66**:2330-36
- Klebba, P. E., M. A. McIntosh, and J. B. Neilands.** 1982. Kinetics of biosynthesis of iron-regulated membrane proteins in *Escherichia coli*. *J Bacteriol* **149**:880-8.
- Ködding J, Killig F, Polzer P, Howard SP, Diederichs K, Welte W.** 2005 Crystal structure of a 92-residue C-terminal fragment of TonB from *Escherichia coli* reveals significant conformational changes compared to structures of smaller TonB fragments. *J Biol Chem.* **280**(4):3022-8)
- Kreft J, Vazquez-Boland J.A., Altrock S., Dominguez-Bernal G., Goebel W.** 2002 Pathogenicity islands and other virulence elements in *Listeria*. *Curr Top Microbiol Immunol* **264**: 109–125.
- Krieg S, Huché F, Diederichs K, Izadi-Pruneyre N, Lecroisey A, Wandersman C, Delepelaire P, Welte W.** 2009 Heme uptake across the outer membrane as revealed by crystal structures of the receptor-hemophore complex. *Proc Natl Acad Sci U S A.* **106**(4):1045-50
- Lambrechts A, K. Gevaert, P. Cossart, J. Vandekerckhove and M. Van Troys.** 2008. *Listeria* comet tails: the actin-based motility machinery at work. *Trends Cell Biol.* **18**:220–227.
- Larsen, R. A., and Postle, K.** 2001. Conserved residues Ser(16) and His(20) and their relative positioning are essential for TonB activity, cross-linking of TonB with ExbB, and the ability of TonB to respond to proton motive force. *J. Biol. Chem.* **276**, 8111–8117

- Lauer P, Chow MY, Loessner MJ, Portnoy DA, Calendar R.** 2002. Construction, characterization, and use of two *Listeria monocytogenes* site-specific phage integration vectors. *J Bacteriol.* **184**(15):4177-86.
- Lavrrar JL, Christoffersen CA, McIntosh MA.** 2002. Fur-DNA interactions at the bidirectional *fepDGC-entS* promoter region in *Escherichia coli*. *J Mol Biol.* **322**:983-995.
- Ledala, N., M. Sengupta, et al.** 2010. Transcriptomic response of *Listeria monocytogenes* to iron limitation and Fur mutation. *Appl Environ Microbiol* **76**: 406-416.
- Lee W.C, M.L. Reniere, E.P. Skaar, M.E.P. Murphy.** 2008. Ruffling of metalloporphyrins bound to IsdG and IsdI, two heme-degrading enzymes in *Staphylococcus aureus*. *J. Biol. Chem.* **283**:30957-30963.
- Lefevre J, Delepelaire P, Delepierre M, Izadi-Pruneyre N.** 2008. Modulation by substrates of the interaction between the HasR outer membrane receptor and its specific TonB-like protein, HasB. *J Mol Biol* **378**:840-851.
- Lei, B., L. M. Smoot, H. M. Menning, J. M. Voyich, S. V. Kala, F. R. Deleo, S. D. Reid & J. M. Musser.** 2002. Identification and characterization of a novel heme-associated cell surface protein made by *Streptococcus pyogenes*. *Infect Immun* **70**: 4494-4500.
- Lei B, M. Liu, J.M. Voyich, C.I. Prater, S.V. Kala, F.R. DeLeo, J.M. Musser.** 2003. Identification and characterization of HtsA, a second heme-binding protein made by *Streptococcus pyogenes*. *Infect. Immun.* **71**:5962-5969.
- Letain, T.E., and Postle, K.** 1997 TonB protein appears to transduce energy by shuttling between the cytoplasmic membrane and the outer membrane in *Escherichia coli*. *Mol Microbiol* **24**: 271-283
- Letoffe, S.; Ghigo, J. M.; Wandersman, C.** 1994. Secretion of the *Serratia marcescens* HasA protein by an ABC transporter. *J. Bacteriol* **176**:5372-5377.
- Letoffe S, Redeker V, Wandersman C.** 1998. Isolation and characterization of an extracellular haem-binding protein from *Pseudomonas aeruginosa* that shares function and sequence similarities with the *Serratia marcescens* HasA haemophore. *Mol Microbiol* **28**:1223-1234.
- Letoffe S, Nato F, Goldberg ME, Wandersman C.** 1999. Interactions of HasA, a bacterial haemophore, with haemoglobin and with its outer membrane receptor HasR. *Mol Microbiol* **33**:546-555

- Letoffe S, Omori K, Wandersman C.** 2000. Functional characterization of the HasA(PF) hemophore and its truncated and chimeric variants: determination of a region involved in binding to the hemophore receptor. *J Bacteriol* **182**:4401–4405.
- Letoffe S, Delepelaire P, Wandersman C.** 2004. Free and hemophore-bound heme acquisitions through the outer membrane receptor HasR have different requirements for the TonB-ExbB-ExbD complex. *J Bacteriol* **186**:4067–4074.
- Letoffe S, Wecker K, Delepierre M, Delepelaire P, Wandersman C.** 2005. Activities of the *Serratia marcescens* heme receptor HasR and isolated plug and beta-barrel domains: the beta-barrel forms a heme-specific channel. *J Bacteriol* **187**:4637–4645
- Liu M, Tanaka WN, Zhu H, Xie G, Dooley DM, Lei B.** 2008. Direct heme transfer from IsdA to IsdC in the iron-regulated surface determinant (Isd) heme acquisition system of *Staphylococcus aureus*. *J Biol Chem* **283**:6668–6676
- Locher KP, Rosenbusch JP.** 1997. Oligomeric states and siderophore binding of the ligand-gated FhuA protein that forms channels across *Escherichia coli* outer membranes. *Eur J Biochem.* **247**(3):770-5
- Locher, K. P., Rees, B., Koebnik, R., Mitschler, A.,Moulinier, L., Rosenbusch, J. P. & Moras, D.** 1998. Transmembrane signaling across the ligand-gated FhuA receptor: crystal structures of free and ferrichrome-bound states reveal allosteric changes. *Cell* **95**:771–778.
- Maresso, A. W., T. J. Chapa & O. Schneewind.** 2006. Surface protein IsdC and Sortase B are required for heme-iron scavenging of *Bacillus anthracis*. *J Bacteriol* **188**: 8145-8152.
- Marques M B, Weller P F, Parsonnet J, Ransil B J, Nicholson-Weller A .**1989 Phosphatidylinositol-specific phospholipase C, a possible virulence factor of *Staphylococcus aureus*. *J Clin Microbiol.* **27**: 2451–2454.
- Marraffini LA, Dedent AC, Schneewind O.** 2006. Sortases and the art of anchoring proteins to the envelopes of gram-positive bacteria. *Microbiol Mol Biol Rev* **70**(1):192-221
- Masse E, Gottesman S.** 2002 A small RNA regulates the expression of genes involved in iron metabolism in *Escherichia coli*. *Proc Natl Acad Sci USA* **99**:4620-4625.
- Masse E, Escorcía FE, Gottesman S.** 2003 Coupled degradation of a small regulatory RNA and its mRNA targets in *Escherichia coli*. *Genes Dev* **17**:2374-2383.
- Mazmanian, S. K., H. Ton-That, and O. Schneewind.** 2001. Sortase-catalyzed anchoring of surface proteins to the cell wall of *Staphylococcus aureus*. *Mol. Microbiol.* **40**:1049–1057

- Mazmanian, S. K., Ton-That, H., Su, K., and Schneewind, O.** 2002. An iron-regulated sortase anchors a class of surface protein during *Staphylococcus aureus* pathogenesis. *Proc Natl Acad Sci U S A* **99**: 2293-2298.
- Mazmanian S.K., Skaar E.P., Gaspar A.H., Humayun M., Gornicki P., Jelenska J., et al.** 2003 Passage of heme-iron across the envelope of *Staphylococcus aureus*. *Science* **299**: 906–909
- McLauchlin, J. a.** 1990. Human listeriosis in Britain, 1967-85, a summary of 722 cases. 1. Listeriosis during pregnancy and in the newborn. *Epidemiol Infect* **104**(2): 181-201
- Miller, J.H.** 1972. Experiments in molecular genetics. Cold Spring Harbor Laboratory, Cold Spring Harbor, NY
- Morita T, Maki K, Aiba H.** 2005 RNase E-based ribonucleoprotein complexes: mechanical basis of mRNA destabilization mediated by bacterial noncoding RNAs. *Genes Dev* **19**:2176-2186
- Mounier J., Ryter A., Coquis-Rondon M., Sansonetti P.J.** 1990. Intracellular and cell-to cell spread of *Listeria monocytogenes* involves interaction with F-actin in the enterocytelike cell line Caco-2. *Infect. Immun.* **58**: 79-82.
- Murphy ER, Payne SM.** 2007 RyhB, an iron-responsive small RNA molecule, regulates *Shigella dysenteriae* virulence.. *Infect Immun.* **75**(7):3470-7.
- Murray, E.G.D., Webb, R.E., Swann, M.B.R.** 1926. A disease of rabbits characterized by a large mononuclear leucocytosis, caused by a hitherto undescribed bacillus *Bacterium monocytogenes* (n. sp.). *J. Pathol. Bacteriol.* **29**: 407– 439.
- Muryoi N, Tiedemann MT, Pluym M, Cheung J, Heinrichs DE, Stillman MJ.** 2008. Demonstration of the iron-regulated surface determinant (Isd) heme transfer pathway in *Staphylococcus aureus*. *J Biol Chem.* **283**(42):28125-36)
- Navarre W., Schneewind O.** 1999. Surface proteins of gram-positive bacteria and mechanisms of their targeting to the cell wall envelope. *Microbiol Mol Biol Rev.* **63**:174-229.
- Neidhardt, F. C., P. L. Bloch, and D. F. Smith.** 1974. Culture medium for enterobacteria. *J Bacteriol* **119**:736-47.
- Neilands, J.B.** 1976. Siderophores: diverse roles in microbial and human physiology. *Ciba Found Symp* **51**:107-24
- Neilands, J.B.** 1995. Siderophores: structure and function of microbial iron transport compounds . *J Biol chem.* **270**:26723-26726

- Newton SM, Igo JD, Scott DC, Klebba PE.** 1999. Effect of loop deletions on the binding and transport of ferric enterobactin by FepA. *Mol. Microbiol* **32**:1153-65
- Newton, S. M., P. E. Klebba, C. Raynaud, Y. Shao, X. Jiang, I. Dubail, C. Archer, C. Frehel, and A. Charbit.** 2005. The *svpA-srtB* locus of *Listeria monocytogenes*: Fur-mediated iron regulation and effect on virulence. *Mol. Microbiol.* **55**:927–940.
- Newton SM, Trinh V, Pi H, Klebba PE.** 2010. Direct measurements of the outer membrane stage of ferric enterobactin transport: postuptake binding. *J Biol Chem.* **285**(23):17488-97
- Ochsner UA, Johnson Z, Vasil ML.** 2000. Genetics and regulation of two distinct haem-uptake systems, *phu* and *has*, in *Pseudomonas aeruginosa*. *Microbiology* **146**(Pt 1):185–198.
- Parsons, L. M., F. Lin, and J. Orban.** 2006. Peptidoglycan recognition by Pal, an outer membrane lipoprotein. *Biochemistry* **45**:2122–2128.
- Perkins-Balding D, Ratliff-Griffin M, Stojiljkovic I.** 2004. Iron transport systems in *Neisseria meningitidis*. *Microbiol Mol Biol Rev.* **68**(1):154-71.
- Pilpa R.M, E.A. Fadeev, V.A. Villareal, M.L. Wong, M. Phillips, R.T. Clubb.** 2006. Solution structure of the NEAT (NEAr Transporter) domain from IsdH/HarA: the human hemoglobin receptor in *Staphylococcus aureus*. *J. Mol. Biol.* **360**:435–447
- Pishchany G, Dickey SE, Skaar EP.** 2009. Subcellular localization of the *Staphylococcus aureus* heme iron transport components IsdA and IsdB. *Infect Immun.* **77**(7):2624-34
- Pluym M, Vermeiren CL, Mack J, Heinrichs DE, Stillman MJ.** 2007. Heme binding properties of *Staphylococcus aureus* IsdE. *Biochemistry.* **46**(44):12777-87
- Pohl E, Haller J, Mijovilovich A, Meyer-Klaucke W, Garman E, Vasil ML.** 2003. Architecture of a protein central to iron homeostasis: crystal structure and spectroscopic analysis of the ferric uptake regulator. *Mol. Microbiol.* **47**:903–15.
- Portnoy D.A., Auerbuch V., Glomski I.J.** 2002 The cell biology of *Listeria monocytogenes* infection: the intersection of bacterial pathogenesis and cell-mediated immunity. *J Cell Biol* **158**: 409–414.
- Postle K, Kadner RJ.** 2003. Touch and go: tying TonB to transport. *Mol Microbiol.* **49**(4):869-82
- Pradel E, Guiso N, Menozzi FD, Locht C.** 2000. *Bordetella pertussis* TonB, a Bvg-independent virulence determinant. *Infect Immun* **68**:1919–1927

- Pucciarelli, M. G., E. Calvo, C. Sabet, H. Bierre, P. Cossart, and F. Garcia- Del Portillo.** 2005. Identification of substrates of the *Listeria monocytogenes* sortases A and B by a non-gel proteomic analysis. *Proteomics* **5**:4808–4817.
- Quiocho FA, Ledvina PS.** 1996. Atomic structure and specificity of bacterial periplasmic receptors for active transport and chemotaxis: variation of common themes. *Mol Microbiol* **20**(1):17-25.
- Ramaswamy V, Cresence VM et al.** 2007. *Listeria* - Review of Epidemiology and Pathogenesis. *J Microbiol Immunol Infect.* **40**:4-13
- Raymond, K. N.; Dertz, E. A.; Kim, S. S.** 2003. Enterobactin: An archetype for microbial iron transport. *PNAS* **7**: 3584–3588
- Reniere ML, Torres VJ, Skaar EP.** 2007. Intracellular metalloporphyrin metabolism in *Staphylococcus aureus*. *Biometals.* **20**(3-4):333-45
- Retzer MD, Yu RH, Schryvers AB.** 1999. Identification of sequences in human transferrin that bind to the bacterial receptor protein, transferrin-binding protein B. *Mol.Microbiol.* **32**:111-21
- Riedel CU, Monk IR, Casey PG, Morrissey D, O'Sullivan GC, Tangney M, Hill C, Gahan CG.** 2007. Improved luciferase tagging system for *Listeria monocytogenes* allows real-time monitoring in vivo and in vitro. *Appl Environ Microbiol.* **73**(9):3091-4.
- Rohrbach MR, Braun V, Köster W.** 1995. Ferrichrome transport in *Escherichia coli* K-12: altered substrate specificity of mutated periplasmic FhuD and interaction of FhuD with the integral membrane protein FhuB. *J Bacteriol.* **177**(24):7186-93.
- Rossi MS, Fetherston JD, Letoffe S, Carniel E, Perry RD, Ghigo JM.** 2001. Identification and characterization of the hemophore-dependent heme acquisition system of *Yersinia pestis*. *Infect Immun* **69**:6707–6717.
- Ryter S.W., R.M. Tyrrell.** 2000. *Free Radic. Biol. Med.* **28**:289–309
- Schiering N, Tao X, Zeng H, Murphy JR, Petsko GA, Ringe D.** 1995. Structures of the apo- and the metal ion-activated forms of the diphtheria toxin repressor from *Corynebacterium diphtheriae*. *Proc. Natl. Acad. Sci. USA* **92**:9843–50.
- Schmitt MP, Holmes RK.** 1991. Iron-dependent regulation of diphtheria toxin and siderophore expression by the cloned *Corynebacterium diphtheriae* repressor gene *dtxR* in *C. diphtheriae* C7 strains. *Infect Immun.* **59**(6):1899-904.

- Schmitt MP.** 1997. Utilization of host iron sources by *Corynebacterium diphtheriae*: identification of a gene whose product is homologous to eukaryotic heme oxygenases and is required for acquisition of iron from heme and hemoglobin. *J Bacteriol* **179**:838–845
- Schneewind, O., P. Model, and V. A. Fischetti.** 1992. Sorting of protein A to the staphylococcal cell wall. *Cell* **70**:267–281.
- Schneider, W., Schwyn, B.** 1987. *Aquatic surface Chemistry*. Wiley: New York, pp 167-195
- Schneider S, Paoli M** 2005 Crystallization and preliminary X-ray diffraction analysis of the haem-binding protein HemS from *Yersinia enterocolitica*. *Acta Crystallogr Sect F Struct Biol Cryst Commun.* **61**(Pt 8):802-5)
- Schneider S, K.H. Sharp, P.D. Barker and M. Paoli.** 2006. An induced fit conformational change underlies the binding mechanism of the heme transport proteobacteria-protein HemS. *J. Biol. Chem.* **281**: 32606–32610.
- Schuller DJ, Wilks A, Ortiz de Montellano PR, Poulos TL.** 1999. Crystal structure of human heme oxygenase-1. *Nat Struct Biol* **6**:860–867
- Scott, D. C., Z. Cao, Z. Qi, M. Bauler, J. D. Igo, S. M. Newton & P. E. Klebba.** 2001. Exchangeability of N termini in the ligand-gated porins of *Escherichia coli*. *J Biol Chem* **276**:13025-13033.
- Sebulsky MT, Heinrichs DE.** 2001. Identification and characterization of *fhuD1* and *fhuD2*, two genes involved in iron-hydroxamate uptake in *Staphylococcus aureus*. *J Bacteriol.* **183**(17):4994-5000
- Sebulsky MT, Shilton BH, Speziali CD, Heinrichs DE.** 2003. The role of *FhuD2* in iron(III)-hydroxamate transport in *Staphylococcus aureus*. Demonstration that *FhuD2* binds iron(III)-hydroxamates but with minimal conformational change and implication of mutations on transport. *J Biol Chem.* **278**(50):49890-900
- Sebulsky MT, Speziali CD, Shilton BH, Edgell DR, Heinrichs DE.** 2004. *FhuD1*, a ferric hydroxamate-binding lipoprotein in *Staphylococcus aureus*: a case of gene duplication and lateral transfer. *J Biol Chem.* **279**(51):53152-9.
- Sharp K.H, S. Schneider, A. Cockayne, M. Paoli.** 2007. Crystal structure of the heme-IsdC complex, the central conduit of the Isd iron/heme uptake system in *Staphylococcus aureus*. *J. Biol. Chem.* **282**:10625–10631.
- Shao Y.** 2007. Genetic and biochemical characterization of hydroxamate transporters in *Listeria monocytogenes*. Ph.D dissertation

- Skaar EP, Gaspar AH, Schneewind O.** 2004a. IsdG and IsdI, heme-degrading enzymes in the cytoplasm of *Staphylococcus aureus*. *J Biol Chem.* **279**(1):436-43.
- Skaar EP, Humayun M, Bae T, DeBord KL, Schneewind O.** 2004b. Iron-source preference of *Staphylococcus aureus* infections. *Science* **305**:1626–1628.
- Siburt C. J. P., R. P. L., Weaver K. D., Noto J. M., Mietzner T. M., Cornelissen C. N., Fitzgerald M. C. and Crumbliss A.L.** 2009. Hijacking transferrin bound iron: protein–receptor interactions involved in iron transport in *N. gonorrhoeae*. *Metallomics* **1**:249.
- Smith K, Youngman P.** 1992. Use of a new integrational vector to investigate compartment-specific expression of the *Bacillus subtilis* spoIIM gene. *Biochimie.* **74**(7-8):705-11.
- Sprencel, C., Z. Cao, Z. Qi, D. C. Scott, M. A. Montague, N. Ivanoff, J. Xu, K. M. Raymond, S. M. Newton, and P. E. Klebba.** 2000. Binding of ferric enterobactin by the *Escherichia coli* periplasmic protein FepB. *J. Bacteriol.* **182**:5359–5364.
- Stauff DL, Torres VJ, Skaar EP.** 2007. Signaling and DNA-binding activities of the *Staphylococcus aureus* HssR-HssS two-component system required for heme sensing. *J Biol Chem.* **282**(36):26111-21
- Stauff DL, Bagaley D, Torres VJ, Joyce R, Anderson KL, Kuechenmeister L, Dunman PM, Skaar EP.** 2008. *Staphylococcus aureus* HrtA is an ATPase required for protection against heme toxicity and prevention of a transcriptional heme stress response. *J Bacteriol.* **190**(10):3588-96
- Steen, A., G. Buist, K. J. Leenhouts, M. El Khattabi, F. Grijpstra, A. L. Zomer, G. Venema, O. P. Kuipers, and J. Kok.** 2003. Cell wall attachment of a widely distributed peptidoglycan binding domain is hindered by cell wall constituents. *J. Biol. Chem.* **278**:23874–23881.
- Stojiljkovic I, K. Hantke.** 1994a. Transport of haemin across the cytoplasmic membrane through a haemin-specific periplasmic binding-protein-dependent transport system in *Yersinia enterocolitica*. *Mol. Microbiol.* **13**:719-732
- Stojiljkovic I, Baumler A, Hantke K.** 1994b. Fur regulon in gram-negative bacteria: Identification and characterization of new iron-regulated *Escherichia coli* genes by a fur titration assay. *J. Mol. Biol.* **236**:531–45.
- Stojiljkovic I., V. Hwa, L. de Saint Martin, P. O’Gara, X. Nassif, F. Heffron and M. So,** 1995. The *Neisseria meningitidis* haemoglobin receptor: its role in iron utilization and virulence. *Mol Microbiol* **15**:531–541.

- Stojiljkovic I, J. Larson, V. Hwa, S. Anic and M. So.** 1996. HmbR outer membrane receptors of pathogenic *Neisseria* spp.: iron-regulated, hemoglobin-binding proteins with a high level of primary structure conservation. *J Bacteriol* **178**:4670–4678.
- Stojiljkovic I, Schryvers AB.** 1999. Iron acquisition systems in the pathogenic *Neisseria*. *Mol Microbiol* **32**:117-23
- Stojiljkovic I, Perkins-Balding D.** 2002. Processing of heme and heme-containing proteins by bacteria. *DNA Cell Biol.* **21**(4):281-95.
- Stork M., Di Lorenzo M., Mourino S., Osorio C.R., Lemos M.L., Crosa J.H.** 2004 Two tonB systems function in iron transport in *Vibrio anguillarum*, but only one is essential for virulence. *Infect Immun* **72**:7326–7329
- Tarlovsky, Y., M. Fabian, E. Solomaha, E. Honsa, J. S. Olson & A. W. Maresso.** 2010. A *Bacillus anthracis* S-layer homology protein that binds heme and mediates heme delivery to IsdC. *J Bacteriol* **192**:3503-3511.
- Thompson, J.M., Jones, H.A., and Perry, R.D.** 1999. Molecular characterization of the hemin uptake locus (*hmu*) from *Yersinia pestis* and analysis of *hmu* mutants for hemin and hemoprotein utilization. *Infect. Immun.* **67**:3879–3892).
- Tilney L.G., Portnoy, D.A.** 1989. Actin filaments and the growth, movement, and spread of the intracellular bacterial parasite, *Listeria monocytogenes*. *J. Cell Biol.* **109**: 1597-1608.
- Tong Y, Guo M.** 2007. Cloning and characterization of a novel periplasmic heme-transport protein from the human pathogen *Pseudomonas aeruginosa*. *J Biol Inorg Chem* **12**:735–750.
- Tong Y, Guo ML.** 2009. Bacterial heme-transport proteins and their heme-coordination modes. *Arch Biochem Biophys.* **481**(1):1-15.
- Ton-That, H., H. Mazmanian, K. F. Faull, and O. Schneewind.** 2000. Anchoring of surface proteins to the cell wall of *Staphylococcus aureus*. I. Sortase catalyzed *in vitro* transpeptidation reaction using LPXTG peptide and NH₂-Gly₃ substrates. *J. Biol. Chem.* **275**:9876–9881.
- Ton-That H, Marraffini LA, Schneewind O.** 2004. Protein sorting to the cell wall envelope of Gram-positive bacteria. *Biochim Biophys Acta.* **1694**(1-3):269-78).
- Torres VJ, Pishchany G, Humayun M, Schneewind O, Skaar EP.** 2006. *Staphylococcus aureus* IsdB is a hemoglobin receptor required for heme iron utilization. *J Bacteriol.* **188**(24):8421-9

- Torres VJ, Stauff DL, Pishchany G, Bezbradica JS, Gordy LE, Iturregui J, Anderson KL, Dunman PM, Joyce S, Skaar EP.** 2007 A *Staphylococcus aureus* regulatory system that responds to host heme and modulates virulence. *Cell Host Microbe*. **1**(2):109-19
- Torres VJ, Attia AS, Mason WJ, Hood MI, Corbin BD, Beasley FC, Anderson KL, Stauff DL, McDonald WH, Zimmerman LJ, Friedman DB, Heinrichs DE, Dunman PM, Skaar EP.** 2010 *Staphylococcus aureus* fur regulates the expression of virulence factors that contribute to the pathogenesis of pneumonia. *Infect Immun*. **78**(4):1618-28
- Unno M., T. Matsui, M. Ikeda-Saito.** 2007. Structure and catalytic mechanism of heme oxygenase. *Nat. Prod. Rep.* **24**:553–570.
- Vazquez-Boland J.A., Kuhn M., Berche P., Chakraborty T., et al,** 2001. *Listeria* pathogenesis and molecular virulence determinants *Clin Microbiol Rev.* **14**:548-640.
- Villareal V.A, R.M. Pilpa, S.A. Robson, E.A. Fadeev, R.T. Clubb.** 2008. The IsdC protein from *Staphylococcus aureus* uses a flexible binding pocket to capture heme. *J. Biol. Chem.* **283**:31591–31600.
- Vollmer W, Höltje JV.**2004. The architecture of the murein (peptidoglycan) in gram-negative bacteria: vertical scaffold or horizontal layer(s)? *J Bacteriol.* **186**(18):5978-87.
- Wandersman C, Stojiljkovic I.** 2000. Bacterial heme sources: the role of heme, hemoprotein receptors and hemophores. *Curr Opin Microbiol.* **3**(2):215-20.
- Wandersman, C., and P. Delepelaire.** 2004. Bacterial iron sources: from siderophores to hemophores. *Annu Rev Microbiol* **58**:611-47.
- Watanabe J.M, Y. Tanaka, A. Suenaga, M. Kuroda, M. Yao, N. Watanabe, F.Arisaka, T. Ohta, I. Tanaka, K. Tsumoto.** 2008. Structural basis for multimeric heme complexation through a specific protein-heme interaction: the case of the third neat domain of IsdH from *Staphylococcus aureus*. *J. Biol. Chem.* **283**:28649–28659.
- Weinberg ED.** 1978. Iron and infection. *Microbiol Rev.* **42**(1):45-66
- Weinberg, E.D.** 1990. Roles of trace metals in transcriptional control of microbial secondary metabolism. *Biol. Metals.* **2**:191-96
- Wejman J.C, D. Hovsepian, J.S. Wall, J.F. Hainfeld, J. Greer.**1984. Structure of haptoglobin and the haptoglobin-hemoglobin complex by electron microscopy. *J. Mol. Biol.* **174**:319–341

- Wong J.C., J. Holland, T. Parsons, A. Smith and P. Williams.** 1994. Identification and characterization of an iron-regulated hemopexin receptor in *Haemophilus influenzae* type b. *Infect. Immun.* **62**:48–59
- Wrigglesworth, J.M.; Baum, H.** 1980. Iron in Biochemistry and Medicine, II Academic Press: London , pp 29-86
- Wu R, E.P. Skaar, R. Zhang, G. Joachimiak, P. Gornicki, O. Schneewind, A.Joachimiak.** 2005. Staphylococcus aureus IsdG and IsdI, heme-degrading enzymes with structural similarity to monooxygenases. *J. Biol. Chem.* **280**:2840–2846.
- Wyckoff EE, D. Duncan, A.G. Torres, M. Mills, K. Maase, S.M. Payne.** 1998. Structure of the *Shigella dysenteriae* haem transport locus and its phylogenetic distribution in enteric bacteria. *Mol. Microbiol.* **28**:1139–1152.
- Wyckoff EE, Schmitt M, Wilks A, Payne SM.** 2004. HutZ is required for efficient heme utilization in *Vibrio cholerae*. *J Bacteriol.* **186**(13):4142-51
- Wyckoff EE, Mey AR, Payne SM.** 2007 Iron acquisition in *Vibrio cholerae*. *Biometals.* **20**(3-4):405-16.
- Yeowell, H. N., and J. R. White.** 1982. Iron requirement in the bactericidal mechanism of streptonigrin. *Antimicrob Agents Chemother* **22**:961-8.
- ZHU, W., HUNT, J.T., RICHARDSON, A.R., and STOJILJKOVIC, I.** 2000a. Use of heme compounds as iron sources by pathogenic *Neisseriae* requires the product of the *hemO* gene. *J. Bacteriol.* **182**:439–447
- ZHU, W., WILKS, A., and STOJILJKOVIC, I.** 2000b. Degradation of heme in Gram-negative bacteria: The product of the *hemO* gene of neisseriae is a heme oxygenase. *J. Bacteriol.* **182**, 6783–6790.)
- Zhu H, Liu M, Lei B.** 2008. The surface protein Shr of *Streptococcus pyogenes* binds heme and transfers it to the streptococcal heme-binding protein Shp. *BMC Microbiol.* **8**:15.
- Zhu H, Xie G, Liu M, Olson JS, Fabian M, Dooley DM, Lei B.** 2008. Pathway for heme uptake from human methemoglobin by the iron-regulated surface determinants system of *Staphylococcus aureus*. *J Biol Chem.* **283**(26)
- Zong, Y., T. W. Bice, H. Ton-That, O. Schneewind, and S. V. Narayana.** 2004. Crystal structures of *Staphylococcus aureus* sortase A and its substrate complex. *J. Biol. Chem.* **279**:31383–31389.

Zunszain P.A., J. Ghuman, T. Komatsu, E. Tsuchida, S. Curry. 2003. Crystal structural analysis of human serum albumin complexed with hemin and fatty acid. *BMC Struct. Biol.* 3:6